A STUDY ON ENGINEERING BEHAVIOUR OF GEOSYNTHETICS REINFORCED SOIL

ANKUR MUDGAL

DEPARTMENT OF CIVIL ENGINEERING

DELHI TECHNOLOGICAL UNIVERSITY

SHABAD DAULATPUR, DELHI – 110042

AUGUST 2020

A STUDY ON ENGINEERING BEHAVIOUR OF GEOSYNTHETICS REINFORCED SOIL

By

ANKUR MUDGAL

Department of Civil Engineering

Submitted

in fulfillment of the requirements of the degree of

DOCTOR OF PHILOSOPHY

to the

DEPARTMENT OF CIVIL ENGINEERING

DELHI TECHNOLOGICAL UNIVERSITY

SHABAD DAULATPUR, DELHI – 110042

AUGUST 2020

To my mentors, family and friends.

I couldn't have done this without you.

Thank you Almighty for your blessings during my work.

CERTIFICATE

This is to certify that the thesis entitled, '**A Study on Engineering Behaviour of Geosynthetics Reinforced soil**' being submitted by **Mr. Ankur Mudgal** to the Delhi Technological University, Delhi for the award of the degree of **DOCTOR OF PHILOSOPHY** is a record of the bonafide research work carried out by him. Mr. Ankur Mudgal has worked under my supervision for the submission of this thesis, which, to my knowledge, has reached the requisite standard.

The thesis or any part thereof has not been presented or submitted to any other University or Institute for any degree or diploma.

Prof. Raju Sarkar
Professor
Department of Civil Engineering
Delhi Technological University
New Delhi, India

Prof. A.K. Shrivastava
Professor
Department of Civil Engineering
Delhi Technological University
New Delhi, India

ACKNOWLEDGEMENT

I would like to express my gratitude to my supervisors ***Prof. Raju Sarkar*** *and* ***Prof. A.K Shrivastava,*** *for their continuous guidance, supports and encouragement during my research. Their continued support and visionary thoughts have been a strong motivation for me. The work ethics and discipline learnt from their will help me throughout my academic career.*

I am also thankful to Prof. Nirendra Dev and other faculty members of the Department of Civil Engineering, Delhi Technological University, Delhi for their extended cooperation throughout my PhD study.

I am also thankful to HEICO and its staff for providing me their lab's space and research facilities for extending my work. Special thanks to Mr. Abhay Tiwari for his valuable suggestions during the research work.

Also, I would like to thank my friend Dr. Prateek Negi and Dr. Prakash Chittora for his unconditional support in my research work and during Preparation of this thesis. I am also thankful to my fellows Akshit Mittal, Shubham Gupta, Aman Middha, Prachi Lingwal, Meenakshi Singh, Ibadur Rahman, and Ritesh Kurar, for their valuable discussions and cooperation throughout this programme.

Lastly, I feel privileged and grateful to my parents, Mrs. Aarti Mudgal and Mr. Jagdish Mudgal, my brother Deepak Mudgal and my sister Pooja Sharma for everything in my life and the fact that I have reached here today. Everything that I have achieved is because of their blessings, encouragement, and support. Thanks to all of you, I really appreciate everything that you have done for me.

ABSTRACT

The bearing capacity of a foundation reduces in case of cohesive soil with low to medium plasticity, which thus requires the proper solutions for significant improvement in the load-carrying capacity of the foundation. Geosynthetics are an effective way of increasing the shear strength of the soil, which results in lesser settlement and higher load-bearing capacity of foundation hence giving a safe and economical solutions. On the other hand, Various civil engineering structures such as bridge abutments and embankments require the construction of foundations on sloping grounds, is significantly reduces the bearing capacity of the foundation. Geosynthetic reinforcements can also be a low-cost method of enhancing the bearing capacity of such foundations and act as settlement reducer. However, their increments are dependent on the location of the placement of the geosynthetics within the foundation. Hence, in this study, a number of reduced scaled laboratory tests were performed on footing resting on flat and slopping surface. Different parameters such as spacing of the top layer reinforcement (u), number of reinforcement layers (N), vertical spacing between reinforcements (h), effective depth of reinforcement (d), types of reinforcements, slope angle (β), the distance between the edge of the slope and the loading surface (D) have been analysed. The study showed a significant improvement in bearing capacity of the foundation with geosynthetics inclusion, although maximum improvements occurred at the point of optimum placement of geosynthetics. Also, the improvement in the bearing capacity increased until it reached saturation with the increment in the number of layers of geosynthetic, thus signifying the presence of an optimum depth of reinforcement. Strains developed during the testing were also measured using strain gauges bonded onto the geosynthetic, and it is observed that strain development in geosynthetic is interrelated to footing settlement which has a very low strain in reinforcement located beyond the distance $2.5B$ from the footing center, where B is the width of footing. Numerical simulation of experimental setup is done to calculate the bearing capacity

and settlements. Numerical results were compared with experimental results. Computation of the analytical model based on the reduction factor revealed R^2=0.96, thus signifying that this model can be used effectively for computation of the ultimate bearing capacity of reinforced foundations. A statistical regression model was presented, with a confidence level greater than 95%, which included the significant parameters necessary for computation of the ultimate bearing capacity of reinforced foundations. The proposed equation was in close agreement with the experimental results, and the multiple R^2 values and the adjusted R^2 values were obtained as 0.956 and 0.951 respectively for the proposed model in case of footing resting over slopping surface and the multiple R^2 values and the adjusted R^2 values were obtained 0.964 and 0.953 respectively in the case of footing over flat surface.

CONTENTS

LIST OF FIGURES

LIST OF TABLES

LIST OF ABBREVIATIONS

B	Footing width
D	Edge Distance
IF	Improvement Factor
FEM	Finite Elements Method
N	Number of reinforcements
PRS	Percentage Reduction in Settlement
UBC	Ultimate bearing capacity
d	Depth of reinforcement
h	Vertical spacing between two geosynthetics
s	Settlement of footing
u	Top layer spacing
b	Width of reinforcement
β	Slope angle
x:	Relative distance from the center of footing
GGR1	Geogrid
GGR2	Glasgrid
GTX	Geotextile
CMD	Cross machine direction
MD	Machine direction
EA	Secant Stiffness
SG	Strain gauge
N_t	Normalized tensile strength
N_s	Normalized stiffness
$Q_{r(\text{flat surface})}$	Bearing capacity of reinforced soil for flat surface
$Q_{(\text{flat surface})}$	Bearing capacity of unreinforced soil for flat surface
$s_{r(\text{flat surface})}$	Settlement of the reinforced for flat surface
$s_{(\text{flat surface})}$	Settlement of the reinforced for flat surface
$Q_{r(Slope\ \text{surface})}$	Bearing capacity of reinforced soil for slopy surface
$Q_{(Slope\ \text{surface})}$	Bearing capacity of unreinforced soil for slopy surface
$s_{r(Slope\ \text{surface})}$	Settlement of the reinforced for slopy surface
$s_{(\text{Slope surface})}$	Settlement of the reinforced for slopy surface
UBC	Ultimate bearing capacity of soil
$q_{u(R)}$	Ultimate bearing capacity of the foundation under reinforced soil
$q_{(u)b}$	Ultimate bearing capacity of the foundation under reinforced soil
D_f	Embedment depth of the footing
γ_t	Unit weight of the soil in the reinforced region
K_S	Coefficient of punching shear
T_i	Tensile force mobilized in the ith reinforcement layer
T_u	Ultimate tensile strength of the reinforcement
δ	Mobilized frictional angle at the punching shear upper surface
α_i	Horizontal angle of the reinforcement
c_a	Unit adhesion of the soil along the line D_P
D_P	Depth of punching shear zone
ANM1	Analytical model 1

ANM2	Analytical model 2
ω	Reduce width
R_k	Reduction factor 1
RF	Reduction factor 2
$q_{u(eccentric,N)}$	Ultimate bearing capacity of an eccentrically loaded square footing with N layers of reinforcements
$q_{u(centric,N)}$	Ultimate bearing capacity of a centrally loaded square footing with N layers of reinforcements
μ	Unknown parameters in the model
γ	Unknown parameters in the model

CHAPTER 1
INTRODUCTION

1.1 General

The geosynthetic is a universal term that can be used for all the categories of synthetic products, and these synthetic products are used in conjunction with soil, rock, and other construction materials like fly ash, pond ash and stone dust, etc. These geosynthetics are made of synthetic polymers like polyethylene, polyamide, polyester, and polypropylene, etc. The most common synthetic products include geogrid, geotextile, geocell, geomembrane, and geonets. Since the last three decades, these geosynthetics are significantly used as soil reinforcement in many civil engineering structures, like pavement, foundation soil, and retaining wall. Among them, the use of geosynthetics in foundation soil has recently received more attention.

1.2 Description of the problem

In geotechnical engineering, the construction of the shallow foundation over the existing clay or cohesive soil layer of low to medium plasticity adversely affects the performance of foundation on soil in terms of ultimate bearing capacity and settlement. Excessive footing settlement can damage the superstructure, thus adversely affects the longevity of the structure. A shallow foundation constructed over geosynthetics reinforced soil has not only better performance in terms of bearing capacity and settlement but also from an economic point of view over conventional methods like deep foundation and soil replacement by a thick layer of strong granular fill, the replacement will be costly because of limited availability of stronger good quality granular materials. The simplicity of the basic principles and the economic benefits over the conventional approaches made the geosynthetic-reinforced foundation soil very attractive to the designers.

The geosynthetic-reinforced soil can be used in many geotechnical applications like the foundation of the building, bridge approach slab, industrial and pavement foundation, etc. Among them, the application of geosynthetics reinforced soil foundation in the design of building and bridge approach foundation to improve the bearing capacity of the soil, and to minimize the resulting excessive settlement is also very useful. One proposed solution is the use of reinforced soil foundation in geotechnical engineering is to design the foundation and to transfer the structural load into soil strata. A shallow foundation is illustrated in Fig. 1.1. From the literature study, it is cleared that when reinforcement is provided below the footing, the size of the footing reduces, and a uniform pressure is distributed, which also reduces the higher settlement of the footing.

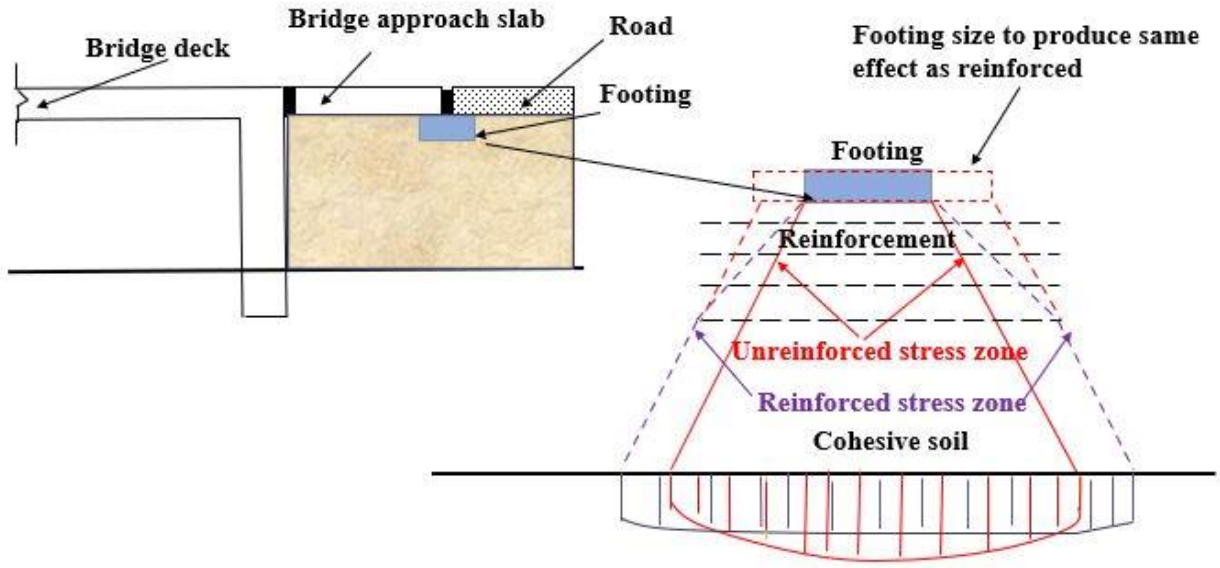

Fig. 1.1 Reinforced soil foundation load transfer mechanism (Chen et. al 2007)

1.3 Function and mechanism

Many researchers have introduced different theories of the basic concept of soil reinforcement. One of the approaches of soil reinforcements using rigid reinforcements like metals, fiber-reinforced plastics, etc. can be described using either an induced-stresses concept or an induced deformations concept. As per the induced stresses concept, the development of friction at the

soil-reinforcement interface and high stiffness of reinforcement provides a cohesive strength to the soil- reinforcement system. On the other hand, in the case of induced-deformations concept, tensile reinforcements involve anisotropic restraint of the soil deformations. The use of flexible reinforcements, like geosynthetics in soil, does not fall within these concepts (Shukla, 2002). The performance of rigid reinforcement and flexible reinforcements in soil reinforcement is different in terms of load settlement behavior of footing. Reinforced soil foundation with the inclusion of flexible reinforcement has the ability to take more load and higher extensibility than soil reinforced with rigid reinforcement of unreinforced soil. However, the soil reinforced with both the reinforcements, *i.e.*, rigid and flexible reinforcement, have a similarity to restrain the growth of internal tensile strain in soil and develop the tensile stress. The foundation soil, in inclusion with geosynthetics, can be considered to have four different significant roles of the bearing capacity improvement and settlement reduction of footing.

1.3.1 Confinement effect: Confinement effect in the soil mass occurs when a downward load of footing acts on soil mass, which results in a relative movement of soil and reinforcement, thus mobilize a friction force at the soil reinforcement interface. An interlocking can be induced by soil and reinforcement interaction, which inhibits the lateral deformations resulting in a reduction of the vertical deformation of the whole soil mass. This action of reinforcement is referred to as the confinement effect (1.2-a).

1.3.2 Membrane effect: With the application of load, soil, along with footing, moves downward and causes the deformations in the reinforcement. This deformed reinforcement (tensile) resists the applied pressure and provides vertical support to overlaying soil mass subjected to loading. This action of reinforcement is called membrane effect (1.2-b) (Shukla and Chandra, 1994a). For a beneficial use of membrane effect in reinforced soil foundation, reinforcement should experience a certain amount of deformation, which develops the tension

forces in reinforcement. However, geosynthetics should have sufficient stiffness and length so that it never fails in pullout and tension. The geogrid and geotextile with higher stiffness can be used in membrane effect in case of excessive deformation of reinforced foundation soil.

1.3.3 Deep footing effect: Along with the above two reinforcement mechanisms, a deep footing effect can be induced in reinforced foundation soil. It should be noticed that the meaning of deep footing here is different than the concept of using a traditional deep foundation for the load transfer mechanism in soil. Here in this deep footing mechanism, the soil reinforced to a depth of *d* (effective reinforcement depth) loaded under the surface footing is very similar to the unreinforced soil loaded with the same depth $d = D_f$. This effect is applicable up to a depth of 1.5 *B*. Huang and Tatsuoka, (1990) have considered this effect in their analytical work to compute the bearing capacity of reinforced soil. The mechanism is shown in Fig (1.2-c).

1.3.4 Rigid boundary effect: If the cover depth of the reinforcement (*u*) is higher than the specific values, then the reinforcement behaves like a boundary, and failure of soil mass is likely to occur above the first reinforcement layer. The rigid boundary effect was first introduced by (Binquet and Lee 1975b) shown in Fig. (1.2-d). Researchers like Mandal 1992; Omar et al., 1993b; Chen et al., 2007 have confirmed this finding by conducting several laboratory tests.

1.4 Applications of geosynthetics in real-life problem

The following sections discuss some live geotechnical applications in the field. There are already more than ten times types of geosynthetics. However, in the present study, the focus has been kept on geogrids and geotextiles.

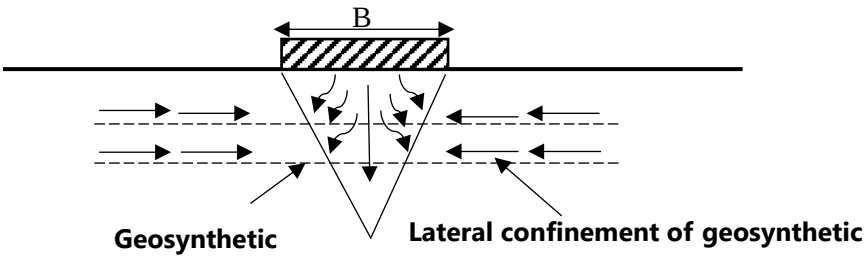

(a) Confinement effect

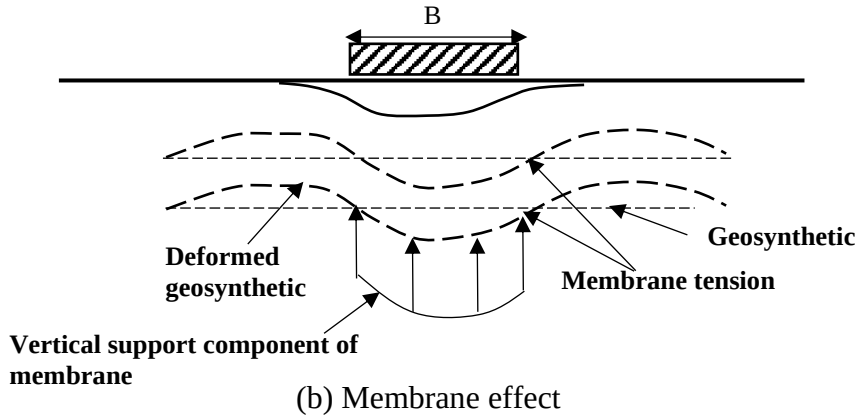

(b) Membrane effect

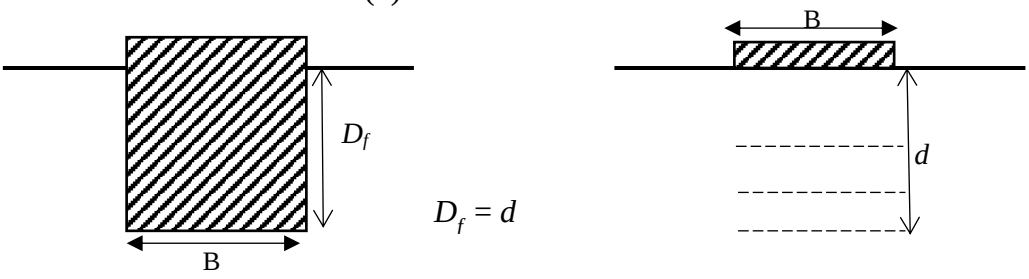

(c) Deep footing effect (Huang & Tatsuoka ,1990)

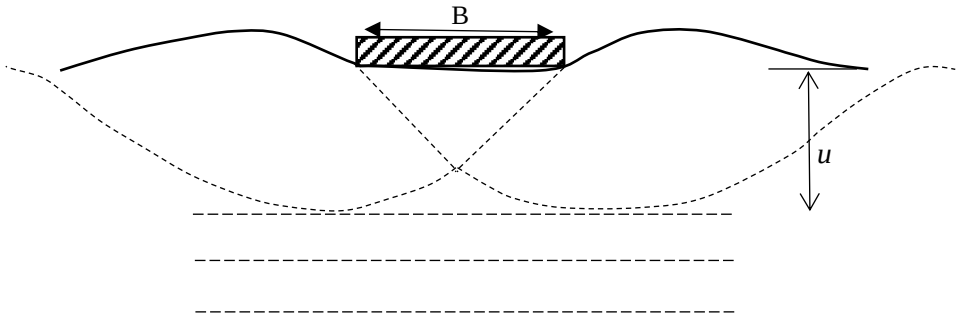

(d) Rigid boundary effect (Binquet & lee, 1975 b)

Fig. 1.2 Various failure mechanisms

1.4.1 Application of geosynthetics in pavement

In a road construction project at Kharagpur, India, a pavement was designed for 100 MSA traffic with a life of 15 years. Due to less availability of aggregates, the engineers proposed a solution to reducing the thickness of the pavement by introducing 3-D geogrids. They designed the service road in two sections, one of them was 500 m in length with 3-D geogrid, and another was 150 m long without 3-D geogrid. A falling weight deflectometer (FWD) test was conducted over the pavement section by IIT, Kharagpur as shown in Fig. 1.3 (a). The FWD test setup consists of an impulse loading device in which a transient load is applied to the pavement, and the deflected shape of the pavement surface is measured. The working principle of FWD test is shown in Fig. 1.3 (c). The observed results in the section with the geogrid were within limits, hence the geogrid was installed in the entire project. The details of the considered sections for FWD tests are given below.

(1) Pavement with geogrid - 25 mm SDBC, 50 mm DBM, 150 mm WMM, A layer of Tenax 3 D grid S, 200 mm GSB, Subgrade.

(2) Pavement without Geogrid- 25mm SDBC, 50mm DBM, 250 mm WMM, 200 mm GSB, Subgrade.

The test results showed that the average back-calculated elastic moduli of bituminous, WMM, GSB, and subgrade layers obtained for the section with geogrid are- 6746, 285, 257, and 147 MPa. The average back-calculated elastic moduli obtained for the section without geogrid are- 7388, 230, 156, and 156 MPa. It has been seen from the back-calculated moduli of the granular base and granular sub-base that the provision of geogrid improved the strength of these two layers even though the thickness of the geogrid reinforced section was less than that in the section without geogrid (conventional). In the case of WMM base layer of the pavement section with geogrid modulus, value is about 24% larger than the value obtained for section without geogrid even though the thickness of WMM layer with geogrid is 150 mm compared to 250

mm thickness provided in the section without geogrid. It can also be seen that the granular sub-base modulus for the pavement with geogrid is 64% more than the modulus of the GSB of the pavement section without Geogrid. Fig. 1.3 (c) show the laying down of geogrid in pavement.

(a) FWD test, IIT Kharagpur

(b) Laying down of geogrid in pavement

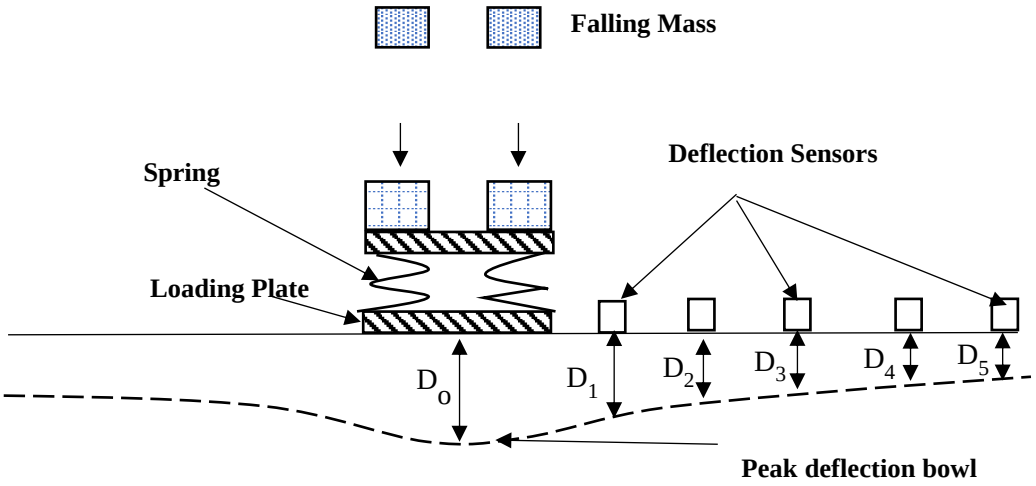

(c) Falling weight deflectometer

Fig. 1.3 Thickness reduction using 3-D geogrid at NH-6 Dhankauri- Kharagpur section (IIT Kharagpur, 2000)

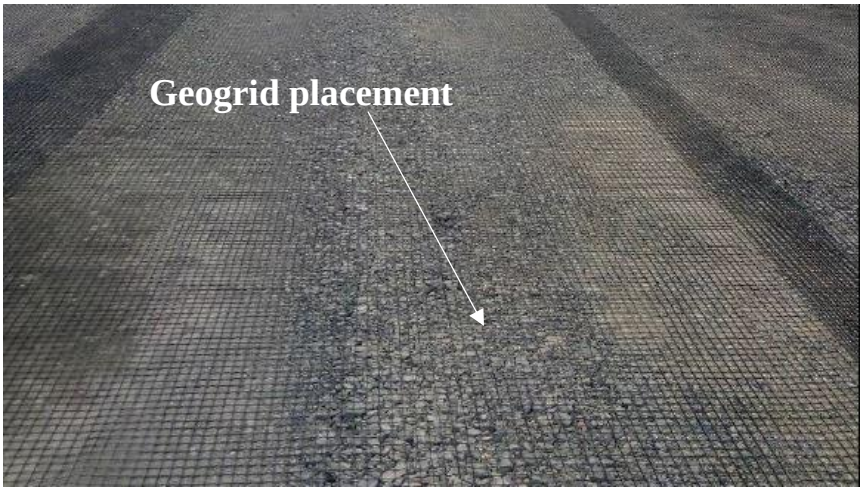

Fig. 1.4 Laying down of geogrid in granular sub base (HMBS Textile, 2017)

Some practical examples also reveal that geosynthetics can be utilized in pavement stabilization. HMBS Textile, (2017) have used Tenax 3-D geogrid in granular sub-base at Charama District, Chhattisgarh. They observed that by reinforcing the granular base layers with Tenax geogrids, construction could be carried out cost-effectively, quickly, and with less environmental impact due to reduced excavation depths (up to 40% less). Fig. 1.4 shows the proper placement of a 3-D geogrid layer in pavement section.

1.4.2 Application of geosynthetics in blanket thickness reduction system

A blanket or a sub-ballast layer is a layer of coarse materials which is provided between the ballast and subgrade and spread over the entire formation width. The purpose of the blanket is to distribute the traffic load on the subgrade layer. HMBS textiles, (2018) used Tenax 3-D grid S (Bi oriented geogrid) at the interface of subgrade and blanket to reduce the thickness at Jhansi to Bhimsen, U.P., India. By using the geogrid, the required quantities of blanket material were reduced, which was being imported from the far location. Thus, an increase in cost and time for transportation was minimized.

Tenax 3-D Grid S (Bi oriented geogrid) was prepared at the interface of subgrade and blanket. These 3-D Grid S are specifically designed for railway applications where the load applied to

the soil mainly develops longitudinally, which is also referred to as plane strain condition. The 3-D geogrid is scientifically better than traditional flat or triangular mesh geogrid. The thickness of threads and nodes produce lateral confinement, which combined with a specific mesh for every kind of soil, maximum the interlocking between soil geogrid. This results in higher performance that enables a better distribution of loads. Therefore, the development of holes and ruts decreases, and the thickness of the bore layer required for roads and railways decreases. The thickness of blanket material was reduced from 600 mm to 400 mm, saving in a huge volume of blanket material, thereby cost increasing the speed of the project. Fig. 1.5 (b) shows the reduction of blanket thickness using Tenax 3-D geogrid.

Another case study of the Slovenia railway line has been presented. The railway line Trieste Wien, in the Slovenian segment, was passing over soils with extremely low bearing capacity, with an elastic modulus lower than 20 MPa (somewhere even 5-10 MPa). This fact was causing severe problems to the line. The maximum speed had to be reduced to 40-50 km/h. Being necessary to operate by removing one track and keeping the other one in function, it was not possible to dig and remove the bad subsoil (clayey silts and clays) to a depth greater than 0.50-0.60 m. As the minimum required modules for the subbase (blanket), according to Slovenian rules, is 50 MPa, it was necessary to stabilize the base of the embankment with properly selected geosynthetics. In the Sentjur-Celje segment, depending upon the characteristics of the subgrade, an extruded PP bi-oriented geogrid Tenax LBO 401 SAMP has been used. The geogrid was used laid on a nonwoven geotextile when the subbase had very poor characteristics, and it was necessary to have both a reinforcing and a filtration-separation effect. Fig. 1.6 shows the proper installation of the geogrid and geotextile in the over the subgrade layer.

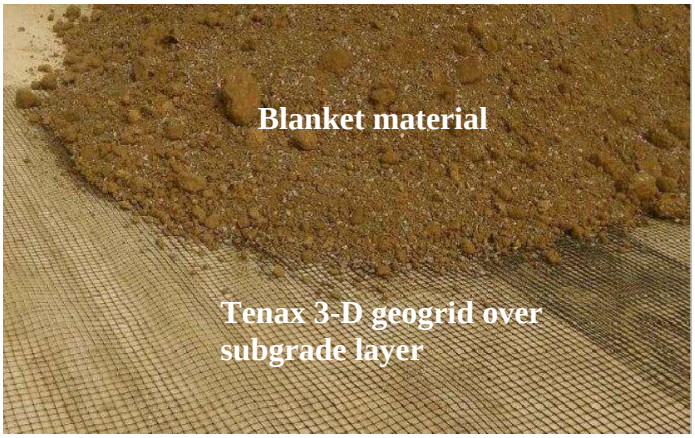

(a) Geogrid over subgrade layer

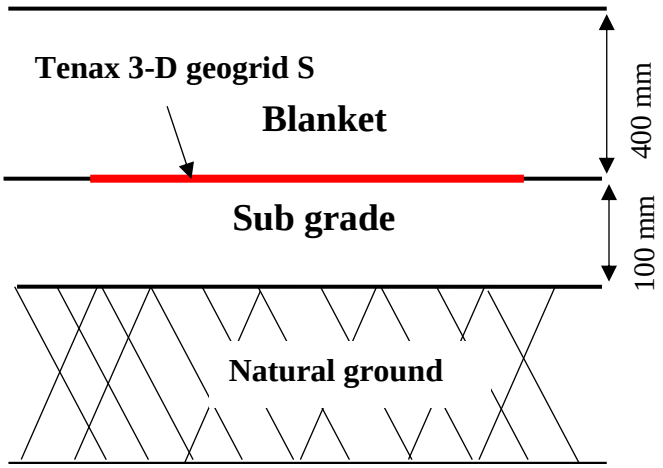

(b) Schematic diagram of geogrid reinforced embankment layers

Fig. 1.5 Reduction of blanket thickness using Tenax 3-D geogrid (HMBS Textile, 2018)

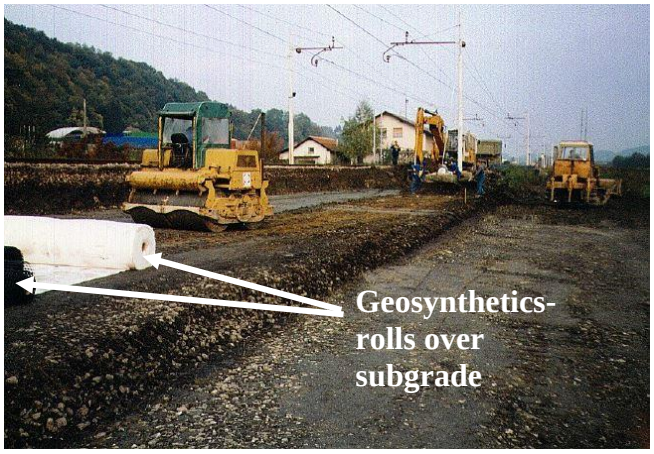

(a). Preparation of the subgrade

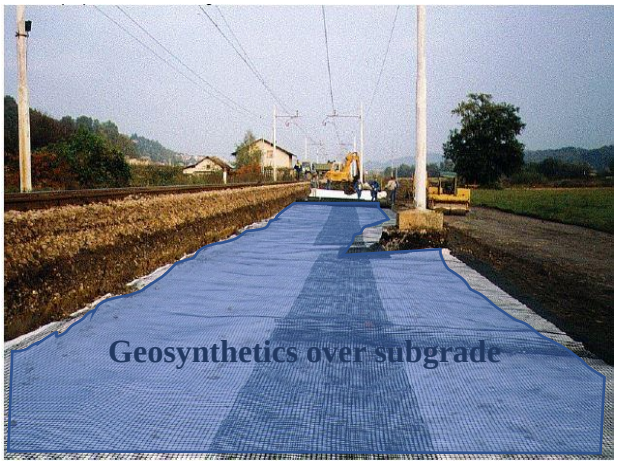

(b) Laying down of geosynthetics

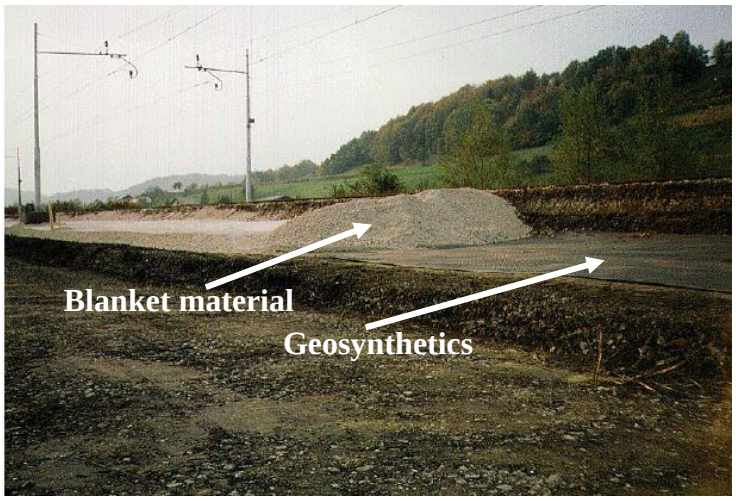

(c) Laying down of the blanket layer

Fig. 1.6 Application of geosynthetics in railway embankment at Slovenia, Trieste Wien (Slovenia railway, 2000)

A study on a large-scale plate load test at Bern-Luzern (Swiss Federal Railway) has been presented. The purpose of the test was to check the strength of the subsoil over which a rail embankment was prepared. The subsoil was for the first 8-12 m was consist of sands, with peat and a CBR ranging between 2 to 4 % (Elastic modulus between 2 to 6 MPa). The poor conditions were causing increasing maintenance resulting in rehabilitation every 1-2 years. When it was decided to double the line, different solutions were studied in order to achieve an elastic modulus of 50 MPa. Large-scale tests have been conducted with a different solution in terms of aggregate, thickness, and geogrids used were PET woven grid 55 kN/m, and PP extruded geogrids, the thickness of coarse aggregate was 400 mm or 300 mm. The results obtained are shown in Fig. 1.7. The extruded geogrid was allowing a reduction in thickness to 300 mm. Fig. 1.8 also shows the laying down of geogrid in railway embankment.

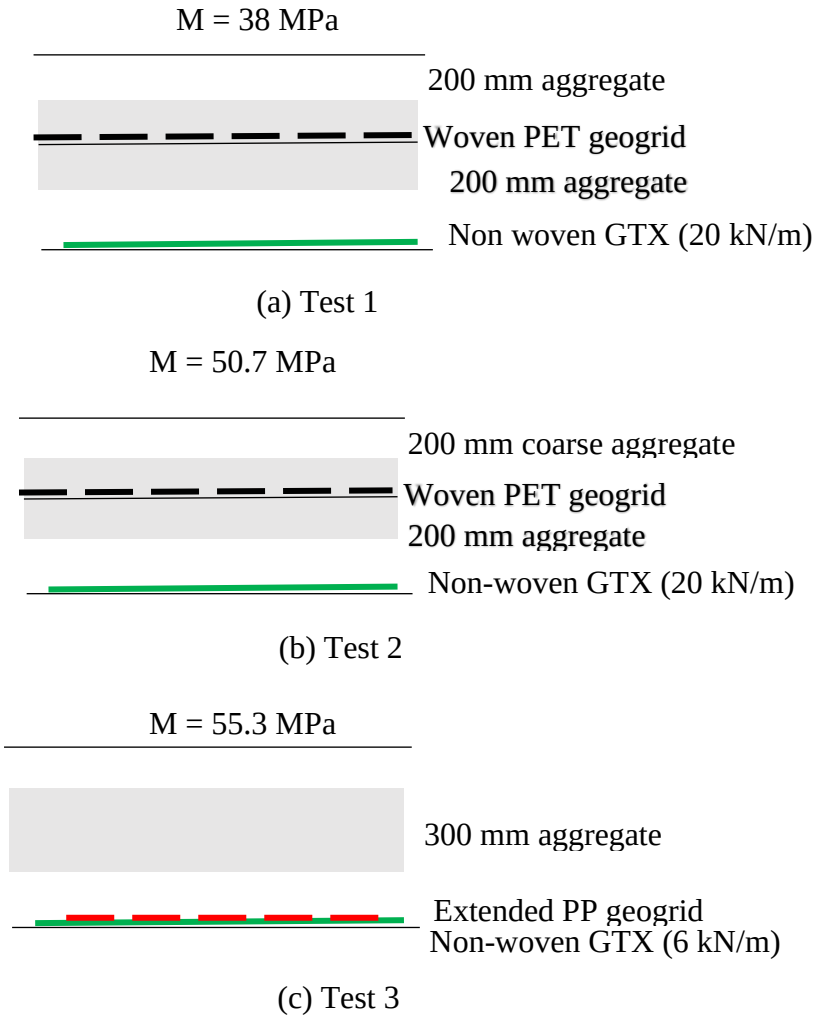

Fig. 1.7 Plate load tests in various field conditions (Swiss Federal Railway, 2000)

(a) Laying down of geosynthetics

(c) Laying down of geosynthetics

Fig. 1.8 Geosynthetics applications in railway embankment (Swiss Federal Railway, 2000)

1.5 Objectives of the study

The major emphasis of the study is towards estimating the improvement in bearing capacity of the foundations over flat ground and sloping ground, with the application of different geosynthetics. A number of experimental studies are available on reinforced foundation in sand using different geosynthetics. However, such studies on reinforced cohesive soil are still unexplored. Also, the loading used in the studies is limited to centric loading. In the present study, attempts have been made to understand the behavior of geosynthetics reinforced foundation in cohesive soil under centric and eccentric loading.

The experimental work has been conducted in two parts. In the first part the tests have been performed on small-scaled footing on cohesive soil. In the second part, the behavior of reinforced soil foundation over sloping ground has been studied. The objectives of the present study are as follows:

(1) To analyze the effect of various parameters like initial reinforcement depth (u), a number of reinforcement layers (N), an optimum depth of reinforcement (d), load eccentricity (e), Slope angle (β), the distance between the edge of the slope and the loading surface (D) mechanical properties of geosynthetics in the improvement of bearing capacity of cohesive soil.

(2) To understand the morphology of failure patterns of geosynthetics by conducting SEM analysis.

(3) To examine the strain distribution in soil reinforced bed by strain gauges.

(4) To develop the empirical model based on experimental results, which included the significant parameters necessary for computation of bearing capacity of reinforced foundations.

(5) To validate the results based on numerical analysis with experimental results for wide and easy application.

(6) To modify the analytical model available in a literature study for the estimation of bearing capacity of reinforced foundation soil and comparing the output of the analytical model with experimental results of present work.

1.6 Outline of the Thesis

The thesis comprises of eight chapters. C**hapter 1** introduces the various use of geosynthetics in many geotechnical applications. Then it describes that what is beneficial use of reinforcements in foundation soil. The objectives of the present work to achieve them are described. **Chapter 2** discusses the various studies conducted by different researchers, and the study includes experimental, numerical, and analytical work. **Chapter 3** presents the materials and methods adopted to achieve the desired objectives. **Chapter 4** describes a discussion of results obtained from the experimental studies on small scale model footing over flat ground, and the results obtained by the empirical study are also compared with earlier work available in the literature. **Chapter 5** describes the results of experimental work on small-scaled footing tests to observe the effect of slope geometry on the bearing capacity of reinforced soil foundation. **Chapter 6** discuss the validation of numerical results from experimental results and scale effect study. **Chapter 7** describes the model development based on empirical study. This chapter also presents the modification of the analytical model available in the literature for the calculation of the bearing capacity of square footing under different loading conditions. **Chapter 8** presents the conclusions and future scope. A brief program of the study is presented in Fig 1.8

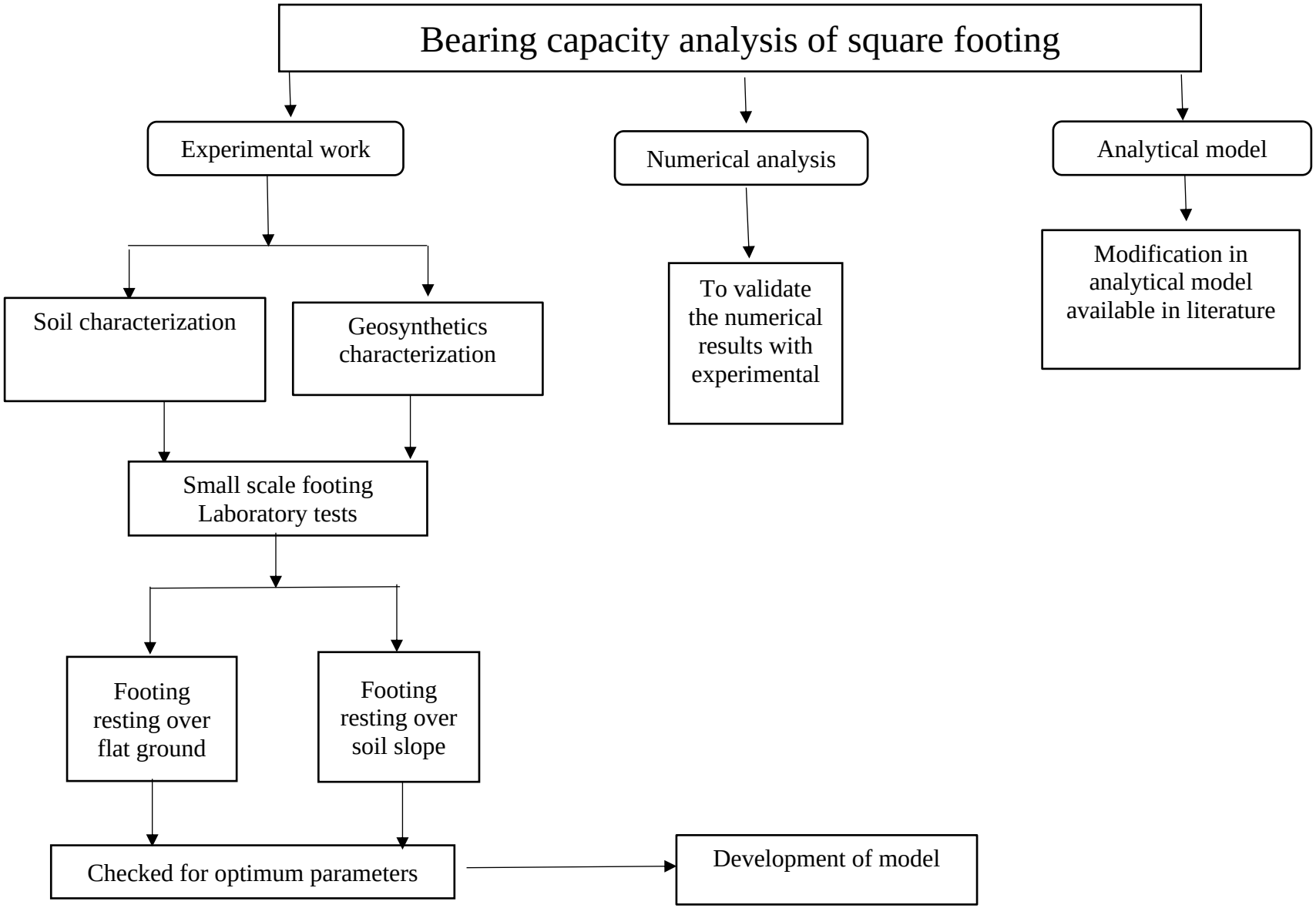

Fig. 1.8 Brief description of the study

REFERENCES

1. Binquet, J., and Lee, K.L. (1975b), "Bearing capacity analysis on reinforced earth slabs", *Journal of Geotechnical Engineering Division, ASCE*, Vol. 101, pp. 1257-1276.
2. HMBS Textiles (2016), "Pavement stabilization at Vaggampalle to Dhoronalat junction PKG-6 NH-565 Andhra Pradesh", *A case study,* Andhra Pradesh, India.
3. HMBS Textiles (2017), "Pavement stabilization at 5 km ahead from charama dist-kanker Chhattisgarh", *A case study,* Dhamtari, India.
4. Huang, C. C., and Tatsuoka, F. (1990), "Bearing capacity of reinforced horizontal sandy ground", *Geotextiles and Geomembranes*, Vol. 9, pp. 51-82.
5. IIT, Kharagpur (2013), "Thickness reduction using 3D Geogrid at NH-6, Dhankuni Kharagpur Section, Near Kolaghat", *A case study,* Kharagpur, India.
6. Madhav, R.M., (1988), "A new model for geosynthetic reinforced soil", *Computers and Geotechnics*" Vol. 6. pp. 277-290.
7. Shukla, S.K., and Chandra, S. (1994), "A generalized mechanical model for geosynthetic-reinforced foundation soil", *Geotextiles and Geomembranes,* Vol. 13, pp. 813-825.
8. Shukla, S.K. (2002), "Geosynthetics and their applications", *Thomas Telford Publishing.* London, ISBN 978-0-7277-3117-3 (Hardbound) and 978-0-7277-3783-0 (E-Book), doi: 10.1680/gata.31173.
9. Wayne, M. H., Han, J., and Akins, K. (1998), "The design of geosynthetic reinforced foundations", *Geosynthetics in foundation reinforcement and erosion control systems*, Vol. 10, pp. 1-18.
10. Mandal, J. N., and Sah, H. S. (1992), "Bearing capacity tests on geogrid-reinforced clay", *Geotextiles and Geomembranes,* Vol. 11, pp. 327-333.

11. Omar, M. T., Das, B. M., Yen, S. C., Puri, V. K., and Cook, E. E. (1993), "Ultimate bearing capacity of rectangular foundations on geogrid-reinforced sand", *Geotechnical Testing Journal*, Vol. 16, pp. 246-252.
12. Chen, Q., Abu-Farsakh, M., Sharma, R., and Zhang, X. (2007), "Laboratory investigation of behavior of foundations on geosynthetic-reinforced clayey soil", *Journal of the Transportation Research Board*, Vol. 2004, pp. 28-38.

CHAPTER 2

LITERATURE SURVEY

2.1 Introduction

Since the last three decades, different studies have been proposed for a possible solution to enhance the bearing capacity of foundation soil with the inclusion of different reinforcing materials. In the field of geosynthetics, many researchers have evaluated the benefits of reinforcements in the improvement of bearing capacity of soil foundation through improvement factors (*IF*), this improvement factor shows the quantum of benefits of reinforcement in terms of bearing capacity of foundation soil. Experimental and numerical studies from the literature show that the reinforcement inclusion in the soil significantly improves the bearing capacity of foundation. Many researchers studied the following parameters:

(1) First reinforcement depth (*u*),

(2) Adequate depth of reinforcement (*d*),

(3) Number of reinforcement layers (*N*),

(4) Width of reinforcement (*b*),

(5) Vertical spacing between two reinforcements (*h*),

(6) Type of soil and reinforcement,

(7) Slope angle (β),

(8) Slope edge distance (*D*).

2.2 Physical modeling

A first comprehensive study on the effect of reinforcement on the bearing capacity of the soil was put forward by Binquet and Lee, (1975b), wherein sand reinforced with aluminum foil strips overlain by strip footing showed substantial increase in ultimate bearing capacity of the reinforced soil, thus signifying the potential of reinforcements in the soil. Since then, the

profuse amount of research was carried out by researchers with the inclusion of different reinforcing materials to enhance the load-carrying capacity of foundation. The literature review on physical modeling has been studied in two different soils, i.e. sand and clay.

2.2.1. Reinforced sandy soil

The performance of geogrid and geotextile was analyzed by Guido et al., (1986) for evaluating its potential as reinforcement for enhancing the bearing capacity. The study proffered that there exists an optimum placement depth for the respective geosynthetics within the foundation beyond which placement is not advantageous.

The effect of geogrid reinforcement in the bearing capacity of foundation soil has been investigated by Yetimoglu et al., (1994). A series of model footing tests on rectangular footing over sand reinforced with geogrid has been conducted. All the experiments were performed using a tank made of steel with dimensions: 700 mm in length, 700 mm in width, and 1000 mm in height. A steel plate was considered as the rectangular model footing of size 127 mm × 101.5 mm (L × B) and 12.5mm in thickness. Sandy soil with a relative density equal to 72% was used in the study, while a Terragrid GS1000 uniaxial geogrid was used as a reinforcing material. For single reinforced sand, the results of the test indicate that the optimum value of top reinforcement depth was observed at 0.3 times the width of footing, while for two reinforcement layers, the optimum value of vertical spacing (*h/B*) was observed at 0.2. The results also show that an increment in *BCR* was observed as the number of reinforcement layers was increased up to $N = 4$. This value of optimum reinforcement layers was corresponding to a maximum depth of reinforcement of 1.5D or 1.5B. The test results showed that beyond this optimum value, the *BCR* value slightly decreases.

Das and Omar (1994) presented the experimental results of model footing tests on surface strip foundations reinforced with geogrid. Six different sizes of footing were used in the experiment having the widths $B = 50.8$, 76.2, 101.6, 127, 152.4, and 177.8 mm. The length of each footing

was considered as 304.8 mm. Fine round silica sand was having C_u = 1.53, and C_c = 1.10 was used. Soil bed was tested in a rectangular tank of size 1.96 m × 305 mm ×914 mm. The results obtained from the experiment showed that the *BCR* of the sand bed reinforced with geogrid reduces with an increase in the footing width. When the footing width is more than 13-14 cm, the *BCR* reaches practically a constant value.

Lee and Manjunath (2000) conducted a series of small-scale footing tests on unreinforced and reinforced soil slope under strip footing loading. The study aimed to examine the effect of geosynthetics on the bearing capacity of foundation over soil slope. Experimental results demonstrate that the development in the improvement of the ultimate bearing capacity of foundation significantly increases with the inclusion of geosynthetics placed at an appropriate location in the soil slope. The effective depth of reinforcement, which resulted in the highest *BCR*, was found to be 0.5B. They suggested that bearing capacity reduces as the slope angle increases and a reduction in edge distance. Their results also indicated that bearing capacity almost becomes insignificant when the footing is placed at an edge distance of five times the footing width.

Yoo (2001) prepared a physical model of footing resting over the reinforced earth slope. The parameters were varied, such as a number of reinforcement layers, reinforcement length, location to the topmost reinforcement layer, and vertical spacing between two reinforcements. The model was prepared in a steel box frame, with size 1.8m × 0.5 m and 1.2 m in height. The testing bed was constructed using fine sand, having a value of *C*u and *C*c = 1.61, 0.36, respectively. Two 2D geogrids of tensile strength 55 kN/m were used. He suggested that footing performance on the sloping ground improves when the footing is placed on the crest of the slope, thus the overall supporting power of footing resting over reinforced soil slope increases.

The results of model footing tests of strip footing over sand bed reinforced with multiple layers of geogrids were presented by Shin et al., (2001). The dimension of the steel tank are: Length = 100 cm, width = 17.6 cm and height = 60 cm. The model footing was made of wood and measured 172 mm (length, L) and 67mm (width, B). A poorly graded silica sand having C_u and C_c values of 1.51 and 1.1, respectively, was used in the test. A biaxial geogrid was used for soil reinforcement. Experimental results showed that the value of the effective depth of reinforcement was observed at *d/B* equal to 2.

The potential benefits of reinforcement, which were used in place of a sand layer constructed near a slope, was investigated by Sawwaf (2006). The study was carried out in the laboratory by conducting physical model tests on the footing. The model footing was used of width 75 mm, and geogrids were as reinforcing material. Parameters considered in the study are the footing location relative to the slope crest and depth of the replaced sand layer and. The results obtained from the experiment indicate that the geogrid inclusion in replaced soil enhances the footing performance in terms of allowable footing settlement.

Latha and Somwanshi, (2007) presented the results obtained from the experimental work of model footing tests on reinforced sand foundation bed. The results show the optimum value of spacing between two reinforcements is half the footing width, and effective depth of reinforcement is two times the footing width, and they suggested that the configuration of the reinforcement is more important than the tensile strength of the reinforcements.

A series of laboratory model footing tests on circular footing resting over the semi-infinite reinforced sandy bed was conducted by Basudhar et al. (2007). The study highlights the effect of a number of reinforcement layers, layout and configurations, and footing size on bearing capacity of the soil. Their observed results showed that a number of reinforecement layers increase equivalent sequent modulus (E_q) increases. As the size of the footing was increased, the value of the sequent modulus decreased.

Latha and Somwanshi (2009) conducted a systematic study on the influence of geosynthetics on the strength of the reinforced sand bed. The parameters that were used in the study are the layout and configuration of reinforcement, strength, and type of reinforcement. The sand bed was prepared with and without reinforcement in a tank of size 900 × 900 mm in the area and 600 mm in height. Geosynthetics like uniaxial geogrid, weak 2D geogrid, strong 2D geogrid, and a geonet were used in the study. A 25 mm thick rigid steel plate was used as a footing prototype and measured 150 mm^2 in area. All the reinforcements were provided as planer reinforcement, and the parameters were varied like variation of the width of geosynthetic, number of geosynthetic layers, geosynthetics depth from the base of the footing. On the basis of the obtained experimental results, they recommended the vertical spacing of reinforcement layers (h) is half of the footing width, and the influence depth of reinforcement (d) is two times the footing width (B).

The eccentricity effect on footing resting over reinforced soil was studied by Sawwaf, (2009). During the test, the effect of configurations of the geosynthetic with different lengths and layers were investigated. The results show that the performance of footing under eccentric loading was significantly improved by the placement of geogrid layers leading to an economical design of the footing. Tafreshi and Dawson (2010) discussed the study based on experimental work on laboratory footing tests resting over a planar reinforced sand bed. The tests were conducted on model strip footing. The parameters considered in the testing program included the quantity of the reinforcements and the width of reinforcement. The model footing tests were carried out in a test bed-loading frame consisting of a steel box, the data acquisition system, and the loading system. Following dimensions of the box was considered: 750 mm × 375 mm × 150 mm (L×B×H). A rigid plate was used as a model footing and measured, Length = 148 mm, width = 75 mm, and 20 mm in thickness. Uniform silica sand having a specific gravity of 2.68 and grain sizes between 0.85 and 2.18 mm was used in the test.

Based on the experimental work, they found that the improvement factor (*IF*) initially increases when *u/B* rises from 0 to 0.1; beyond this, the value of *IF* decreases with increase in reinforcement depth. Different sizes of reinforcements were used, which show that no significant improvement in bearing capacity is expected when reinforcement width increases, higher than 5.5B. They also suggested that with an increase in the number of planar reinforcement layers, the footing settlement decreases along with enhancement in supporting power of the foundation bed. The influence of the interference phenomenon on the load-carrying capacity of closely constructed footings over the reinforced soil was studied by Javdanian et al., (2012). They derived the model and correlation parameters for quantifying load carrying capacity for different interfering footings on reinforced sand. They concluded that the optimum value of first reinforcement depth *u/B,* and width of reinforcement *b/B* was achieved at 0.3, and 5 respectively.

Dash (2012) performed a series of model footing tests on the strip footing over reinforced soil. The aim of the study is to understand the effect of reinforcement on the load distribution mechanism of foundation soil. The parameters considered in the study are the development of strain in the reinforcement, pressure-settlement distribution, and the load dispersion in the reinforcement. The experiment was conducted in a steel tank of size 1200 mm in length, 333.2 mm in width, and 370.0 mm in height. A steel footing with the following dimensions: 33× 31 cm in area and 32.5 cm in thickness was used in the test. A uniformly graded river sand was used in the study. Based on the experimental work, they have concluded that the footing performance is affected by aperture size, stiffness, and tensile strength of reinforcement.

Various parameters like first reinforcement depth (*u*), the vertical spacing of reinforcements (*h*), tensile strength, geosynthetic type, the shape of footing, and depth of embedment (D_f), were considered by Farsakha et al. (2013). The results indicated that the layout of reinforcement had a significant effect on the behavior of footing over reinforced sand. Two or

greater than two layers of reinforcements, settlement of the footing can be minimized to about 20%. The study also showed that there is a better performance of reinforced sand with a composite of geotextile and geogrid than when sand is reinforced with geogrid or geotextile alone. Reinforcement also distributes the load more uniformly hence reducing stress concentration.

Farsakh et al., (2013) investigated the behavior of geosynthetic reinforced sand foundation by conducting experimental work on a model footing. The parameters considered in the study are first reinforcement depth, the vertical spacing between two geosynthetic sheets and number of reinforcement layers, stiffness, and type of reinforcement. Physical strain distribution in reinforcement was also studied. The overall study demonstrated that the reinforcement configuration and layout have a crucial role in the performance of reinforced soil foundation.

In the experimental work of laboratory footing tests, Mehrjardi et al. (2016) used sand with different gradations, specifically fine sand and coarse-grained sand, for their behavior with geogrids. The study proffered that the inclusion of the geogrid enhanced the strength of soil bed, and the bearing capacity of the foundation was found to similar or even higher to the foundation built on flat ground. Also, the study showed that the increase in the reinforcement length higher than 4B does not enhance the bearing capacity.

Tavangar and Shooshpasha (2016) performed a plate load test on two different square plates of area 27 cm^2 and 35 cm^2. The effect of the initial height of reinforcement from the base of the footing (*u/B)*, the spacing between two geotextiles (*h/B)*, and the number of geotextile layers(*N*) on the performance of footing in bearing capacity improvement. The study dealt with the effects of using nonwoven geotextiles in the improvement of *BCR* on the medium dense sand. Based on their research, they recommend the optimum value of *h/B* and *u/B* is 0.3 and 0.15 respectively. The main advantage of the nonwoven geotextile in soil reinforcement, is its high flexibility in comparison with other geosynthetics.

Roy and Deb (2017) studied the strain distribution along the geosynthetics. For this purpose, a series of model footing test was conducted on sandy soil overlain by soft clay with a geogrid at the interface. A total of eight number of strain gauges were attached with geogrid located at four different locations like below the center and edge of footing and the distance equivalent to the footing width (B) from the center of footing. Each location was having two strain gauges, one located at the top of geogrid while others at the bottom of geogrid. The mean of two values was considered as strain in reinforcement. The results demonstrated that the strain value was largest at just below the footing. The magnitude of the strain reduces as the distance from the center of footing increases and also increases as the settlement of footing increases.

2.2.2 Reinforced clay

A physical model of strip footing resting over reinforced clay was prepared by Sakti and Das (1987). The purpose of the experiment was to check the role of geosynthetics in the reinforcement of the clayey soil. A nonwoven polypropylene geotextile was used in the study. The model test box was used in the study with the following dimensions: 76.2 cm in length, 65.2 cm in width, and 61 cm in height. The model footing used for the laboratory tests was 76.2 mm wide, 228.6 mm long, and 9.5 mm thick. The plasticity index of the soil was 11 (%). Following general observations were made from the data:

(1) For a single layer of geotextile, the optimum value of *BCR* was observed when *u/B* lies between 0.35 to 0.4.

(2) For a given number of geotextile layers (*N*), the value of *BCR* reduces with increasing *d/B* value. However, when *d/B* = 1.0, the *BCR* was also approximately equal to 1.0. The study also showed that the geotextile reinforcements placed beyond the depth equal to *B* do not create an increase in the ultimate bearing capacity.

Samtani and Sonpal (1989) investigated the bearing capacity aspects of clay reinforced with metal strips. The foundation bed was prepared in a square box of 914.4 mm^2 in area 762 mm

in height. A cast-iron strip of 495.3 mm × 76.2 mm in plan area was fabricated as a strip footing. A black cotton soil (Plasticity index = 28.5%) having cohesion c_u = 159.4 kPa and ϕ_u = 16.5˚ has been used. The foundation bed was prepared by compacting the soil at optimum moisture content. The load was applied to footing by reaction frame with the help of a mechanical jack. Experimental results demonstrated that the footing performance over cohesive soil increases with the inclusion of strips in cohesive soil.

An experimental study on geogrid reinforced clay subgrades was conducted by Mandal and Sah (1992). For the study purpose, a physical model was prepared in a steel cubical tank of size 460 mm^3. A steel plate was chosen as a footing with dimensions: 100 mm square, and 48 mm thick. Clay subgrade was prepared with marine clay having liquid limit 72%, and plastic limit 41%. The results of the tests were presented in the form of pressure settlement curves. The results indicate that the *BCR* value significantly increases from 1.22 to 1.36, corresponding to *u/B* value from 0 to 0.175. They have also recommended that if *u/B* value is more than 0.175, *BCR* value significantly decreases. The highest percentage reduction in settlement (*PRS*) of geogrid reinforced compacted clay was observed about 45%, and it was found when geogrid was placed at a distance of 0.25 B from the bottom of the footing.

The behavior of bearing capacity of strip footing over-saturated reinforced clayey slope was analyzed by Shin and Das (1992). The experimental results show that the first layer of geogrid should be placed at a depth of 0.4 *B* below the footing base for the requirement of the maximum magnitude of bearing capacity ratio derived from reinforcement, and the maximum depth of reinforcement is about 1.72*B*, which contributed to bearing capacity improvement.

The performance of strip footing over reinforced slope was studied by Shin and Das (1996). For this purpose, a slope of angle 35˚-50˚was prepared in the laboratory, which was reinforced with 2D geogrid for all the experimental work. The location of the first reinforcement depth from the base of footing, adequate depth of reinforcement, and the vertical separation between

two reinforcement layers were varied. For preparing the slope model, a steel tank inside dimensions: 1.2m in length, 152.4mm in width, and 610 mm in depth was used. The footing was made of hardwood with size: width = 76.1mm, length = 152.4 mm, and thickness 38.1mm. A natural clay of 20% plasticity index was used in the slope preparation. The experimental results showed that the optimum value of *BCR* occurred when the first location of geogrid was at a depth of 0.4 B from the base of the footing where B is footing width. The maximum depth of reinforcement which contribute to the bearing capacity improvement is about 1.72 times the width of footing. After the contribution of Shin and Das (1996), in the study of clayey soil reinforcement, Chen et al. (2007) have started the research work towards cohesive soil reinforcement. They performed a number of laboratory tests to check the performance of footing by using geosynthetics in clay with low to medium plasticity. A model footing of size 152 mm × 152 mm was used as square footing. Three different geogrids, along with a geotextile were used as reinforcement in the study. The parameters were studied in the research: initial depth of reinforcement, the vertical separation between two conjugated layers, the number of reinforcement layers, and type of reinforcement. Test results revealed that the optimum value of the first reinforcement depth was found at $u/B = 0.33$. They also observed that as a number of reinforcement layers increases the bearing capacity of foundation increases and appeared to become almost insignificant after $N = 4$ and $N = 3$, which are situated at a depth of 1.33B and 1.00B for geogrids and geotextile-reinforced clay, respectively.

2.3 Numerical analysis

Sawwaf (2007) studied the benefit of providing geogrid on a replaced sand layer near the slope crest. FEM analysis on a model slope 2D plane strain conditions were carried out using a square footing of dimension 75mm × 75mm. The parameters considered in the study were replaced sand depth and footing location with respect to slope crest. The results demonstrate that the

placement of geogrid in replaced sand inhance the footing performance and reduces the footing settlement.

Sawwaf (2009) studied the nonlinear behavior of sand using the hardening soil model. The footing was treated as elastic beam elements with significant normal stiffness (EA) and flexural rigidity (EI). A refined mesh was applied then prescribed loading was adopted using the load control method. The boundary conditions were selected in such a way so that the vertical wall was constrained horizontally and free vertically while the bottom part of the model was fully fixed. The parameters like size, number, and eccentricity of layers have been investigated. Test results reveal that the inclusion of four geogrid layers increases the ultimate bearing capacity from 105.6 kN/m^2 to 174.2 kN/m^2.

Javdanian et al., (2012) worked on finite element analysis on reinforced soil foundation in Plaxis 2D software. In the FEM study, A Mohr-Coulomb model and plane strain condition with 15-node triangular elements were used. Geometrical parameters depend on the depth of the first layer of layer (*u*), reinforcement width (*b*), the vertical spacing of reinforcement (*h*), and total reinforcement depth (*d*). The results demonstrated that the optimum value of *u/B* value was approximately equal to 0.3, while for *b/B* and *h/B* value, the optimum value was found at 5 and 0.3, respectively.

K.S. Gill et al. (2012) conducted a series of 2D finite element analysis on geogrid reinforced footing soil slope system to validate the experimental results of the small-scale model test and to understand the soil deformation behavior. In the study, it was observed that the number of reinforcement layers increases the load-carrying capacity of the footing slope as the number of geogrid layers increases from 1 to 4 the load-carrying capacity increases from 120% to 180%. Further increment in geogrid layers in soil mass only 25% improvement in ultimate bearing capacity was observed.

Javdanian (2017) conducted numerical analysis on reinforced soil slope using the Finite-Difference program FLAC. The study concluded that geosynthetic reinforcement could be the most cost-effective method for stabilizing the soil and thus can increase the bearing capacity of footings over steep soil slopes. Also, the optimum width of the reinforcement was obtained at 5B, and any further increase width of reinforcement did not significantly impact the bearing capacity. Cicek et. al., (2019) studied the performance of the first reinforcement layer depth (u) for sand subbase of pavement or construction by conducting the laboratory plate load tests. In the study, a single type of geotextile and two different geogrids was used as a reinforcement. A sandy soil having C_u and C_c equal to 2.5 and 1, respectively, was used in the study. The footing tests were conducted in a steel tank of dimensions 100 cm in length, 50 cm in width, and 100 cm in depth. A strip steel plate of width (B) = 10 cm and thickness (t) = 25 mm was used as a model footing. Laser sensors displacement gauges were installed over the footing in order to measure the footing settlement. Bearing ratios were estimated by measuring the bearing pressure. The laboratory footing results unreinforced, and geotextile reinforced soil was validated with FEM results. The results demonstrated the influence of the different types of reinforcements for different locations of first reinforcement depth. They also observed that the bearing ratio and pressure settlement behavior changed with the first reinforcement depth.

2.4 Analytical approach

Based on laboratory footing tests on soil reinforced foundation, Binquet and Lee (1975a, 1975b) proposed three modes of failures of the reinforced soil bed. The following are the proposed failure modes.

(1) Failure of the foundation soil above the topmost reinforcement layer see Fig. 2.1(a) This failure generally occurs when the first reinforcement depth is more than 2/3rd times foundation width.

(2) Pull out of reinforcement layer: This failure is likely to happen when the first reinforcement depth is less than the 2/3rd times the foundation width and also less than three number of reinforcement layers see Fig. 2.1(b).

(3) Rupture of geosynthetic: This type of failure mostly occurs when reinforcement layers are more than 3 and depth of first reinforcement located at u < 0.67 B. In this type of failure, reinforcement fails just beneath the edge of the footing or center of footing see Fig. 2.1(c).

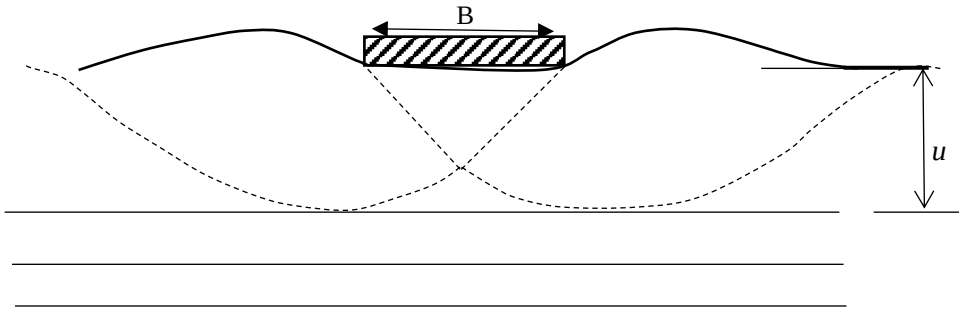

(a) Bearing capacity failure above the reinforcement

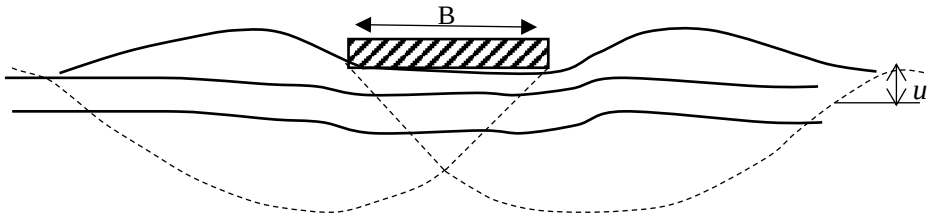

(b) N < 3 and u/B < 2/3

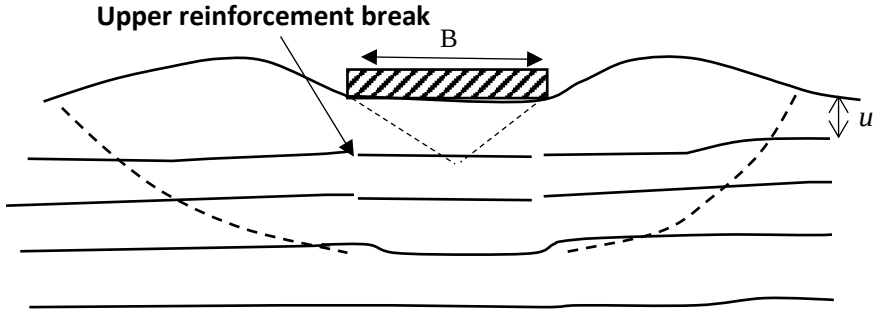

(c) N > 3 and u/B < 2/3

Fig. 2.1 Possible modes of failure (Binquet and Lee 1975 a)

From the above two modes of failure, i.e., mode b, and mode c, it is cleared that the improvement in bearing capacity of soil foundation depends on the strength of reinforcing ties. It is also cleared that the footing performance also depends on the lowest strength of any layer of ties. The design criteria for mode b and mode c is expressed as

$$T_D < \frac{R_y}{FS_y}, \frac{T_f}{FS_f} \quad (2.1)$$

T_D = Force developed in tie force, R_y = tie-breaking strength of the tie layer, T_f = frictional pull out resistance of the tie layer, FS = factor of safety for the condition showed by respective subscript.

Since the failure in reinforcement occurs due to tension force, Binquet and Lee (1975 b) proposed a relation to find the tension force developed in reinforcement at any depth *z*

$$T_{D,}(z, N) = \frac{1}{N}\left[J\left(\frac{z}{B}\right)B - I\left(\frac{z}{B}\right)h\right]q_0\left[\frac{q}{qo} - 1\right] \quad (2.2)$$

Where *z* is the reinforcement depth; N is the number of reinforcement layers; *B* is the width of footing; *h* is vertical spacing between two reinforcements; q is the bearing capacity of reinforced soil; q_0 is the bearing capacity of unreinforced soil; *I* and *J* are the forces in reinforcements.

$$J\left(\frac{z}{B}\right) = \frac{\int_0^{X0} \sigma_z \left(\frac{z}{B}\right) dx}{q\ B} \quad (2.3)$$

$$I\left(\frac{z}{B}\right) = \frac{\tau_{max}\left(\frac{z}{B}\right)}{q\ B} \quad (2.4)$$

Wayne et al., (1998) studied the failure criteria of Binquet and Lee, (1975b), and based on their study, they have introduced four more failure modes of reinforced foundation soil which are following: (a) First mode of failure is very similar with a failure mode proposed by (Binquet and Lee, 1975b) discussed earlier. They suggested that if the first reinforcement depth is more than the specific value, then the first reinforcement layer acts a rigid boundary, and soil mass

failure takes place above the first reinforcement layer. The second mode of failure see Fig. 2.2 (b) is a type of failure of reinforced soil foundation that occurs when the vertical distance between two reinforcements is very large. The failure can be mitigated by keeping the vertical spacing within a specific range. Third bearing capacity failure shown in Fig. 2.2 (c) is likely to occur when the reinforcement length and its tensile strength is not enough to mobilize the friction at the soil interface. Punching can be expected along the reinforced zone and the whole reinforced soil mass act as a deep footing, which is equivalent to a depth of embedded footing. It is noticed that this kind of failure is similar to the failure mode proposed by Huang and Tatsuoka, (1990). The fourth mode of failure is shown in Fig. 2.2 (d) The failure is likely to occur when the reinforcement has sufficient first reinforcement depth (*u*), the proper vertical spacing between two reinforcement layers (*h*), and the maximum reinforcement depth (*d*) is located in the influenced zone. According to Wayne et al. (1998) reinforcement soil mass acts as a two-layer soil system in which weaker soil overlying by stronger granular fill. Based on bearing capacity failure mechanism, they proposed some formulae for the determination of bearing capacity of rectangular footing on reinforced soil without inculcating the confinement effect of the reinforcement in improving the ultimate bearing capacity of the soil. The solutions assumed a two-layered soil structure approach for the estimation of the ultimate bearing capacity of the reinforced soil foundation. Thus it is considered that the punching shear failure will take place in the zone of reinforcement followed by general shear failure in the unreinforced region. A solution of bearing capacity of reinforced soil foundation is given by Wayne et al., (1997)

$$q_{u(R)} = q_{(u)b} + \frac{2c_a d}{B}\left(1 + \frac{B}{L}\right) + \gamma_t d^2\left[1 + \frac{2D_f}{d}\right] \times \frac{K_S tan\emptyset_t}{B}\left(1 + \frac{B}{L}\right) + \frac{2}{B}\left(1 + \frac{B}{L}\right)\sum_{i=1}^{N} T_{ui} - \gamma_t d \quad (2.6)$$

Where, $q_{(u)b}$ is the bearing capacity of soil beneath the reinforcement; D_f = embedment depth of the footing; K_s = coefficient of punching shear; γ_t = the unit weight of the soil in the reinforced zone; $\emptyset_t$ = frictional angle of the soil; N = number of layer of reinforcement; L and

B are the length and the width of the footing respectively; *d* is the total reinforcement depth T_{ui} is the tensile force mobilized in the i^{th} reinforcement layer.

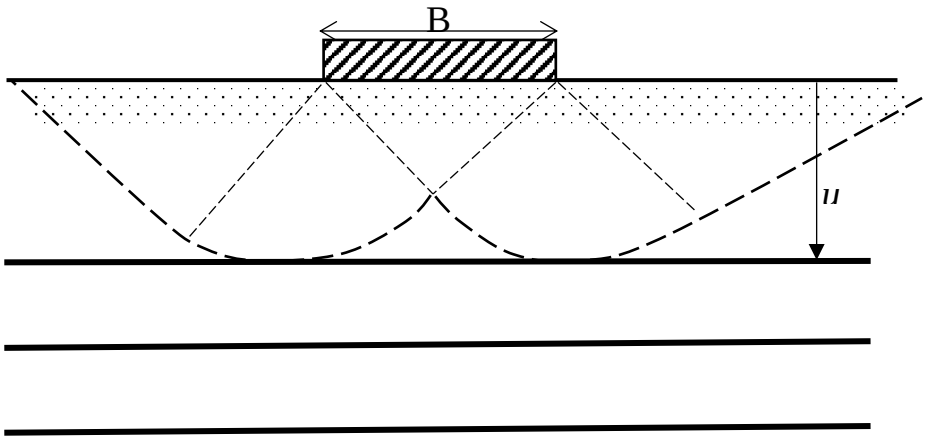

(a) Failure within top reinforcement layer

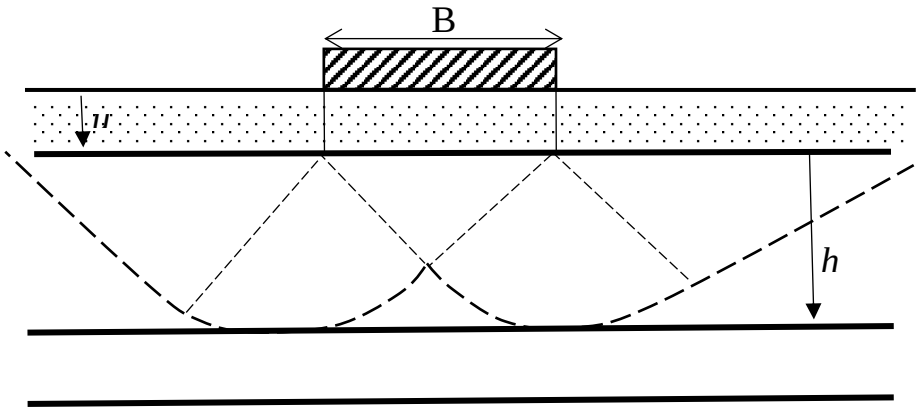

(b) Failure in between reinforcement layers

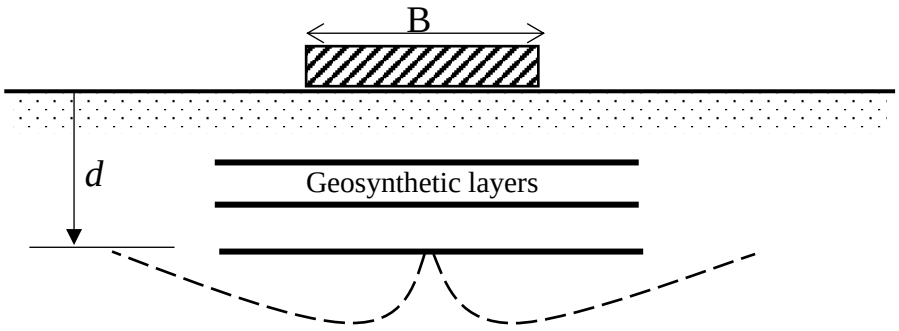

(c) Failure along the reinforcement

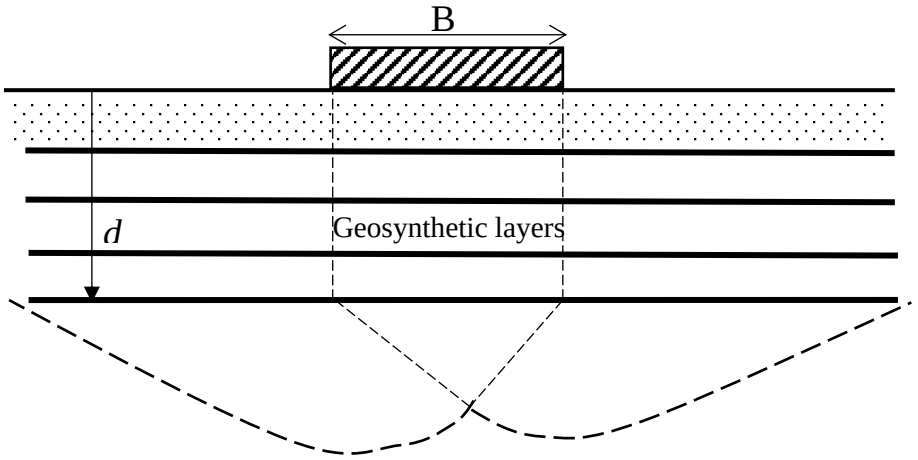

(d) Failure below the reinforcement zone

Fig. 2.2 Failure Mechanism proposed by (Wayne et al., 1998)

An analytical solution for estimation of the ultimate bearing capacity of reinforced soil foundation for silty clay and sand was presented by Sharma et al., (2009). They assumed the same failure mechanism as considered by Wayne et al. (1998). They developed some bearing capacity formulae which incorporate the contribution of reinforcements in the improvement of bearing capacity. The proposed equation for square footing is shown below.

For Sharma et al., (2009):

$$q_{u(R)} = q_{(u)b} + \frac{4c_a d}{B} + 2\gamma_t d^2 \left[1 + \frac{2D_f}{d}\right] \times \frac{K_S tan\emptyset_t}{B} + \frac{4}{B}\sum_{i=1}^{N} T_i tan\delta - \gamma_t d \qquad (2.7)$$

Chen and Abu-Farsakh (2015) proposed a model for determining the ultimate bearing capacity of soil foundations, wherein the effect of confinement and membrane where taken into account. The bearing capacity of the soil in the present study has been compared with the available in the literature, although most of them are for strip footing computations.

Chen and Abu-Farsakh, (2015):

$$q_{u(R)} = q_{(u)b} + \frac{2c_a d}{B} + \gamma_t d^2 \left[1 + \frac{2D_f}{d}\right] \times \frac{K_S tan\emptyset_t}{B} + \frac{2}{B}\sum_{i=1}^{N} T_i cos\alpha_i \, tan\delta + \frac{2}{B}\sum_{i=1}^{N} T_i sin\alpha_i - \gamma_t d \qquad (2.8)$$

Sahu et al. (2016) presented ultimate bearing capacity results obtained from laboratory model footing tests under eccentric loading supported by multi layer of reinforcement. They proposed

a mode of failure of reinforced soil foundation under eccentric loading shown in Fig. 2.3. The failure mechanism was considered as a wide slab and deep foundation effect in which at ultimate load, the soil failure takes place below the last reinforcement layer. Based on the laboratory footing tests, a reduction factor was developed, which is used to calculate the bearing capacity of foundation soil under eccentric loading. The proposed reduction factor is given as, and the reduction factor is

$$\mathrm{RK} = a\left(\frac{d}{B}\right)^{b}\left(\frac{e}{B}\right)^{c} \tag{2.9}$$

Where a, b and c are the dependent on length ratio (*B/L*).

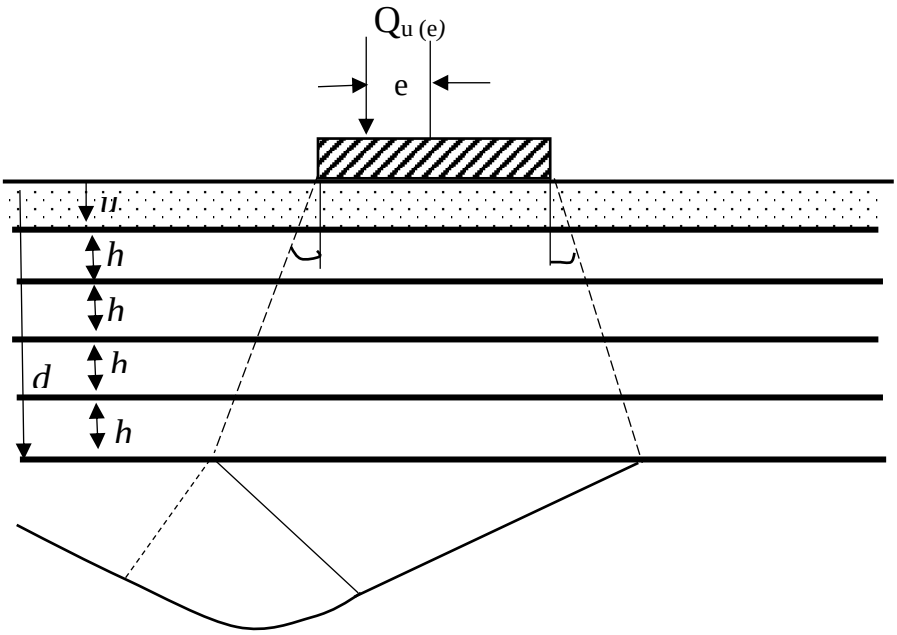

Fig. 2.3 Failure mechanism eccentrically loaded footing

Table. 2.1 Summary of literature study of optimum parameters for reinforcement placements in sand

	Binquet and Lee (1975a)	**Guido et al., (1986)**	**Latha and Somwanshi, (2007)**	**Patra et al., (2005)**	**Farsakha, et al., (2013)**		**Tavangar and Shooshpasha (2016)**	**Javdanian et al., (2012)**	**Das and Omar, (1994)**	**Yetimoglu, et al., (2000)**	**Sawwaf (2009)**
Type of footing	Strip	Square	Square	Strip	Square		Square	Square	Rectangular	Rectangular	Rectangular
Type of reinforcement	Aluminum foil	Geogrid	Geogrid	Geogrid	Geogrid	Geotextile	Geogrid	Geotextile	Geogrid	Geogrid	Geogrid
u/B	0.3	-	0.67	0.35	0.33		0.2	0.3	0.33	0.3	
h/B	-	-	0.67	0.25	0.167		0.3	0.3	0.33	0.3	
d/B	2	1	2	5	1.25		-	-	2	1.5	-
b/B	-	2	5.93	-	-		4	5	-	4.5	1
e/B	-	-	-	-	-		-	-	-	-	0.15

Table. 2.2 Summary of literature study of optimum parameters for reinforcement placements in clay

	Shin et al. (1993)	**Sakti and Das (1987)**	**Mandal and Sah (1992)**	**Chen et. al., (2007)**		**Kolay et. al., (2013)**
Type of footing	Strip	Strip	Square	Square		Rectangular
Type of reinforcement	Geogrid	Geotextile	Geogrid	Geogrid	Geotextile	Geogrid
u/B	0.4	0.35	0.175	0.33		0.667
d/B	1.8	0.35-0.4	-	1.33, 1		-
h/B		-	-	0.167		-
b/B	5	1	-	5		-

2.5 Summary and conclusions

Based on the literature review, the following findings have been reported.

(1) The experimental studies conducted by many researchers like Binquet and Lee (1975a), Sakti and Das (1987), Chen (2007), Das and Omar (1994), Yetimoglu, et al. (2000), Javdanian (2012), Farsakha, et al.(2013) reveals that the first reinforcement depth (*u*) should be located at nearly about 0.33 B below the footing. Some researchers like Tavangar and Shooshpasha (2016), Javdanian (2012), Das and Omar (1994), Yetimoglu, et al. (2000) have also concluded that the vertical spacing between two reinforcement layers (*h*) should be kept at 0.33 B. However, there are some uncertainties have been observed in the effective depth of reinforcement (*d*). Yetimoglu, et al (2000) observed the *d/B* value is 1.5, whereas Binquet and Lee (1975a), Das and Omar (1994), and Latha and Somwanshi, (2007) have found the value of *d/B* is equal to 2. Researchers like Guido et al. (1986), Chen (2007) and Farsakha, et al., (2013) have found the *d/B* value equal to 1, and 1.3, and 1.25, respectively.

(2) The numerical studies conducted by Sawwaf (2007), Sawwaf (2009), Javdanian et al., (2012), and K.S. Gill et al. (2013) showed that the finite element analysis on laboratory model footing could be successfully used to validate the numerical results with experimental work.

(3) A review of past studies indicated that the many works had been done on laboratory small scaled footing tests on the reinforced sand bed e.g. Rowe 1985; Huang and Tatsuoka 1990; Boushehrian 2003; Farsakh 2013; Tafreshi and Dawson 2010. In contrast, some similar works have been done on reinforced clayey soils e.g. Madhav and Poorooshasb 1998; Chen 2007. Since the studies on laboratory model tests related to reinforced cohesive soils are rather limited, the present study shows more laboratory, numerical and analytical model footing tests results on reinforced cohesive soil to observe the expected outcomes.

REFERENCES

1. Abu-Farsakh, M., Chen, Q., and Sharma, R. (2013). "An experimental evaluation of the behavior of footings on geosynthetic-reinforced sand". *Soils and Foundations*, Vol. 53, pp.335-348.
2. Basudhar, P.K., Saha, S., Deb, K., (2007). "Circular footings resting on geotextile-reinforced sand bed," *Geotextiles and Geomembranes* Vol. 25 (6), pp. 377–384 2007.
3. Binquet, J., and Lee, K.L., (1975a). "Bearing capacity tests on reinforced earth slabs." *Journal of Geotechnical Engineering Division*, ASCE, Vol. 101, pp. 1241-1255.
4. Binquet, J., and Lee, K.L., (1975b). "Bearing capacity analysis on reinforced earth slabs." *Journal of Geotechnical Engineering Division, ASCE*, Vol. 101, pp. 1257-1276.
5. Binquet, J., and Lee, K.L., (1975b). "Bearing capacity analysis on reinforced earth slabs*." Journal of Geotechnical Engineering Division, ASCE*, Vol. 101, pp. 1257-1276.
6. Boushehrian, J.H., Hataf, N. (2003) "241 Experimental and numerical investigation of the bearing capacity of model circular and ring footings on reinforced sand," *Geotextiles and Geomembranes*, Vol. 21 (4), pp. 241–256.
7. Chen, Q., Farsakh, A., M., Sharma, R., and Zhang, X. (2007). "Laboratory investigation of behavior of foundations on geosynthetic-reinforced clayey soil". *Journal of the Transportation Research Board*, Vol. 2004, pp. 28-38.
8. Chen, Q., and Abu-Farsakh, M. (2015). "Ultimate bearing capacity analysis of strip footings on reinforced soil foundation". *Soils and Foundations*, Vol. 55, pp. 74-85.
9. Cicek, E., Guler, E., and Yetimoglu, T. (2015). "Effect of reinforcement length for different geosynthetic reinforcements on strip footing on sand soil". *Soils and Foundations,* Vol. 55, pp. 661-677.

10. Das, B.M., and Omar, M., (1994) “The effects of foundation width on model tests for the bearing capacity of sand with geogrid reinforcement” *Geotechnical and Geological Engineering*, Vol. 12, pp. 133-141.
11. Dash and Shivadas, (2012). “Performance Improvement of Railway Ballast Using Geocells”. *Indian Geotechnical Journal*. Vol. 42, pp. 186-193.
12. E. Ciceka, E. Gulerb and T. Yetimoglua, "Effects of reinforcement length for different geosynthetic reinforcements on strip footing on sand soil," *Soil and Foundations*, Vol. 55, pp. 661-677, 2015.
13. El Sawwaf, M. (2007). “Behavior of strip footing on geogrid-reinforced sand over a soft clay slope. *Geotextiles and Geomembranes* Vol. 25, pp. 50-60. doi.org/10.1016/j .geotexmem.2006.06.001.
14. Gill, K.S., Choudhary, A.K., Jha, J.N., and Shukla, S.K (2012). “Experimental and numerical studies of loaded stripfooting resting on reinforced fly ash slope” *Geosynthetics International*, Vol. 20, pp. 13-25.
15. Guido, V. A., Chang, D. K., and Sweeney, M. A. (1986). Comparison of geogrid and geotextile reinforced earth slabs. *Canadian Geotechnical Journal*, Vol. 23, pp. 435-440.
16. Huang, C. C., and Tatsuoka, F. (1990). “Bearing capacity of reinforced horizontal sandy ground”. *Geotextiles and Geomembranes*, Vol. 9, pp. 51-82.
17. Javdanian, H., Haddad, A., and Mehrzad, A., (2012). "Experimental and Numerical Investigation of the Bearing Capacity of adjacent footings on reinforced soil," *Electronic Journal of Geotechnical Engineering*, Vol.17, pp. 2597-2617, 2012.70
18. Javdanian, H. (2012). “Interference effect on bearing capacity of shallow foundations on geosynthetic-reinforced sand”. *5th Asian Regional Conference on Geosynthetics: Geosynthetics for Sustainable Adaptation to Climate Change*, Vol. 8.

19. Javdanian, H. (2017). "On the behaviour of shallow foundations constructed on reinforced soil slope a numerical analysis". *International Journal Geotechnical Engineering*, Vol.14, pp. 188-195.
20. Kolay, P.K., Kumar, S, and Tiwari, D., (2013). “Improvement of Bearing Capacity of Shallow Foundation on Geogrid Reinforced Silty Clay and Sand” *Journal of Construction Engineering*, Vol. 2013, pp.1-10.
21. Lee, K.M. and Manjunath, V.R., (2000). "Experimental and numerical studies of geosynthetic-reinforced sand slopes loaded with a footing". *Canadian Geotechnical Journal*, Vol. 37, pp. 828-842.
22. M. Latha and A. Somwanshi, (2007). "Bearing Capacity of square footings on Geosynthetic reinforced sand," *Geotextile and Geomembranes*, Vol.27, pp. 281-294, 2009.
23. Mandal, J. N., and Sah, H. S. (1992). “Bearing capacity tests on geogrid-reinforced clay”. *Geotextiles and Geomembranes*, Vol. 11, pp. 327-333.
24. P. Kolay, S. Kumar and D. Tiwari, "Improvement of bearing capacity of shallow foundation on Geogrid reinforced silty clay and sand," *Journal of Construction Engineering*, pp. 1-11, 2013.
25. Patra, C.R., Das, B.M., Atalar, C., (2005) “Bearing capacity of embedded strip foundation on geogrid-reinforced sand,” *Geotextiles and Geomembranes*, Vol. 23 (5), pp. 454–462, 2005.
26. Sakti, J. P., and Das, B. M. (1987). “Model tests for strip foundation on clay reinforced with geotextile layers”. *Transportation Research Record*, Vol. 1153. pp. 40-45
27. Samtani, N., Sonpal, R., “Laboratory tests of strip footing on reinforced cohesive soil,” *Journal of Geotechnical Engineering, ASCE* 15 (9), pp. 1326-1330, 1989.

28. Sawwaf, M. (2006). “Experimental and numerical study of eccentrically loaded strip footings resting on reinforced sand”. *Geotextiles and Geomembranes,* Vol. 25. pp. 50-60.

29. Sawwaf, M. (2009). “Experimental and numerical study of eccentrically loaded strip footings resting on reinforced sand.” *Journal of Geotechnical and Geo-environmental Engineering,* Vol. 135, pp. 1509-1518.

30. Sharma, R., Chen, Q., Abu-Farsakh, M., and Yoon, S. (2009). “Analytical modeling of geogrid reinforced soil foundation”. *Geotextiles and Geomembranes,* Vol. 27, pp. 63-72.

31. Sahu, R., Patra, C.R., Das, B.M., and Sivakugan, N., (2016) “Bearing capacity of shallow strip foundation on geogrid-reinforced sand subjected to inclined load” *Journal International Journal of Geotechnical Engineering,* Vol. 10, pp. 183-189.

32. Saha Roy, S., and Deb, K. (2017). “Bearing capacity of rectangular footings on multilayer geosynthetic-reinforced granular fill over soft soil”. *International Journal of Geomechanics*, Vol. 17(9), 04017069.

33. Shin, E. C., Das, B. M., Puri, V. K., Yen, S. C., and Cook, E. E. (1993). “Bearing capacity of strip foundation on geogrid-reinforced clay”. *Geotechnical Testing Journal*, pp. 16(4), Vol. 534-541.

34. Shin, E.C., Das, B.M., Lee, E.S., and Atalar, C., (2002). “Bearing capacity of strip foundation on geogrid-reinforced sand.” *Geotechnical and Geological Engineering*, Vol. 20, pp. 169-180.

35. Skempton, A.W., 1951. “The bearing capacity of clay”. *Proceedings, Building Research Congress,* Vol. 1, pp. 180-189.

36. Tafreshi, S. M., and Dawson, A. R. (2010). "Comparison of bearing capacity of a strip footing on sand with geocell and with planar forms of geotextile reinforcement". *Geotextiles and Geomembranes,* Vol.28, pp.72-84.

37. Tavangar and Shooshpasha (2016). "Experimental and Numerical Study of Bearing Capacity and Effect of Specimen Size on Uniform Sand with Medium Density, Reinforced with Nonwoven Geotextile". Vol.41, pp. 4127-4137.

38. Wayne, M. H., Han, J., and Akins, K. (1998). "The design of geosynthetic reinforced foundations". *Geosynthetics in Foundation Reinforcement and Erosion Control Systems*, Vol. 10, pp. 1-18.

39. Yetimoglu, T., Wu, J.T.H., Saglamer, A., (1994). "Bearing capacity of rectangular footings on geogrid reinforced sand." *Journal of Geotechnical Engineering Division, ASCE*, Vol. 120 (12), 2083–2089.

40. Yoo, C., 2001. Laboratory investigation of bearing capacity behavior of strip footing on geogrid-reinforced sand slope. *Geotextile and Geomembranes,* Vol. 19, pp. 279-298.

CHAPTER 3

EXPERIMENTAL INVESTIGATION

3.1 Introduction

The major emphasis of experimental investigation in the research is to study the effect of various reinforcements in the development of bearing capacity and reduction in settlement of square footing being constructed over cohesive soil. The experimental testing program work has been divided into two parts. The first part of the experimental program deals with the model footing on square footing over flat ground, whereas the second part describes the details of the testing program of square footing resting over soil bed with different angle slope.

3.2 Materials used

3.2.1 Soil

For the present study, A silty clay soil sample has been amassed from Gwalior, Madhya Pradesh, India. The latitude and longitude coordinates of the location are 26.2183 N, 78.1828 E shown in Fig.3.1. The top layer of the soil has been withdrawn with the help of a shovel up to a depth of 0.5 m before gathering the soil sample. The collected sample was procured in the laboratory. Initially, the soil was oven dried for 24 hours, and then it was used for experimental work. The soil sample used in the experiment is shown in Fig. 3.2.and the geotechnical properties of the soil are presented in Table 3.1. On a representative sample of soil, laboratory tests were carried out to determine specific gravity, Atterberg limits, optimum moisture content. Maximum dry unit weight, and shear characteristics as per relevant BIS standard. The grain size distribution curve is presented in Fig. 3.3.

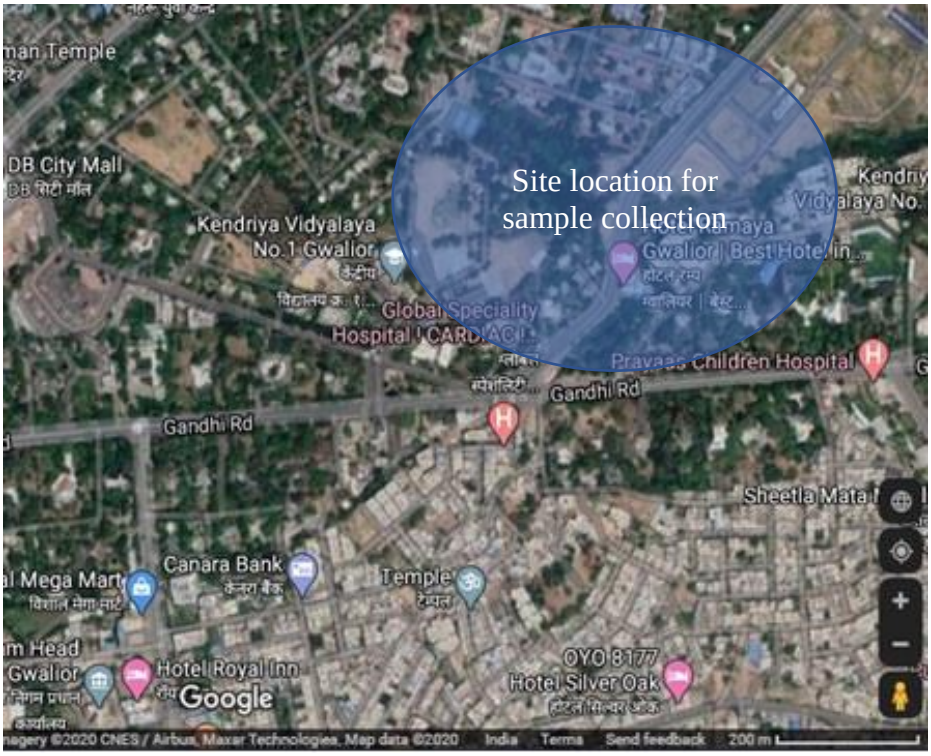

Fig. 3.1 Location of soil sample collection

Fig. 3.2 Soil sample used for experimental work

Table 3.1 Geotechnical properties of the soil

Properties	**Values**	**Protocols/Standards**
Specific Gravity	2.67	IS 2720 (PartIII)
Liquid limit (%)	34.0	IS 2720 (PartV)
Plastic limit (%)	21.0	IS 2720 (PartV)
Plasticity index (%)	13	IS 2720 (PartV)
Maximum dry Unit Weight (kN/m^3)	17.6	IS 2720(Part VII)
Optimum Moisture Content (%)	15	IS 2720(Part VII)
Cohesion (kN/m^2)	16	IS2720(PartXI)
Angle of Friction	22˚	IS2720(PartXI)

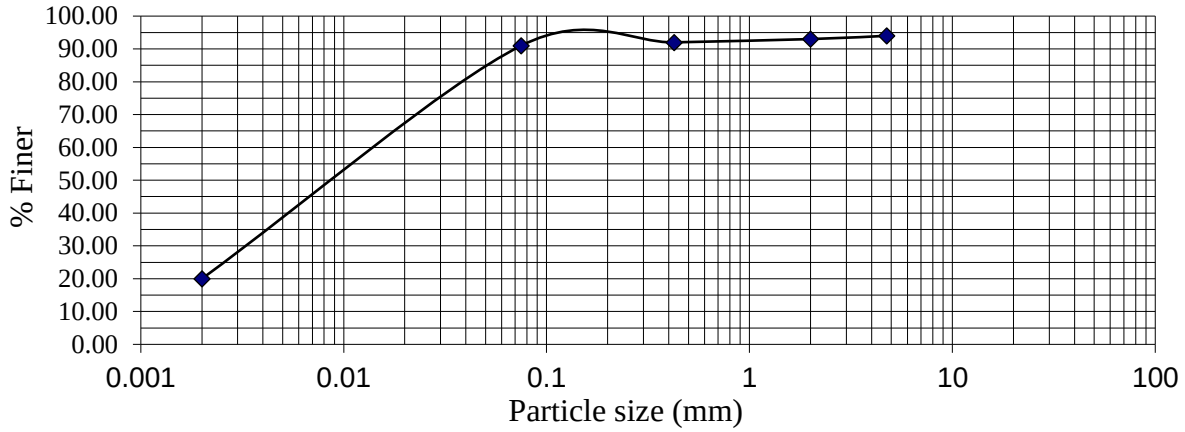

Fig. 3.3 Grain size distribution curve of soil

3.2.2 Geosynthetics

A single type 3D geogrid and glasgrid with different physical and mechanical properties, like aperture size, tensile strength, and tensile modulus were used along with a high tenacity woven geotextile. Geosynthetics samples are shown in Fig. 3.4 (a-c). In the present study, 3D geogrid, glasgrid, and geotextile have been represented as GGR1, GGR2, and GTX, respectively. The properties of the geosynthetics were obtained from the supplier (H.M.B.S. Textiles Pvt. Limited, Delhi) in both the directions, i.e., the traverse direction (across the roll) and the machine direction (longitudinal to the roll). The various properties of the geosynthetics are elaborated in Table 3.2. A unique extrusion technique is used for manufacturing the 3D geogrid

in which a perforated sheet is formed, and the final prepared sheet is shaped in 3D. The process makes a structure like a concaved shaped rib, thereby trapping the soil particles within the aperture, thus mobilizing the friction between the soil and geogrid interface by restricting the relative movement of soil particles and hence inhibit the further displacement. Glasgrid is composed of high tensile strength, continuous glasfibrs, elastomeric polymer, and embedded between two spun bond polyester textiles. The aperture size of glasgrid is smaller than the geogrid. Geotextile is a woven type and made of polypropylene. The geosynthetics were received from the supplier in the form of a roll, with the cross-machine direction being parallel to the roll and the machine direction being perpendicular to roll.

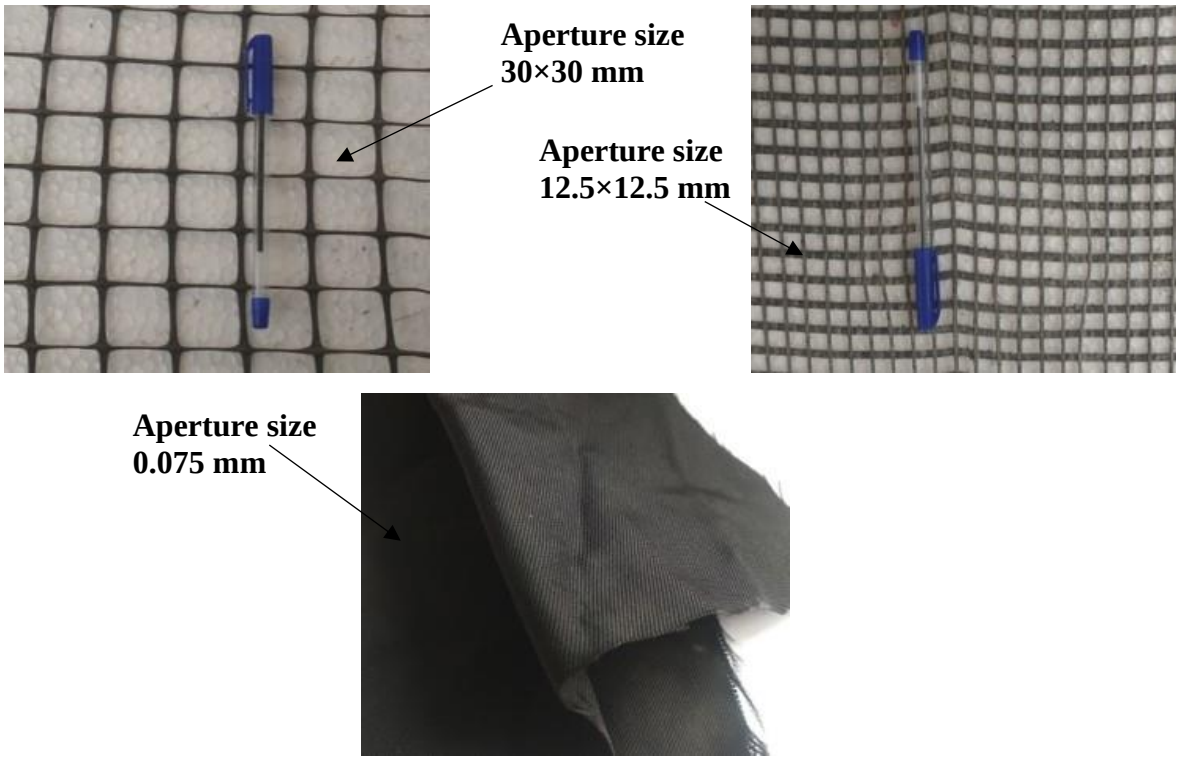

Fig. 3.4 Reinforcements used in foundation soil (a) 3D geogrid (b) Glasgrid (c) Geotextile

Geosynthetics were obtained in the form of rolls and hence were first prepared to be utilized effectively during the tests. For this purpose, four heavy concrete blocks were placed at the corners of the geosynthetics after tests had to be commenced to ensure uniformity of placement throughout.

Table 3.2 Properties of geosynthetics as per MTC

Geosynthetic	Property	Data	Unit	Test Method
3D Geogrid	Type of Polymer	Polypropylene	-	-
	Type of mesh	Quadrangular apertures	-	-
	Structure	Bi-Oriented Geogrid	-	-
	Opening size	30 × 30 (MD × CMD)	mm	
	Stiffness at 0.5% Strain	550 × 350(MD × CMD)	kN/m	ISO-10319
Glass geogrid	Material	Fiberglas	-	-
	Opening size	12.5 × 12.5 (MD × CMD)	mm	-
	Secant Stiffness EA @ 1% Strain	4.6 × 4.6 (MD × CMD)	kN/m	ASTM D4595 EN-ISO 10319:2008
	Tensile Strength	115 × 115 (MD × CMD)	kN/m	ASTM D4595
Geotextile	Tensile Strength	435 × 334 (MD × CMD)	kN/m	IS 1969
	Opening Size	0.075	mm	ASTM D4751
	Weight of fabric	200	g/m^2	ASTM D5261
	Elongation at break	30 × 28 (MD × CMD)	(%)	IS 1969

MD: *Machine direction* ***CMD:*** *Cross machine direction*

3.3 Physical modeling of reinforced foundation over a flat surface

Physical modeling of the square footing over reinforced soil bed has been done in the following steps:

3.3.1 Dimensioning of the test model

A reduced laboratory-scale testing setup was adopted for the study. The testing tank was designed as a rigid structure, with its length, width, and height being 950 mm, 450 mm, and 600 mm, respectively, encompassing the reinforced soil and model footing. A steel plate was used as a model square footing size of 75 mm × 75 mm and 20 mm in thickness. The footing size was chosen based on the model tank's dimension. The size of the testing tank was chosen from the literature study. The footing dimension was selected in such a way that its length,

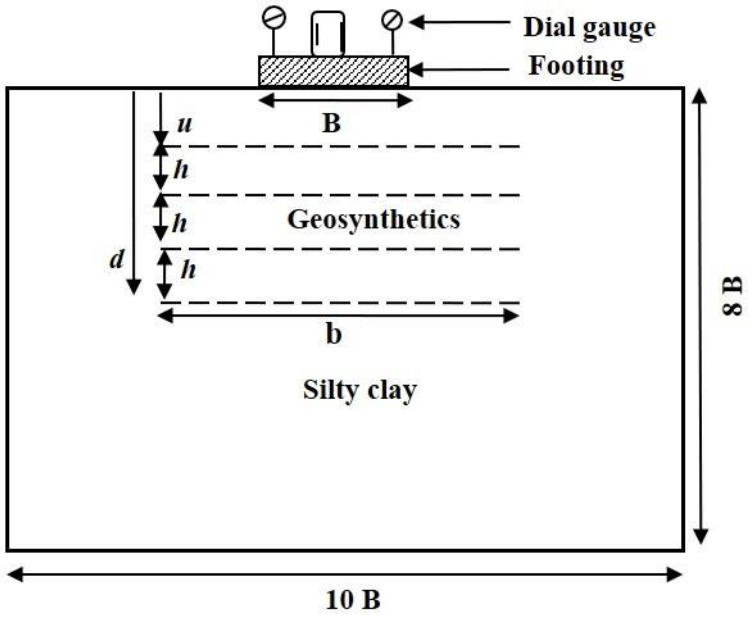

Fig. 3.5 Geometry of foundation bed

width, and height are less than 10B, 6B, and 8B, respectively, so that the boundary effect can be neglected. Fig. 3.5 shows the schematic of the aforementioned model prototype.

3.3.2 Preparation of test model

The testbed was prepared by compacting the soil to such conditions, so as it achieves the maximum dry unit weight. The soil was initially air-dried and pulverized and then passed through a 4.75 mm sieve to achieve suitable soil gradation, similar to those found in typical field conditions. Predetermined moisture content was mixed to the soil sample to attain the desired soil properties. The wet soil sample was placed in airtight conditions for two weeks to achieve moisture equilibrium. After curing the specimen for unreinforced soil, the soil was compacted in three different lifts for each test, to maintain uniform moisture throughout the testing tank. For each layer, the required amount of soil to filled was predetermined by using the volume of tank for each lift and the maximum dry unit weight of the soil, i.e. 17.6 kN/m^3. For example, for one lift of the soil sample, total volume was covered = 0.064 m^3, and the total quantity of soil was required to fill one lift = 115.085 kg. Fig. 3.6 (a) shows the first lift of soil in the tank. However, in the case of reinforced soil bed, the thickness of each layer was decided

according to reinforcement configurations. Fig. 3.6 (b) shows the placement of the horizontal reinforcement layer in soil bed. Each lift was compacted uniformly with the help of a light compaction rammer. Throughout the tests, the height of the fall of the rammer, the number of blows to be given, and the amount of soil to be added were determined to maintain uniformity of the soil sample. A random soil sample was collected during certain tests to check the uniformity of moisture content in the soil samples throughout the test tank. Uniformity of compaction was ensured throughout.

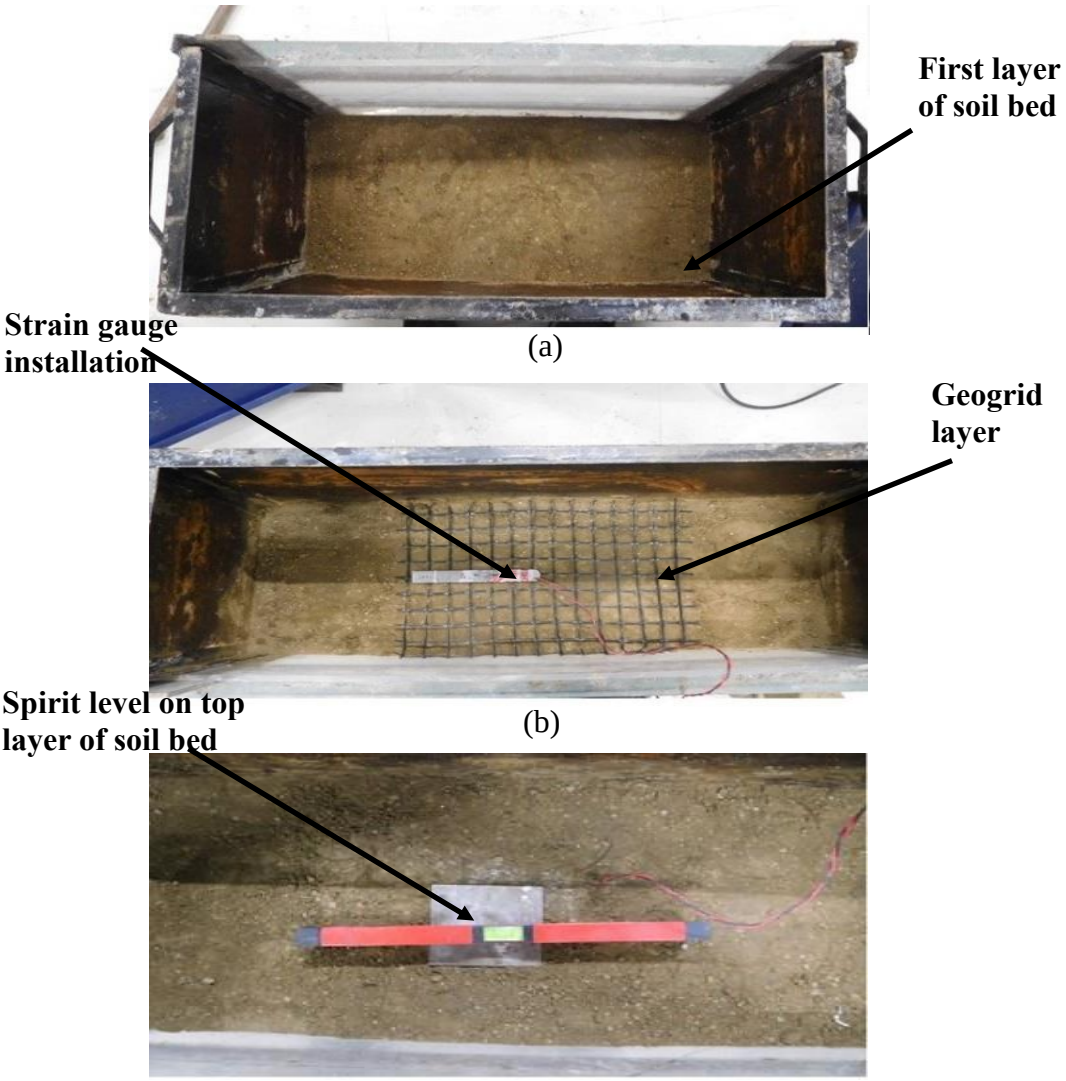

Fig. 3.6 (a) First lift of the compacted soil (b) Placement of geosynthetics layer in soil bed (c) Final top layer of the reinforced clay bed

3.3.3 Experimental program

The model footing tests were conducted in a loading frame assembly with a capacity of 100 kN with the application of reinforcements at different positions in the foundation bed. The purpose of the study was to find out optimum positions for placement of reinforcements in the structure to obtain maximum possible benefit from the reinforcements. The tests were carried out for all the reinforcement materials, i.e., GGR1 (geogrid), GGR2 (glasgrid), GTX (geotextile). Values of *u, d, h, N* were varied in each of the cases to obtain points of maxima. Where u = initial depth of reinforcement, d = influence depth of reinforcement, h = vertical spacing between the two reinforcements. The tests for u/B were carried out by carrying out the test at u/B = 0.17, 0.34, 0.51, 0.68 and 0.85. Similarly, the values of h/B were varied from h/B = 0.08, 0.16, 0.24, 0.32, and 0.5 by fixing the top layer at the optimum depth of top layer. The effect of number of reinforcement layers was estimated by fixing the top layer at maxima and varying the number of reinforcements until the effect of the reinforcement becomes diminished or becomes considerably insignificant for any further extensions in a number of reinforcement layers. Tests for eccentricity were conducted for GGR1, at e/B ratios of 0.04, 0.08, 0.12 and 0.16. Table 3.3 shows the experimental program of reinforced foundation soil over flat ground. The selections of the parameters in the present study are based on the literature study.

3.3.4 Testing Procedure

The physical model was set up to conduct the small-scale tests on reinforced soil foundation. The tank was designed as a rigid structure, the side and back portion of the tank consisted of steel sheets of uniform thickness which were fixed directly to the channel. The front part of the tank consisted of an acrylic sheet of 20 mm thickness for visual observation of footing settlement at various load applications. The acrylic sheet tank was protected by the use of angles across the cross-section of the acrylic to prevent the buckling of the sheet with respect to the steel tank.

Table 3.3 Experimental Program for geosynthetic reinforced foundation soil over flat ground

Type of Reinforcement	***u/B***	***N***	***h/B***	***b/B***	***e/B***	**No. of test**	**Remarks**
Unreinforced soil	-	-	-	-	0	3	To estimate the improvements due to reinforcement
GGR1	0.17, 0.34,0.51,0.68,0.85	1	-	-	0	5	To find out the optimum *u/B* value
	Optimum value of *u/B*	1,2,3,4,5	Optimum value of *u/B*	5	0	5	To check the optimum number of reinforcement layers
	Optimum value of *u/B*	1,2,3,4,5	Optimum value of *u/B*	4,5,6	0	15	To check the optimum value of width of geogrid layers.
	Optimum value of *u/B*	2	0.08, 0.16, 0.24, 0.32, 0.4	5	0	5	To check the optimum value of vertical spacing between two layers of geogrids
	Optimum value of *u/B*	1,2,3,4	Optimum value of *u/B*	5	0.4,0.8, 0.12, 0.16	15	To check the effect of eccentricity
GGR2	0.17, 0.34,0.51,0.68,0.85	1	-	-	0	5	To find out the optimum *u/B* value
	Optimum value of *u/B*	1,2,3,4,5	Optimum value of *u/B*	5	0	5	To check the optimum number of glasgrid layers
	Optimum value of *u/B*	2	0.08, 0.16, 0.24, 0.32, 0.4	5	0	5	To check the optimum value of vertical spacing between two layers of glagrid
GTX	0.17, 0.34,0.51,0.68,0.85	1	-	-	0	5	To find out the optimum *u/B* value
	Optimum value of *u/B*	1,2,3,4,5	Optimum value of *u/B*	5	0	5	To check the optimum number of geotextile layers
	Optimum value of *u/B*	1,2,3,4,5	Optimum value of *u/B*	4,5,6	0	15	To check the optimum values of geotextile width
	Optimum value of *u/B*	2	0.08, 0.16, 0.24, 0.32, 0.4	5	0	5	To check the optimum value of vertical spacing between two layers of geotextile

The tank was polished as far as possible to avoid the deleterious effects of friction on the test results. Petroleum jelly was applied on the inside and the outside of the tank. The loading system consisted of a platen attached to the crosshead of the frame. The load frame was made of four rigid and heavy steel columns of 100 mm diameter attached to a steel column pedestal resting on the surface. A suitable load cell of 25 KN capacity was placed between the loading platen and the foundation model to measure the amount of load generated. Two dial gauges with an accuracy of 0.01mm were used at points diametrically opposite to the footing. The average of the both the readings was considered as s settlement. The testing method was adopted according to ASTM D 1196-93. A sitting load was applied initially over the footing to fix the footing over the soil base, so as to obtain planar strain conditions. Certain tests were repeated to ascertain the authenticity of the results obtained. The average of the two obtained values was reported in the literature.

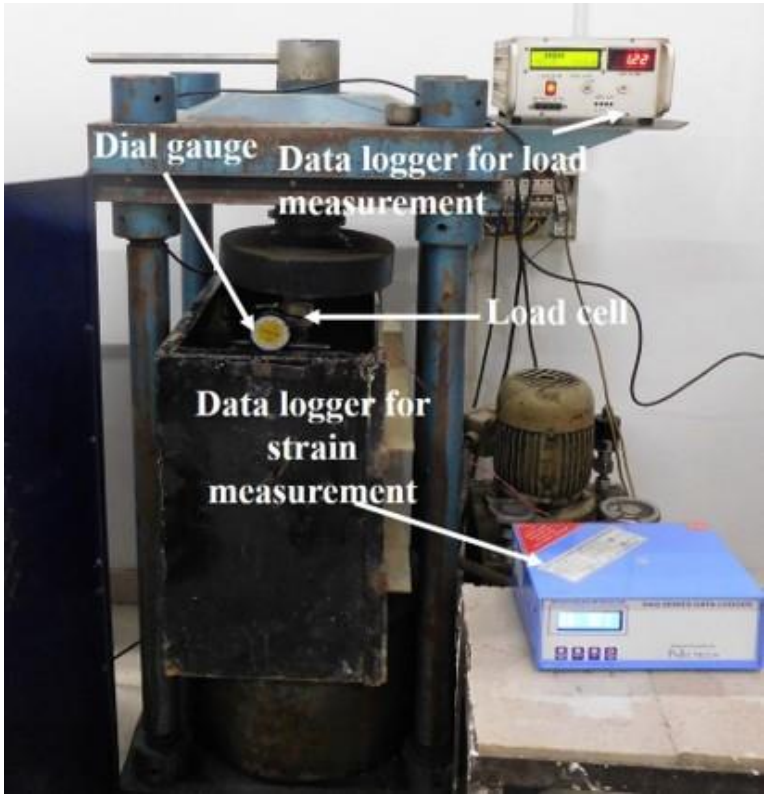

Fig. 3.7 Complete testing setup

3.3.5 Strain Measurement

The physical measurement of strain developed in the reinforcement was also analyzed using strain gauges (SG). SGs were installed in the reinforcement layers located at the optimum depth of the initial reinforcement and maximum depth of reinforcement. The process of strain computation in geosynthetic reinforced model tests is a highly tedious task due to factors such as extensibility of the gauges, opening sizes of the geogrids used, and discontinuity in load transfer (Rajesh and Viswanadham, 2012). This complex process of SG installation warranted skillful handling of the operations, such as application of the gauges on the geosynthetic and choosing the right adhesive for pasting the SGs. For this study, strain gauges with a gauge length of 0.8 mm, gauge factor of 2.2, and a resistance of 350 Ω were used. The surface area of geogrid was not uniform, hence some portion of the geogrid sample of 2 cm as leveled by finishing at the point of bonding.

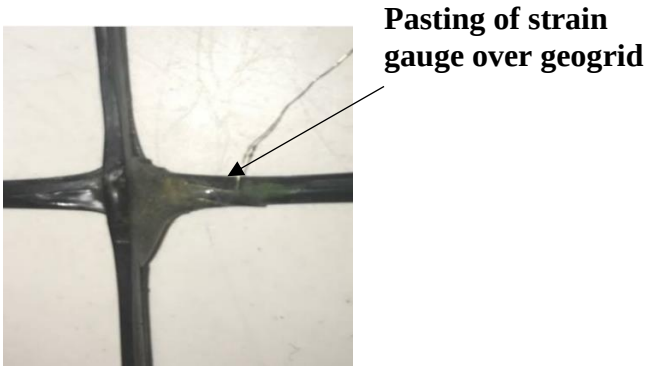

Fig. 3.8 Strain gauge attachment on geogrid

Before bonding the SGs, the surface was cleaned using ethanol. SGs were bonded on geosynthetic by using an epoxy adhesive Araldite. A very thin layer of the adhesive, approximately less than (200 μm) was applied on the cleaned surface. SGs were connected with those wires which were connected with the channels. The output of the physical strain was logged on 16 channel data loggers. The layout of the strain gauges is shown in Fig. 3.9.

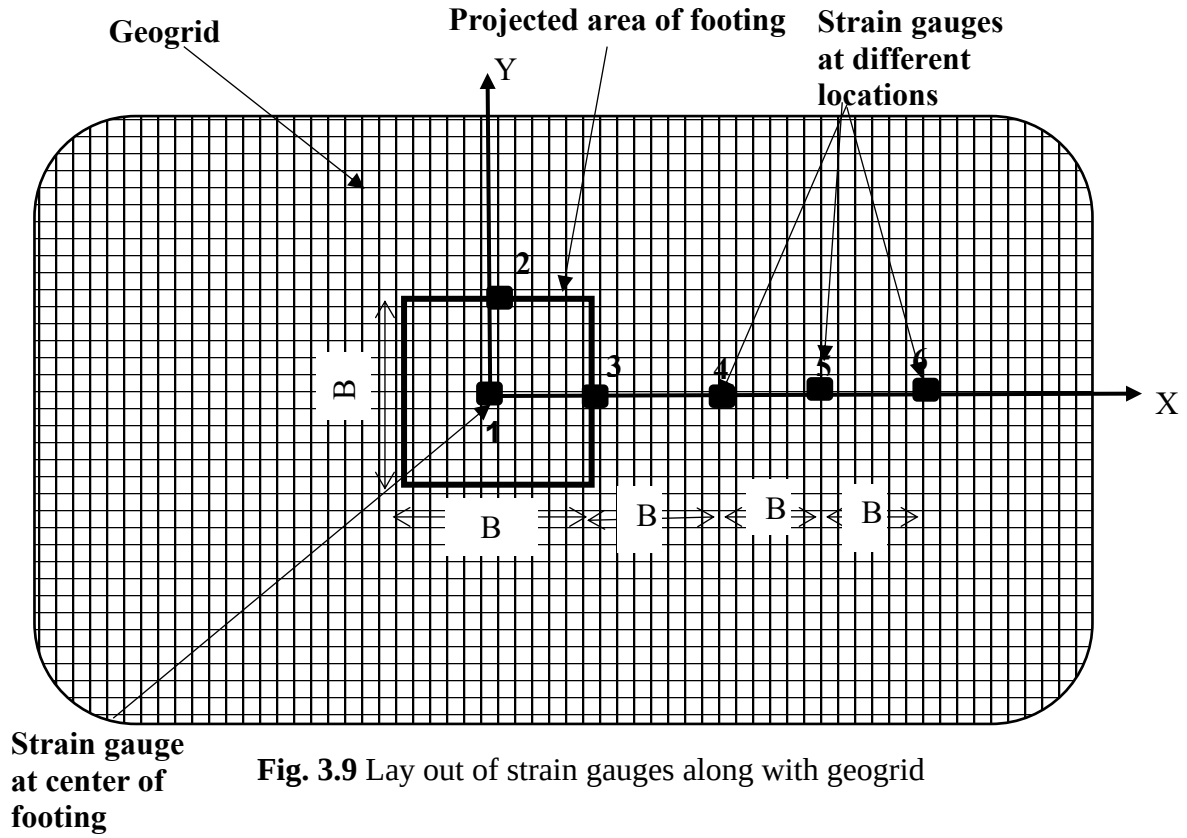

Fig. 3.9 Lay out of strain gauges along with geogrid

3.4 Physical modeling of square footing resting over a slope

Physical modeling of the square footing over a cohesive slope has been done in the following steps.

3.4.1 Dimensioning of the test model

A reduced laboratory-scale testing setup was adopted for the study after considering the possible changes in the results due to the boundary effect. The dimensions of the testing tank were chosen same as in case of footing resting over the flat surface, which are follows: length = 950×450 ×600 mm (L×B×H). A square footing of dimension 75mm × 75mm was chosen as the model footing, and the dimensioning of the tank was done in accordance with the footing width, so as to avert the boundary effect and hence dimensions of 10B, 6B and 8B were chosen as the length, width and height of the tank respectively, where B is the model footing width, i.e. 75 mm. The geometry of the reinforced soil slope is shown in Figure 3.10.

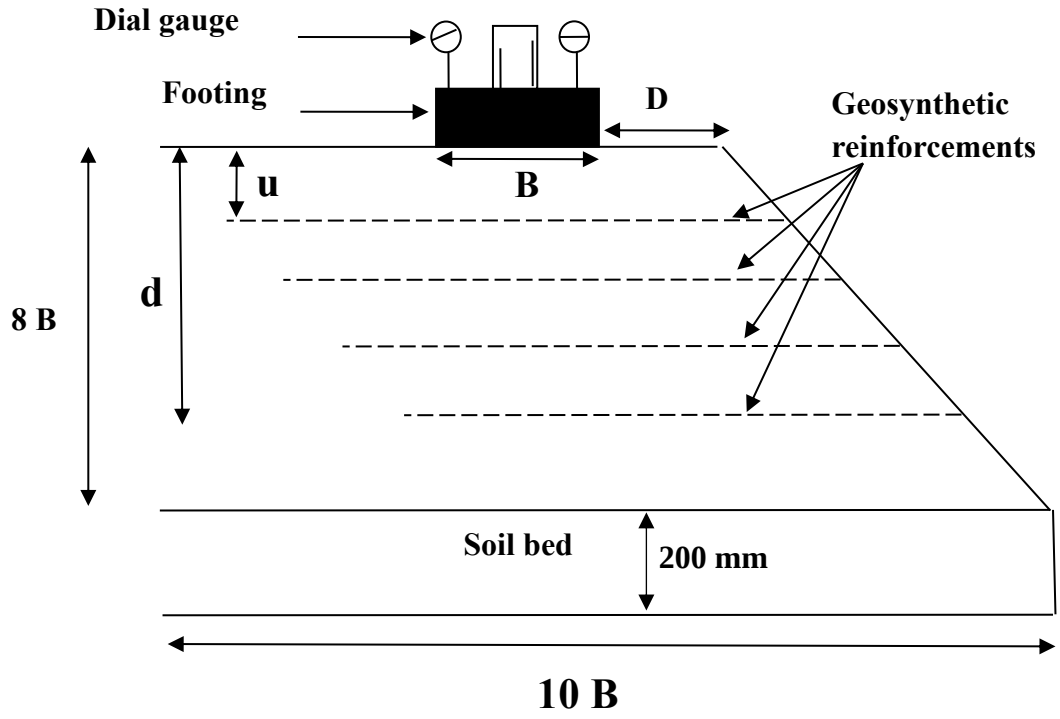

Fig. 3.10 Geometry of soil slope

3.4.2 Soil slope preparation

The tests were conducted in a glass tank of dimension 950 mm × 450 mm × 600 mm. Prior to the commencement of the tests, the soil was pulverized by the addition of water to the soil sample, equivalent to the optimum moisture content of the soil. The slope foundation was compacted in two lifts for each test, each containing soil to fill up the tank up to 100 mm. For each layer, the quantities of soil to be filled were predetermined by using the volume of each lift and multiplying it with the Maximum dry unit weight of the soil, i.e. 17.6 KN/m^3. Each lift was compacted uniformly with the help of a light compaction rammer with a base diameter of 16.2 cm. Throughout the tests, the height of the fall of the rammer, the number of blows to be given and the amount of soil to be added were determined to maintain uniformity of the soil sample. The random soil sample was collected during the course of certain tests to check the uniformity of the soil samples throughout the test tank. The slope was prepared in three lifts in case of unreinforced soil, while for reinforced soil slope, the thickness of each lifts was

dependent on the reinforcement layers. Cubical blocks of soil were prepared for each lift and the excess amount of soil was cut off with the help of a sharp shovel to form a smooth slope. After the creation of the slope structure, a spirit level was used to ascertain the alignment of the slope edge. Fig. 3.9 (a) shows the construction of the second lift of the soil slope. Fig. 3.11 (a) and (b) show the front view and side view of the prepared slope, respectively.

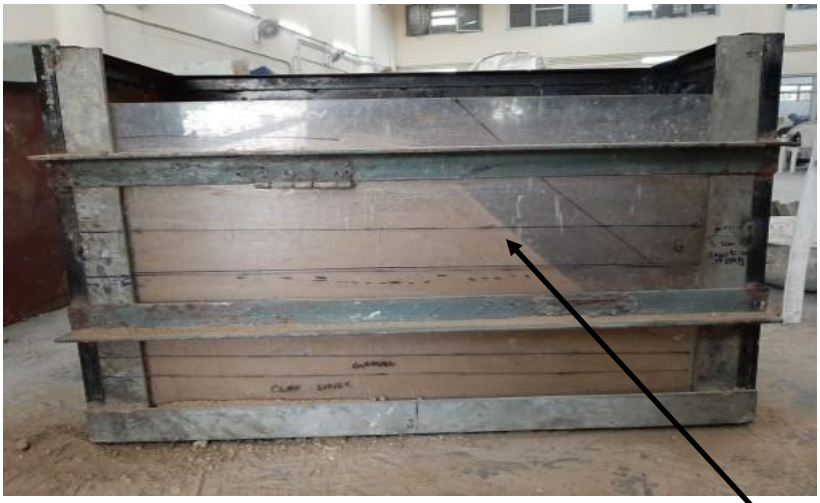

(a)

(b)

Fig. 3.11 Slope preparation (a) Staged construction of the slope (b) Final prepared slope (c) Side view of prepared slope

3.4.3 Experimental Program

The tests were carried out in a compression frame shown in Fig. 3.5 with an overall capacity of 100 kN with the application of reinforcements at different positions in the slope. The purpose of the work is to find out the effect of slope angle, angle edge, and the optimum positions for placement of reinforcements in the structure to obtain maximum possible benefit from the reinforcements by mobilizing the greatest tensile force within the reinforcement. To ascertain the optimums for geosynthetic placements, values of *u*, *d*, *h*, *N* were varied for each of the geosynthetic. The tests for *u/B* were carried out by varying the corresponding values at 0.2, 0.4, 0.6, 0.8, and 1 respectively. Similarly, the values of *h/B* were varied from *h/B* = 0.2, 0.4, 06, 0.8, respectively, by fixing the top layer at the maxima of the top layer spacing obtained from the previous tests. The effect of the number of reinforcement layers was estimated by fixing the top layer at maxima and varying the number of reinforcements until the effect of the reinforcement becomes diminished or becomes considerably insignificant for any further extensions in the number of reinforcement layers. The tests for all the parameters, viz. via. *u/B*, *d/B*, *N* and *h/B* were carried out by fixing the slope angles at 45^{o} and at an edge distance of 1. The tests were carried out for all the reinforcement materials, i.e. GGR1, GGR2 and GTX. The effect of slope geometry was analyzed for GGR1, by varying the slope angles by 35°, 40° and 45° respectively and fixing the value of *D/B* =1. Similarly, the effect of edge distance on bearing capacity of soil as ascertained by fixing the value of slope angle at 45^{o} and varying the values of *D/B* at 0, 1, and 2.

Table 3.4 Testing Program for geosynthetic reinforced foundation soil over slope

Type of Reinforcement	***u/B***	***N***	***h/B***	**β**	***D***	**No. of test**	**Remarks**
Unreinforced soil	-	-	-	45˚	1	3	To estimate the improvements due to reinforcement
GGR1	0.2, 0.4, 0.6, 0.8, 1	1	-	45˚	1	5	To find out the optimum *u/B* value
	Optimum value of *u/B*	5	Optimum value of *u/B*	45˚	1	5	To check the optimum values of number of geogrid layers.
	Optimum value of *u/B*	2	0.2,0.4,0.6,0.8,1	45˚	1	5	To check the optimum value of vertical spacing between two layers of geogrids
	Optimum value of *u/B*	5	Optimum value of *u/B*	35˚, 40˚, 45˚	1	15	To check the effect of slope angle on the bearing capacity of reinforced soil slope
	Optimum value of *u/B*	-	Optimum value of *u/B*	45˚	1, 2, 3		To check the effect of edge distance
GGR2	0.2, 0.4, 0.6, 0.8, 1	1	-	45˚	1	5	To find out the optimum *u/B* value
	Optimum value of *u/B*	5	Optimum value of *u/B*	45˚	1	5	To check the optimum values of number of glasgrid layers.
	Optimum value of *u/B*	2	0.2,0.4,0.6,0.8,1	45˚	1	5	To check the optimum value of vertical spacing between two layers of glasgrids

Type of Reinforcement	***u/B***	***N***	***h/B***	**β**	***D***	**No. of test**	**Remarks**
GTX	0.2, 0.4, 0.6, 0.8, 1	1	-	45˚	1	5	To find out the optimum *u/B* value
	Optimum value of *u/B*	5	Optimum value of *u/B*	45˚	1	5	To check the optimum values of number of geotextile layers.
	Optimum value of *u/B*	2	0.2,0.4,0.6,0.8,1	45˚	1	5	To check the optimum value of vertical spacing between two layers of geotextiles

3.4.4 Testing Procedure

Soil foundation was taken with dimensions of 950 mm, 450 mm, and 200 mm ($L \times B \times D$) respectively. A slope of height 300 mm was prepared over the foundation at a slope angle of 35^o, 40° and 45°as shown in Fig.3.7, in accordance with the experimental program mentioned before. The soil was compacted at 15% moisture content, i.e. at the optimum moisture content. All four sides of the tank consisted of acrylic sheets of 20 mm thickness for visual observation of footing settlement at various load applications. The acrylic sheet was protected by the use of two metal strips fixed vertically at the center of each side of the tank to prevent the buckling of the sheet with respect to the steel tank during the application of load or during soil compaction. The tank was polished as far as possible to prevent the deleterious effects of friction on the test results. Petroleum jelly was applied on the inside and the outside of the tank. The loading system consisted of a platen attached to the crosshead of the loading frame. The frame consisted of two rigid and heavy steel columns of thickness 100 mm each attached to a steel column base resting on the surface. Load measurement was carried out using a stress measurement data logger, which was the part of the loading frame system. Two dial gauges, with an accuracy of 0.01mm each, were used in the experimental study, across the footing. The

average of the two was taken as the settlement of the footing. The low strain rate of 1mm/min was used to simulate undrained conditions. A schematic view of the loading arrangement is shown in Fig. 3.12

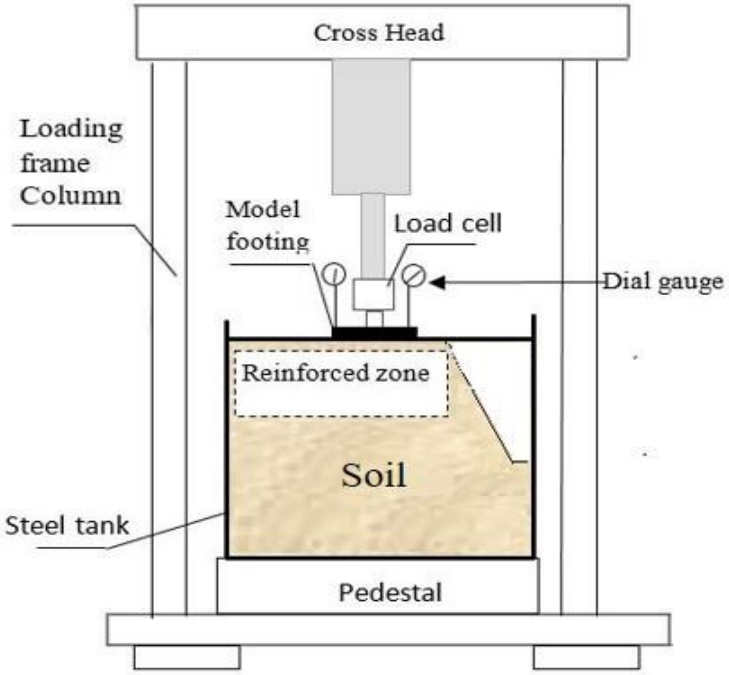

Fig. 3.12 A schematic view of the loading arrangement

3.4.5 Scanning electron microscopic

The morphological analysis of the reinforcements is conducted to study the various failure patterns of the reinforcement during the testing. The study is also used to analysis the role of different reinforcement in the improvement in bearing capacity of reinforced soil foundation. The morphology of the geosynthetic sample was analyzed by Scanning Electron Microscopic (SEM) Hitachi S 3700. The scanning electron microscopic analysis was conducted on different geosynthetic samples. The samples were taken after the testing and chosen from those places where maximum yielding was observed. The pictures of the sampling are shown in Fig. 3.13 (a-c). From Fig. 3.13 (a), maximum yielding has been observed at the edge, similar observations have been observed in the case of GGR2 and GTX shown in Fig. 3.13 (b and c).

Fig. 3.14 shows the SEM photographs of Non-deformed geosynthetics. From Fig. 3.14 (a) it is cleared that that the geotextile is woven type as it indicates that both wrap and weft are interlocked with each other and they are made of multifilament. The fiber arrangement is orthogonal and a very less openings are visible in the whole structure. Fig. 3.14 (b) and (c) shows that the geogrids are 3-D geogrid and glasgrid. From Fig. 3.15 (c) it can be easily seen that the glass grid crystals have uniform coating along its structure.

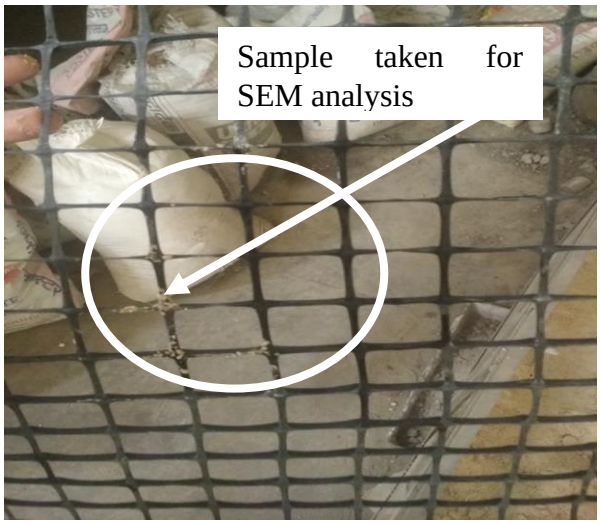

(a) GGR1

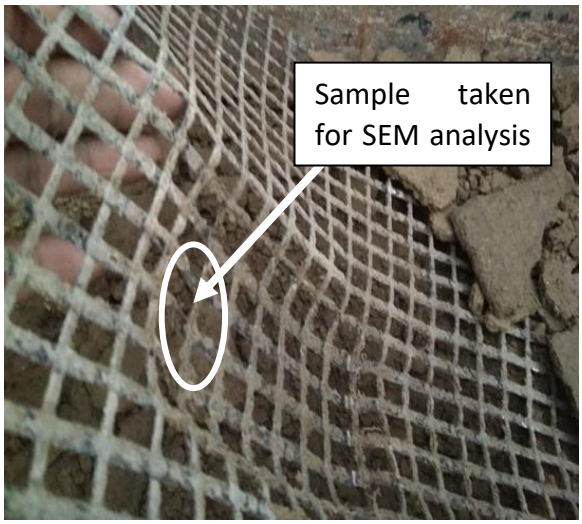

(b) GGR2

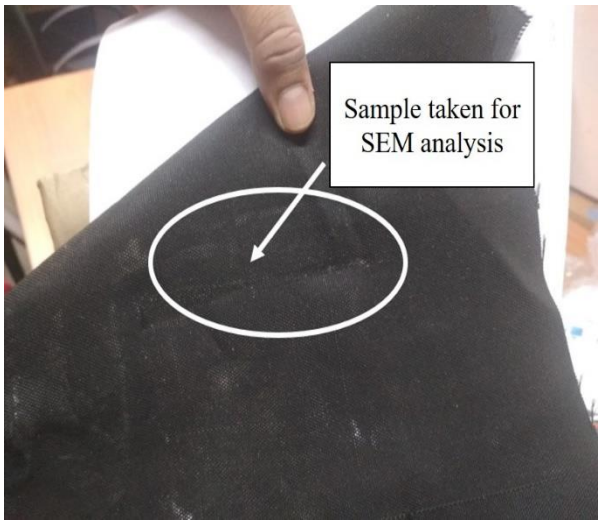

(c) GTX

Fig. 3.13 Samples taken for SEM analysis

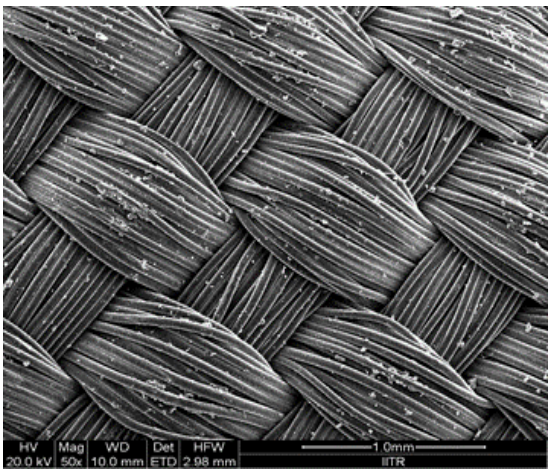

(a) GTX

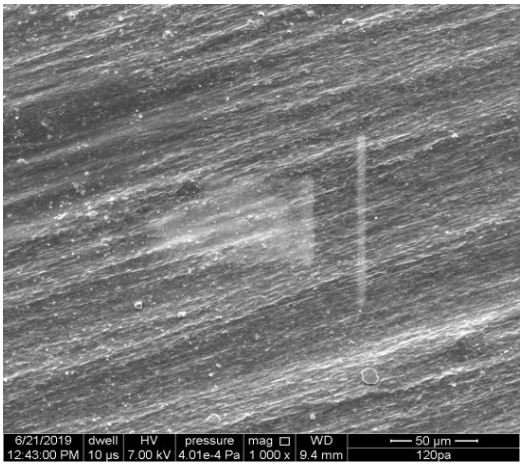

(b) GGR1

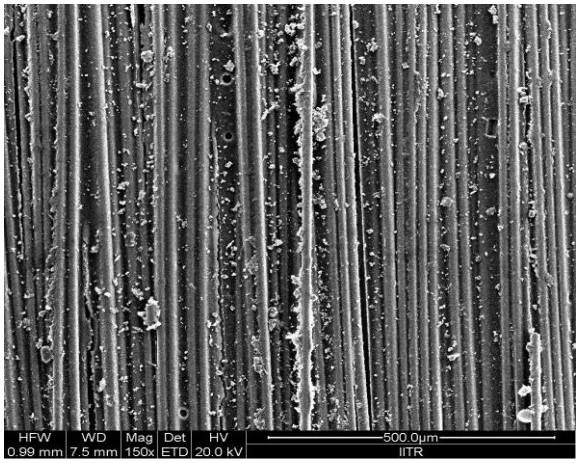

(c) GGR2

Fig. 3.14 SEM analysis for geosynthetics

REFERENCES

1. ASTM, (1997). “Standard test methods for nonrepetitive static plate load tests of soils and flexible pavement components, for use in evaluation and design of airport and highway pavements”. pp. 112-113.

CHAPTER 4

FOOTING RESTING ON FLAT SURFACE

4.1 General

In many civil engineering practices, when the shallow foundations are constructed over the cohesive soil, thus negatively affecting the performance of the foundation in terms of the ultimate bearing capacity and excessive footing settlement. Utilization of geosynthetics as reinforcement can be a possible solution, wherein singular or multi-layered geosynthetics on various forms can increase the load-carrying capacity of the supporting soil. Placement of geosynthetics up to the influence depth (zone up to which shear failure zone of a shallow foundation is formed) can increase the shear strength of the soil. Hence, the position of reinforcement seems to be a necessary condition which affects the efficiency of usage of geosynthetics within the foundational works. A more detrimental situation occurs when eccentric loads act on foundation due to the application of wind loads, oblique loads or due to moments with or without axial forces, which creates not only settlement issues, but also a possibility of tilting of the footing, which decreases overall structural stability. Geosynthetics can provide a better solution in reducing settlement as a result of eccentric loading. The part of the work tries to analyze the beneficial role of geosynthetics in reducing settlement for the foundation over flat ground. Also, the effect of eccentricity under different placement conditions and the eccentricity effect on the bearing capacity at optimum placement locations has also been analyzed. Various parameters have been analyzed in the study, such as top layer spacing for reinforcements (u), the vertical spacing between reinforcements (h), number of reinforcements (N), type of reinforcement, the effect of mechanical properties of reinforcement, eccentricity (e) and the optimum depth of reinforcement (d).

Initially, tests were conducted to determine the optimum top layer spacing of reinforcement. The experiments were conducted for all the geosynthetic materials used in the study. The improvement factor was determined for each settlement ratio (*S.R*) to give an incisive account of the improvement in the bearing capacity of the soil as a result of the application of reinforcements. Improvement factor (*IF*) is defined as the ratio of the bearing capacity of a reinforced soil to that of unreinforced soil, when measured at the same settlement ratio. Hence, the improvement factor can be represented as

$$IF = \frac{Q_r}{Q} \tag{4.1}$$

where Q_r and Q are the bearing capacity of reinforced and unreinforced soil of flat surface, respectively. Here It is noticed that improvement factor is commensurate with bearing capacity ratio (*BCR*) used by many researchers in their studies (Binquet and Lee, 1975a and 1975b; Chen et al., 2007; Farsakh et al.). Along with assessing the improvement in the bearing capacity, another parameter being used for comparison is the percentage reduction in settlement (*PRS*), which can be expressed as follows,

$$PRS = \frac{S_r}{S} \tag{4.2}$$

Where, S_r and S are the settlement of the reinforced and unreinforced soil bed at a given applied pressure, respectively. The percentage reduction factor is similar to the settlement reduction factor suggested and utilized by various researchers (Chen et., 2007; Alawaji., 2017). Ultimate bearing capacity of the soil from pressure settlement curves can be determined by suitable methods present in the literature. (Adams and Collin., 1997; Lee et al., 1999) used the double tangent method for determination of the ultimate bearing capacity of the soil; however, (Sawwaf, 2009) utilized the single tangent method for calculation of the ultimate bearing capacity of the soil. Researchers like (Vesic, 1975) and (Sharma et al., 2009), however, considered bearing capacity at the settlement of 10% of the footing width (*B*) as the bearing

pressure of the soil. For the purpose of this study, double tangent method is being used to compute the ultimate bearing capacity of the soil in accordance with the BIS code. Fig. 4.1 (a) shows the method of computing bearing pressure at the different settlement levels. Fig. 4.1 (b) shows the method of computing bearing capacity using double tangent method. Two tangents are drawn at the ends point, and the intersecting points show the ultimate bearing capacity of the respective soil.

4.2 Effect of top layer spacing

Initially, five tests were conducted on the sample for each of the geosynthetic materials to determine the location of the first reinforcement depth. The general pressure settlement curve of soil bed reinforced with GGR1, GGR2 and GTX obtained during after testing has been shown in Fig.4.2 (a-c) respectively. The pressure settlement curves indicate that there is no distinct peak in the case of unreinforced soil bed, but beyond the settlement of 4%, the slope of the pressure settlement curve becomes almost constant, which indicates that soil has undergone failure. In addition, the pressure settlement curve of reinforced soil shows that soil is much stiffer than those of unreinforced one indicating that geosynthetics used in soil reinforcement substantially reduces the footing settlement. As can be seen from the graph of the improvement factor presented in Fig. 4.3 (a-c) for all reinforcement GGR1, GGR2 and GTX respectively. The improvement factor initially increases and reaches a maximum at *u/B* = 0.34, after which there is a gradual decrease in the value. In the case of reinforcement GGR1, the bearing pressure of unreinforced soil was found to be 324.8 kPa corresponding to *UBC*, which increases as 331.2 kPa (*IF* = 1.02) to 344.2 kPa (*IF* = 1.06) when GGR1 placed at a depth of 0.17B and 0.34B, respectively. Further increment in first reinforcement depth i.e. *u* = 0.51B, 0.68 B to 0.85B, the value of bearing pressure decreases as 337.76 kPa (*IF* =1.04), 334.5 kPa (*IF*=1.03), to 331.98 kPa (*IF*=1.02) respectively. Similarly, for GGR2, the bearing pressure at *UBC* increases from 324.8 kPa (*IF*=1) to 336.3 kPa (1.03) for u = 0.17B to 0.34B,

respectively then it decreases as 327.4kP (*IF*=1), 325.16 kPa (*IF*=1.0) to 324.37 kPa (No improvement) for *u* = 0.51B, 0.68B and 0.85B, respectively. However, geotextile found to be performed negatively for lower settlement values as shown in Fig. 4.3 (c). For higher settlement (*s/B* = 16%), the bearing pressure of unreinforced soil was found to be 581 kPa, which increases as 614 kPa (*IF* =1.056), 663 kPa (*IF* = 1.14), when GGR1 placed at a depth of 0.17B and 0.34B, respectively. Further increment in first reinforcement depth i.e. *u* = 0.51B, 0.68 B to 0.85B, the value of bearing pressure decreases as 656 kPa (*IF* =1.12), 645 kPa (*IF* =1.09), to 633.29 kPa (*IF* =1.06) respectively. Similarly, for GGR2, the bearing pressure increases from 600.23 kPa (*IF* =1.03) to 636.96 kPa (*IF* =1.09) for u = 0.17B to 0.34B, respectively then it decreases as 621.13 kPa (*IF* = 1.07), 612.06 kPa (*IF* = 1.05) to 598.06 kPa (*IF* =1.03) for *u* = 0.51B, 0.68B and 0.85B, respectively. A similar trend has been observed in the case of geotextile, which shows the bearing pressure increases as 627 kPa (*IF* = 1.08), 685 kPa (*IF* =1.18) for a depth of u = 0.17B, 0.34B, respectively. Then it decreases as 663 kPa (*IF* = 1.14), 650.7 kPa (*IF* =1.12), 639.1 (*IF* =1.09) when reinforced was placed at *u* = 0.51B, 0.68 B to 0.85B, respectively. This result is commensurate with those reported by (Sakti and Das, 1987), who conducted laboratory-scale testing of geotextile reinforced foundation. From the above observations, it is concluded that the optimum depth of the first reinforcement has been observed at *u/B* = 0.34 for all three reinforcements. A similar trend was observed in *PRS* curves which is shown in Fig. 4.4. This result comparable to those obtained by (Chen et al., 2007), who reported an optimum *u/B* value of 0.33 for single layer reinforcement tested on clay for a square footing. (Omar et al., 1993) and (Farsakh et al., 2008, 2013) obtained similar result as that obtained by (Chen et al., 2007) for geosynthetic reinforced sand, i.e. the optimum top layer depth was obtained as 0.33. (Badakhshan and Noorzad, 2015) reported similar results while conducting tests for circular footing resting over a granular soil layer, when subjected to eccentric loading, where they reported that the value of maximum bearing capacity where obtained at the same

initial depth for all eccentric loading cases. (Tafreshi and Dawson, 2010) reported *u/B* in range of 0.3-0.35 as the optimum position for placement of planar reinforcement within a reinforced soil foundation. However, (Ramaswamy and Purushothaman, 1992) obtained an optimum *u/B* value of 0.50 for a circular footing on reinforced clay. (Mandal and Sah, 1992) obtained an optimum *u/B* of 0.175 approximately for square footing on a reinforced clay foundation bed. The reason for the variance of results can be attributed to the differences in soil properties and characteristics being used by different researchers in their studies. The reason for the occurrence of an optimum depth of initial layer reinforcement can be attributed to the lack of sufficient depth for $u/B<0.35$ to mobilize sufficient friction between the reinforcement and the soil, which does not yield the beneficial effects of applying a reinforcement within a foundation bed. Also, lack of sufficient confining pressure for the top layer of the soil beyond the footing edges can also be attributed as another reasons for obtaining such results.

4.3 Effect of number of reinforcements and influence depth

For assessment of the effect of a number of reinforcement layers in the further improvement of bearing capacity of the foundation bed, the first reinforcement depth was fixed at 0.34B (i.e., an optimum depth of first reinforcement layer). The vertical spacing between the reinforcement layers also fixed at 0.34B. The number of reinforcements layers was varied from N =1 to 5. The distance of effective depth of reinforcement (d/B), was ascertained for each reinforcement case. For a top layer reinforcement depth (u), and the gap between N numbers of reinforcements being h, the effective depth of the reinforcement can be represented as

$$d = u + (N\text{-}1) \times h \tag{4.3}$$

The pressure-settlement curves were plotted for each number of reinforcement layers to compare with the unreinforced one. Fig.4.5 (a-c) shows the pressure settlement relationship for reinforcements GGR1, GGR2 and GTX respectively. As expected, the value of bearing pressure increases with increment in a number of reinforcement layers. Consider for example

GGR1 case *s/B* = 4%, see Fig. 4.5 (a), at settlement ratio *(s/B* = 4%), the bearing pressure increases as 4.96, 25.0, 48,9 and 57 % for *d/B* = 0.34, 0.68, 1.02, 1.36 and 1.7, respectively. Similarly in case of GTX (see Fig. 4.5 (c)) reinforced soil at *s/B* = 4%, the bearing pressure increases as 5.56, 15.57, 26.89 and 28.14 % for *d/B* = 0.34, 0.68, 1.02, 1.3 and 1.7 respectively. Further placing GGR2 (see Fig. 4.5 (c)) at *d/B* = 0.34, 0.68, 1.02, 1.36 and 1.7, increased the value of bearing pressure as 2.83, 19.38, 47.7, 48.5, 48.31 % respectively. Fig. 4.6 (a-c) shows the variation of *IF* of foundation soil with increment in the number of layers of reinforcement. As can be predicted, an increase in the number of layers of reinforcements substantially increases the overall bearing capacity of the soil. The increase in bearing capacity can be ascribed to the friction between the reinforcement and the soil particle, which improves with the rise in the number of reinforcements. Better interlocking between the soil particles and the geogrid can also be stated as an important reason for this observation. However, the effect of the increase in the number of reinforcements becomes insignificant as the number of reinforcement increases and becomes almost insignificant when the optimum depth is reached. Consider for example GGR1 case *s/B* = 4%, see Fig. 4.6 (a), at settlement ratio *(s/B* = 4%), the improvement factor (*IF)* increases as 1.04, 1.25, 1.48, 1.55 and 1.57 for *d/B* = 0.34, 0.68, 1.02, 1.36 and 1.7, respectively. Similarly in case of GTX reinforced soil, see Fig. 4.6 (c) at *s/B* = 4%, improvement factor (*IF)* increases as 1.11, 1.18, 1.31, 1.36, and 1.36 for *d/B* = 0.34, 0.68, 1.02, 1.3 and 1.7 . Further placing GGR2 at *s/B* = 4% at *d/B* = 0.34, 0.68, 1.02, 1.36 and 1.7, increased the value of improvement factor 1.01, 1.19, 1.45, and 1,46 respectively. A significant rise in the bearing capacity with the application of the third and the fourth layer of reinforcement for all *s/B* ratios when considering the case of central loading. The optimum depth for geogrids, and geotextile was obtained at 1.36B (N=4) and 1.02B (N=3). Hence, below these depths, the inclusion of any other reinforcement would not have any substantial effect when considering the case of central loading. Similar trends for geogrid were reported

by (Shin et al., 1993) wherein the proffered optimum depth for a strip footing was 1.8B. (Chen et al., 2007) also reported that the optimum depth for geogrid and geotextile reinforced square footing resting over a clay foundation was 1.5B and 1.25B respectively. However, when applying eccentric loading on the footing, the increase in the improvement becomes almost negligible after the application of the fourth geogrid. Fig. 4.7 (a-d) shows the relationship between the *IF* vs. *e/B* at different *s/B* ratios for N=1, 2, 3, and 4, respectively. Beyond N=3, the effect of growth in the bearing capacity ratio seems to become insignificant, and thus, N=3 is the optimum number of reinforcement layers in case of an eccentrically loaded footing. Similar results were reported by (Sawwaf, 2009) for the case of a strip footing under eccentric loading. (Badakhshan and Noorzad, 2015) also reported similar trends when they considered circular footing under eccentric loading, which suggested that beyond N=3, an increase in the number of layers of reinforcements had a reducing effect. This effect can be explained on the account that when a footing is eccentrically loaded, the depth of the failure wedge decreases due to the tilt in the footing, due to which the overall depth of reinforcement has a much smaller effect in case of eccentrically loaded footing when compared to a centrally loaded footing. Hence, N=4 and N=3 are the optimum number of reinforcements in the case of centrally and eccentrically loaded footing respectively. The optimum depth of the reinforcements was individually ascertained for each reinforcement by varying the depth of single layer of each reinforcement till the point bearing capacity comparable to the unreinforced soil foundation was not achieved.

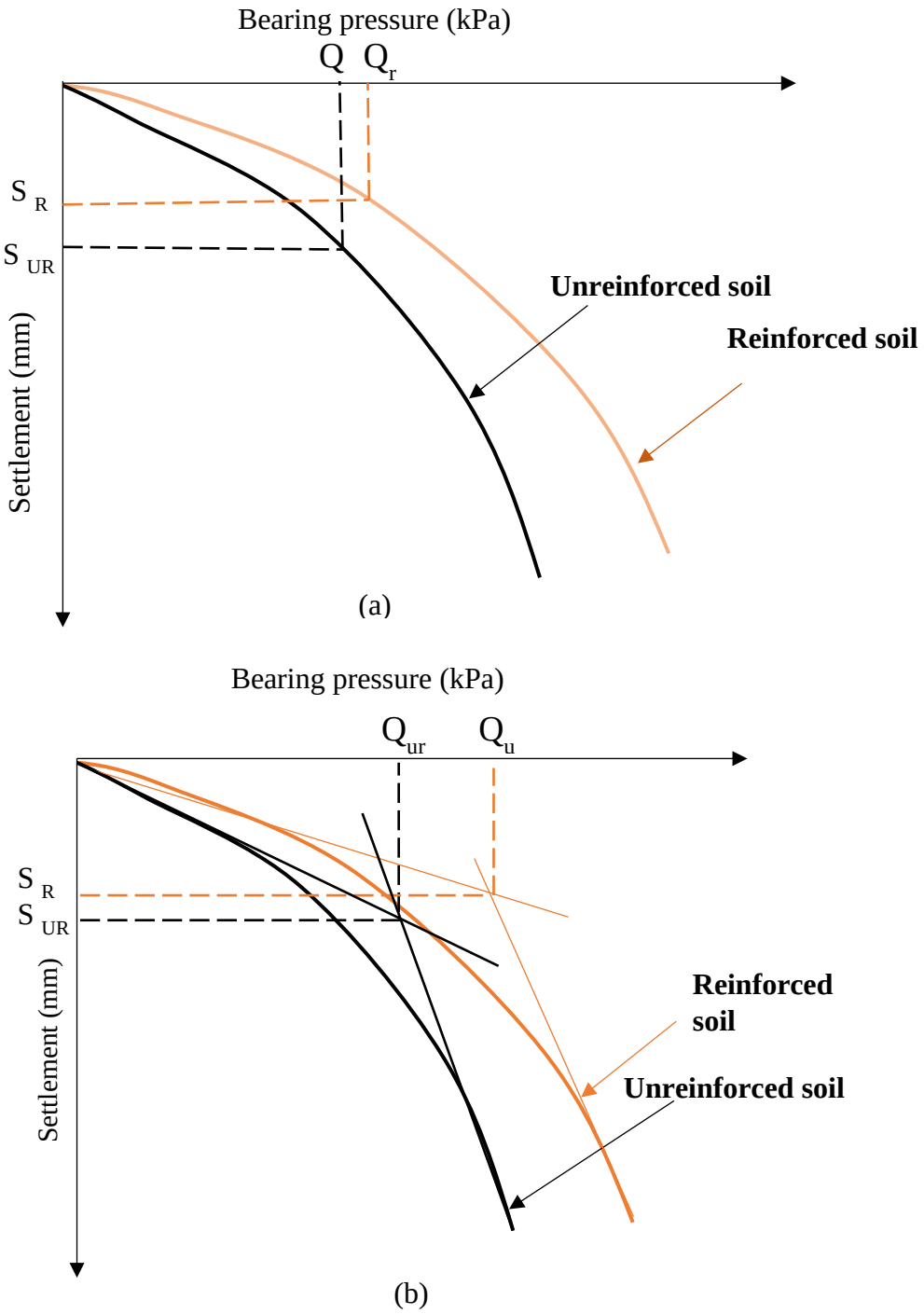

Fig. 4.1 (a) Method to estimate the *IF* using different settlement ratios (b) Double tangent method for ultimate bearing capacity of reinforced and unreinforced soil

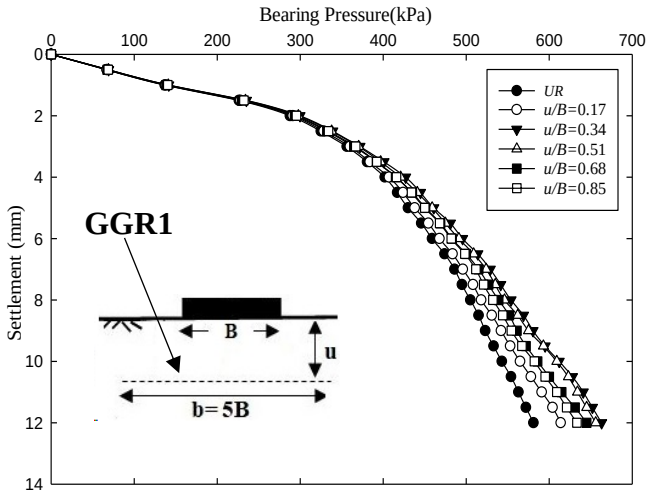

(a)

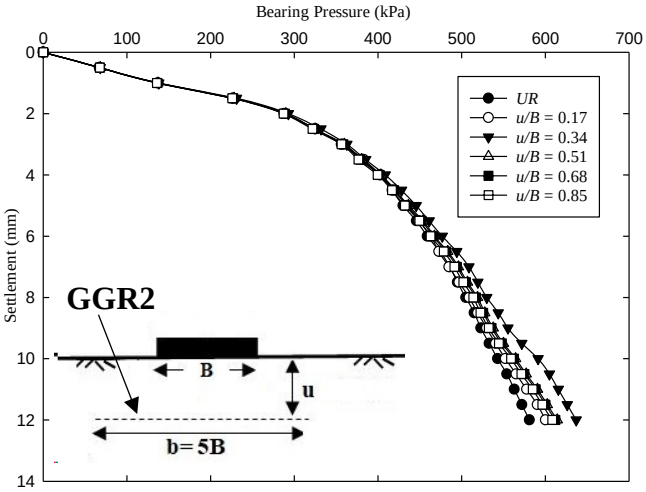

(b)

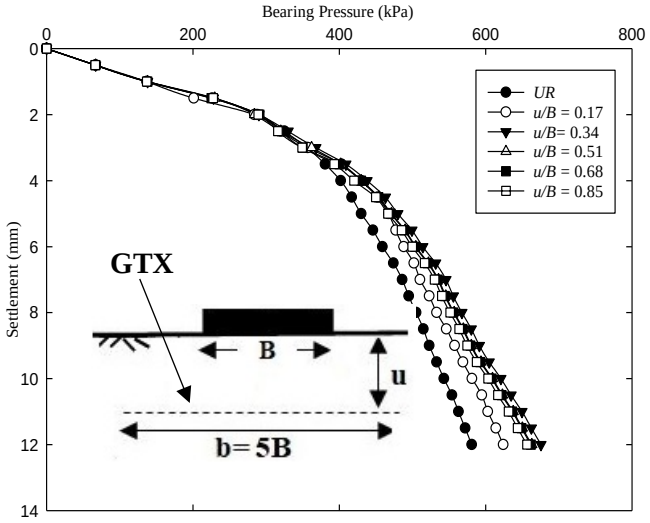

(c)

Fig 4.2 Pressure Settlement Curve for (a) GGR1 (b) GGR2 (c) GTX at different u/B ratios

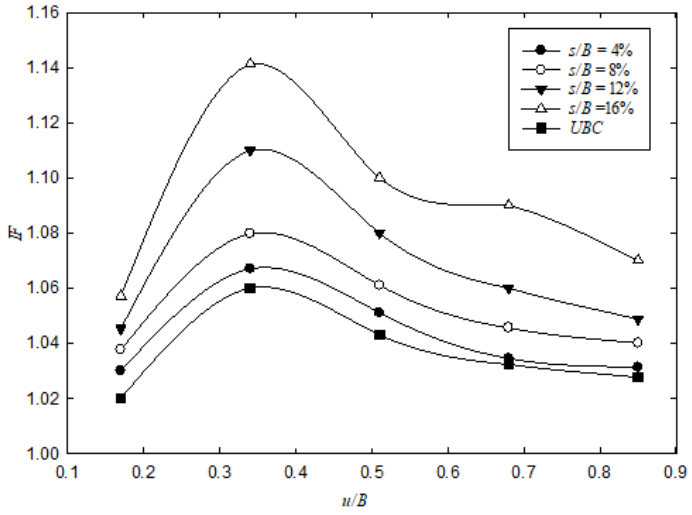

(a)

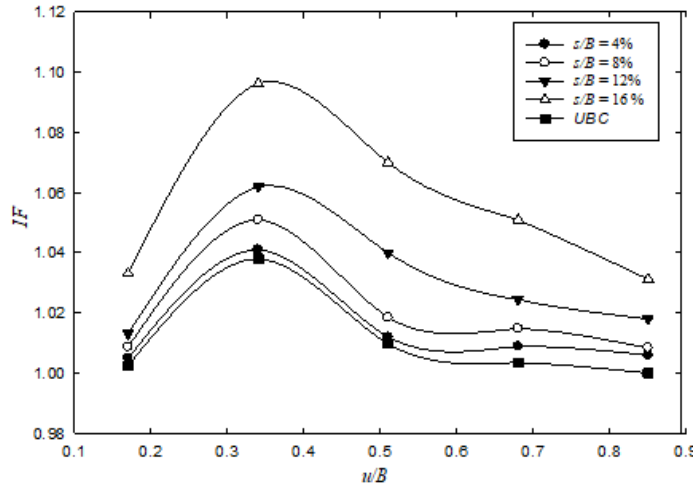

(b)

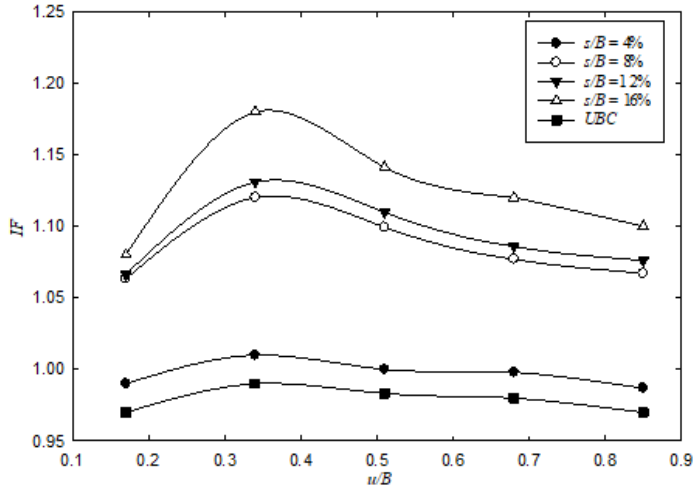

(c)

Fig. 4.3 Improvement factor (*IF*) versus *u/B* for (a) GGR1 (b) GGR2 and (c) GTX

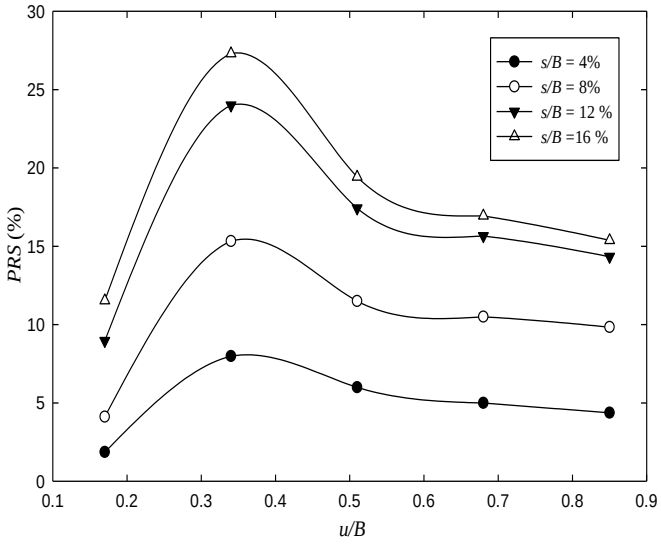

(a)

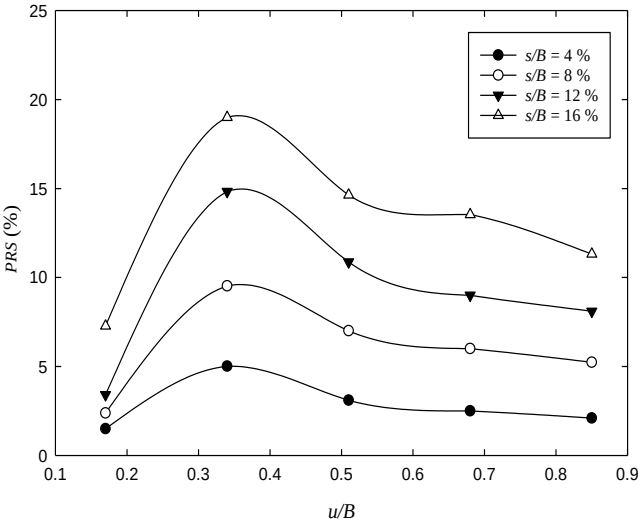

(b)

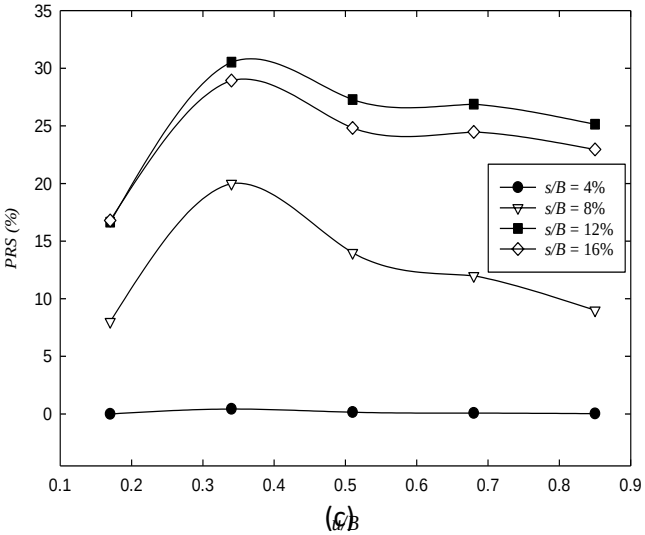

(c)

Fig. 4.3. Improvement factor (*IF*) versus *u/B* for (a) GGR1 (b) GGR2 and (c) GTX

4.4 Effect of the stiffness of the reinforcements

GGR1, GGR2 and GTX of different stiffness are used in the current study. Technical characteristics of geosynthetics are presented in the Table. 3.2. In order to investigate the effect of stiffness of reinforcement in settlement reductions of soil foundation bed, the values of *PRS* were calculated at different settlement ratios. As can be seen from the curves, GGR1 performs better than GGR2 and shows a much higher reduction in a settlement. This signifies that geogrid properties, such as tensile strength, tensile modulus/ stiffness, and aperture size, have a significant role in the performance of the geogrid towards providing efficient reinforcement. Fig. 4.8 (a-c) depict the variation of PRS with multiple geosynthetic layers for different reinforcement widths. The category of the curve is classified into two grades; one for s/B< 4% (lower settlement level) in which ultimate bearing capacity lies and other for s/B >4% (higher settlement level). For the lower settlement level, it can be seen from the graph that GGR1 and GGR2 impart substantial improvement in bearing capacity than GTX. The reason for the same can be explained that at a lower settlement level, geogrid efficiently mobilized the lateral stress resistance capacity due to the confinement effect, which plays a vital role in the reinforcement mechanism. However, for a higher settlement, the performance of geotextile is much better and imparts more improvement than the geogrids.

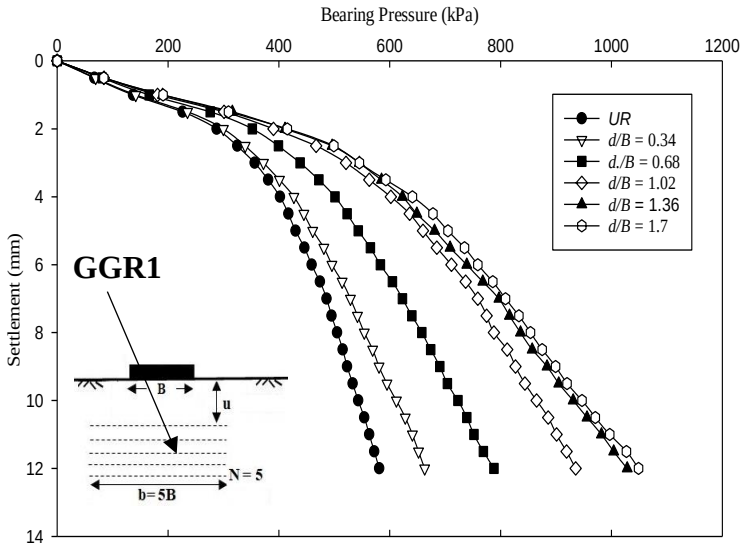

(a)

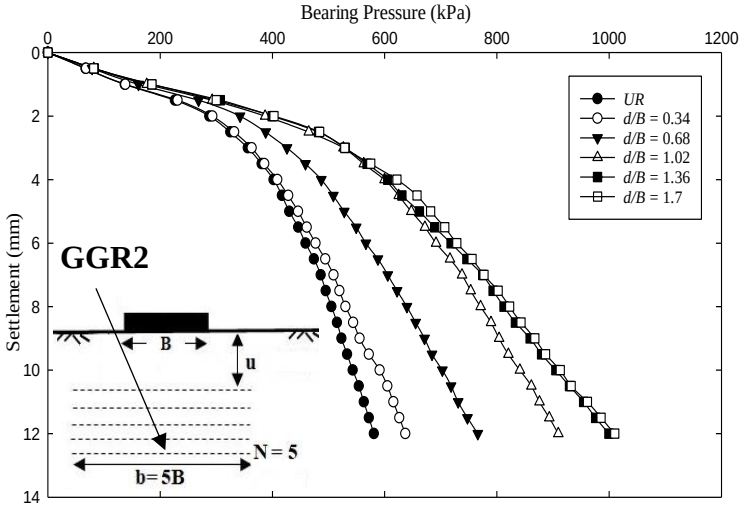

(b)

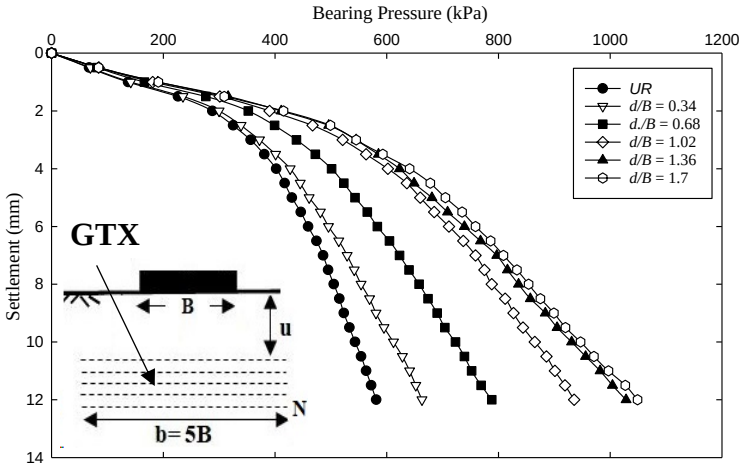

(c)

Fig. 4.5 Pressure Settlement Curve for (a) GGR1 (b) GGR2 (c) GTX at different *d/B* ratios

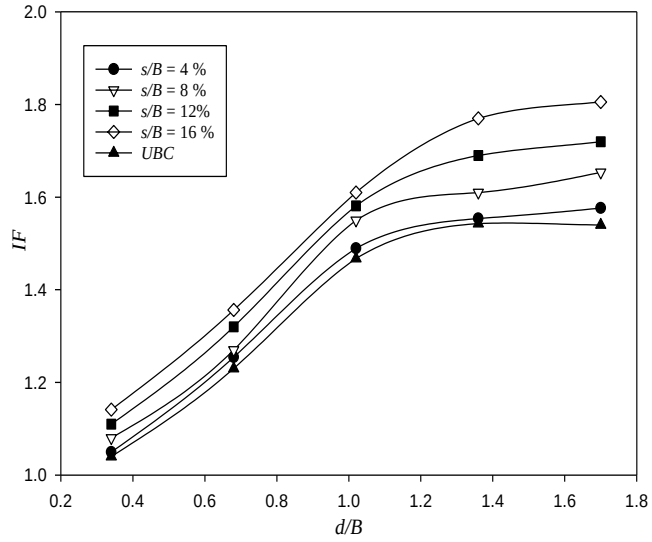

(a)

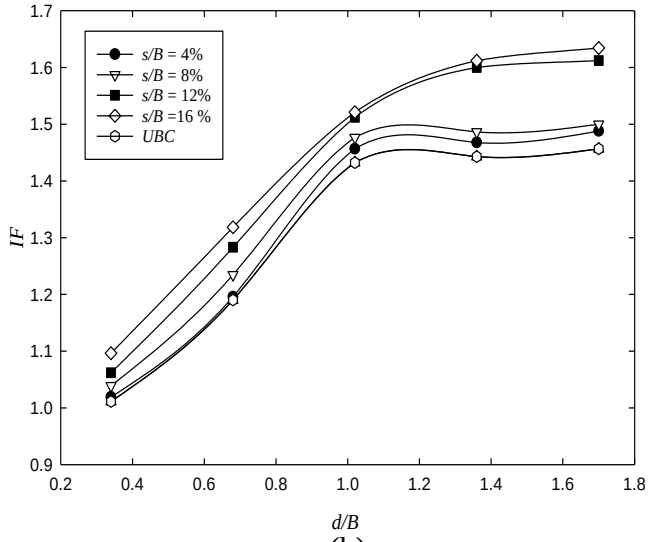

(b)

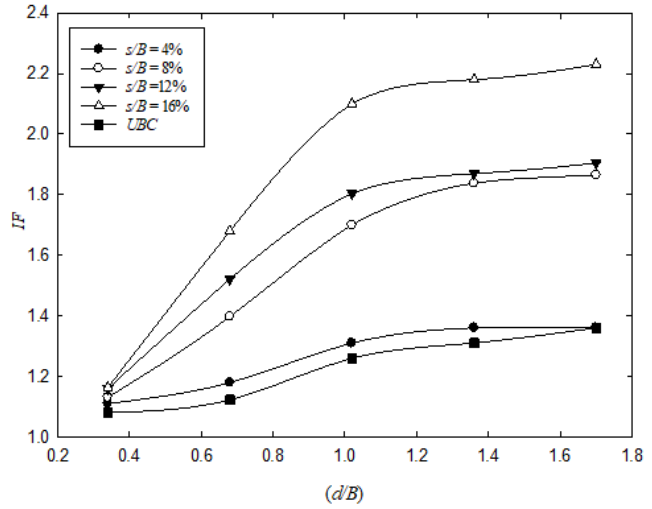

(c)

Fig. 4.6 Improvement factor versus d/B for (a) GGR1 (b) GGR2 and (c) GTX

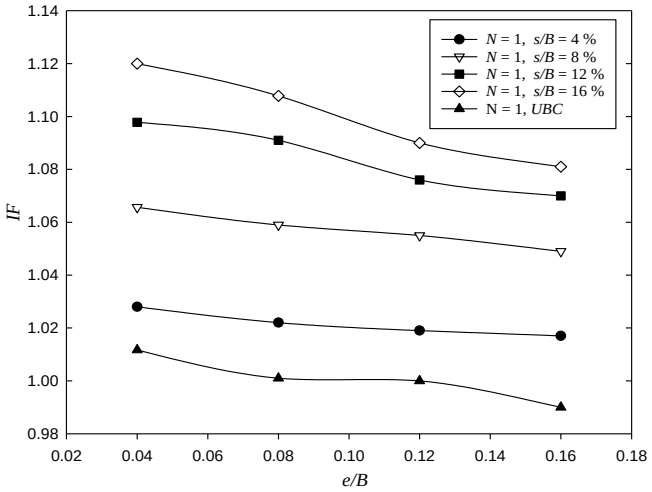
N = 1, s/B = 4 %
N = 1, s/B = 8 %
N = 1, s/B = 12 %
N = 1, s/B = 16 %
N = 1, UBC
IF
e/B

(a)

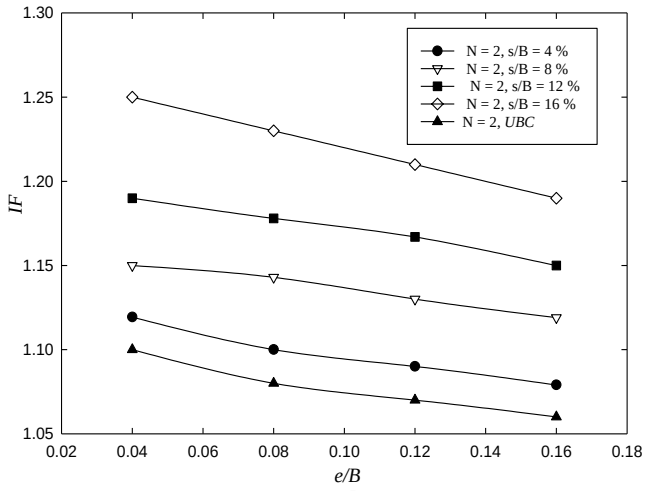
N = 2, s/B = 4 %
N = 2, s/B = 8 %
N = 2, s/B = 12 %
N = 2, s/B = 16 %
N = 2, UBC
IF
e/B

(b)

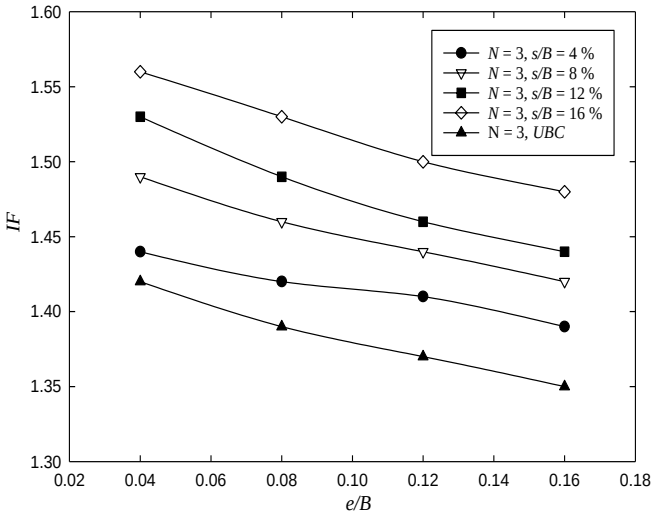
N = 3, s/B = 4 %
N = 3, s/B = 8 %
N = 3, s/B = 12 %
N = 3, s/B = 16 %
N = 3, UBC
IF
e/B

(c)

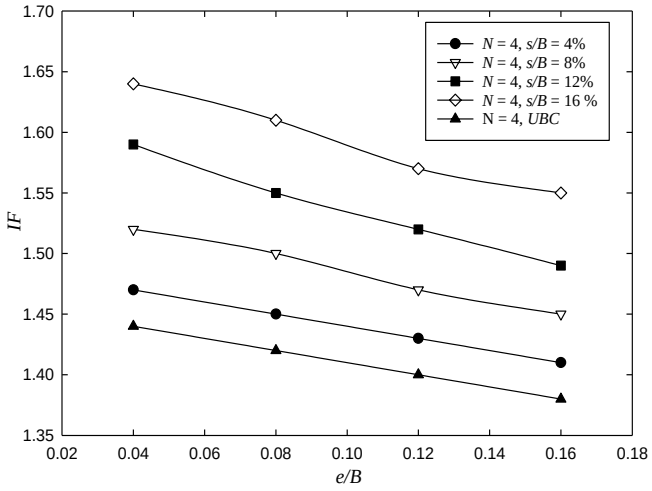

(d)

Fig.4.7 Improvement factor versus *e/B* for GGR1 (a) N=1 (b) N=2 (c) N=3 (d) N=4

The reason behind this can be explained as at certain settlement, geotextile requires higher deformation to perform on its full capacity due to its higher tensile strength. Generally, foundation constructions require to be constructed for the allowable bearing pressure. Geogrid is better performing material than geotextile for limited settlement requirements. However, geotextiles primary function is to act as a filter or in drainage system behind retaining walls, adjacent to roads, and within slopes etc. thus can be considered as reinforcement material where small tensile strength is required. (Biswas et. al.) presented similar findings when they compared the geogrids with geotextile at a certain settlement level.

4.5 Effect of vertical spacing between the reinforcements

The effect of spacing between two corresponding reinforcements was analyzed by varying the distance between two reinforcements by a factor of 0.08 B, 0.16 B, 0.24 B, 0.32 B and 0.4 B. The tests for the same were conducted on three different geosynthetics, which included GGR1, GGR2, and GTX1 respectively. Fig. 4.9 (a-c) show the improvement factor curves with variations of vertical spacing between two reinforcements. It can be seen that 0.16 B is the optimum vertical spacing for all reinforcements.

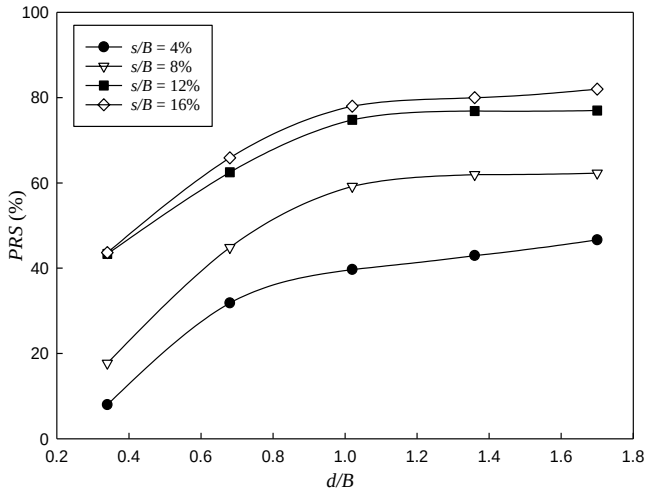

(a)

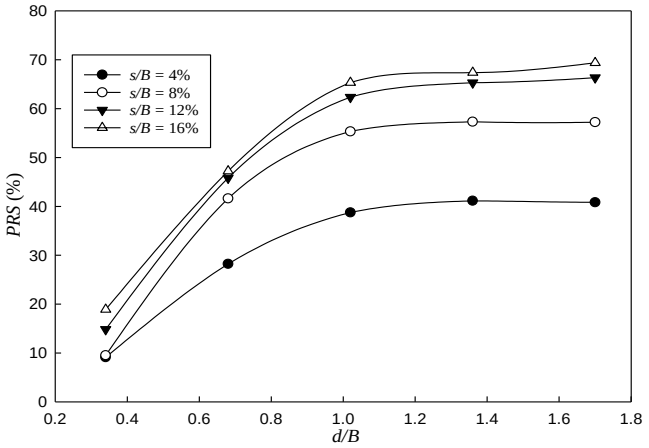

(b)

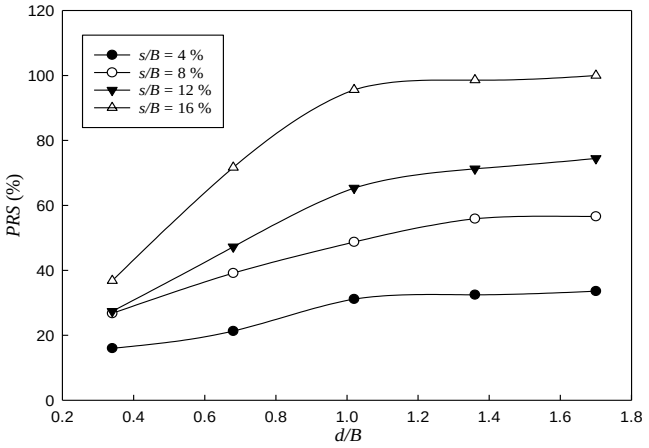

(c)

Fig. 4.8 *PRS* versus *u/B* for (a) GGR1 (b) GGR2 and (c) GTX

Consider, for example, for the GGR1 case, see Fig. 4.9 (a) at *s/B* = 4%. The improvement factor rises as 1.15 to 1.16 for *h/B* ratios 0.08, 0.16 respectively, then decreases to 1.15, 1.14 and 1.12 for *h/B* ratios 0.0.24, 0.32 and 0.4 respectively. Similarly, for GGR2, see Fig 4.9 (b) the improvement factor increases as 1.15 to 1.16 for *h/B* ratios 0.08, 0.16 respectively, then decreases to 1.15, 1.14 and 1.12 for *h/B* ratios 0.0.24, 0.32 and 0.4 respectively. When geotextile was placed, see Fig 4.9 (c) the improvement factor rises as 1.01 to 1.19 for *h/B* ratios 0.08, 0.16 respectively, then decreases to 1.17, 1.14, and 1.01 for *h/B* ratios 0.0.24, 0.32 and 0.4 respectively. The above three observations reveal that the effect of the vertical spacing between the reinforcement reduces significantly when the distance between the reinforcements is increased to 0.16B. The optimum value of vertical spacing was obtained as 0.16B for all the three geosynthetics. Similar results were suggested by (Guido et al., 1986) and (Chen et al., 2007). The probable reason for the optimum vertical spacing is that when reinforcement is provided upto a vertical spacing of 0.16B, soil density occurs maximum due to confinement of soil between two reinforcement layers. As spacing increases density decreases which results in a reduction in strength.

4.6 Influence of reinforcement width

GGR1 and GTX were chosen to check the effect of the width of reinforcement in the improvement of bearing capacity of soil foundation. This influence of reinforcement width was analyzed by the variation of reinforcement width as 4B, 5B, and 6B. Fig. 4.10 (a-c) show the relation between *IF* with number of reinforcement layers (N) at different settlement ratios (*s/B* = 4%, 8%, 12% and 16) for all the reinforcements. From the graphs, it has been observed that *IF* values increase with increasing *b/B* ratios. It is also noted that there is a substantial rise in *IF* with the increment of reinforcement width up to *b/B* equal to 6 for GGR1 and GTX, thus signifying that with any further increment in reinforcement width, improvement in improvement factor is likely to become almost insignificant.

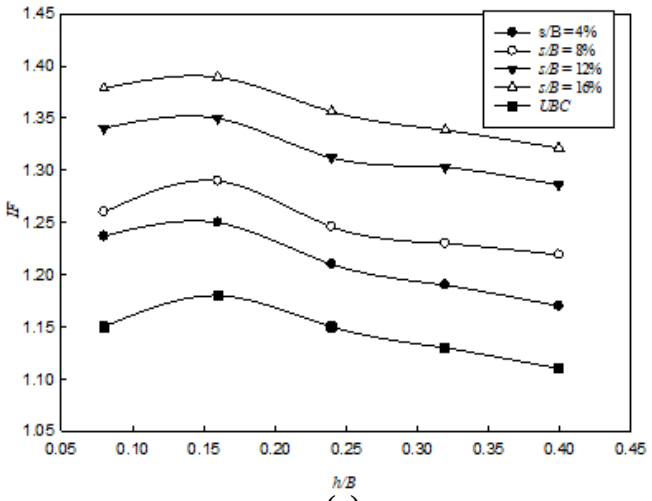

(a)

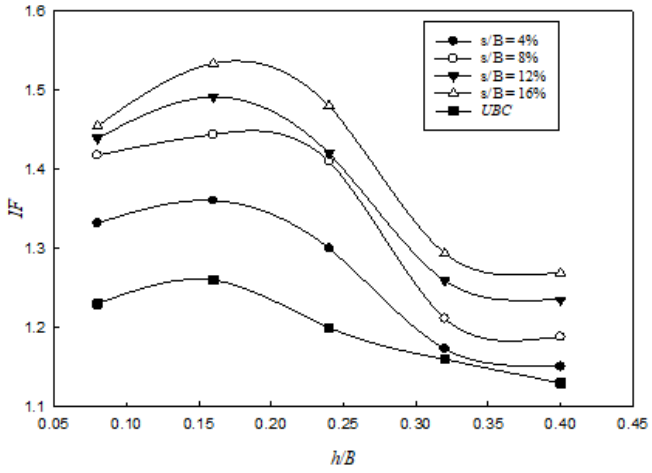

(b)

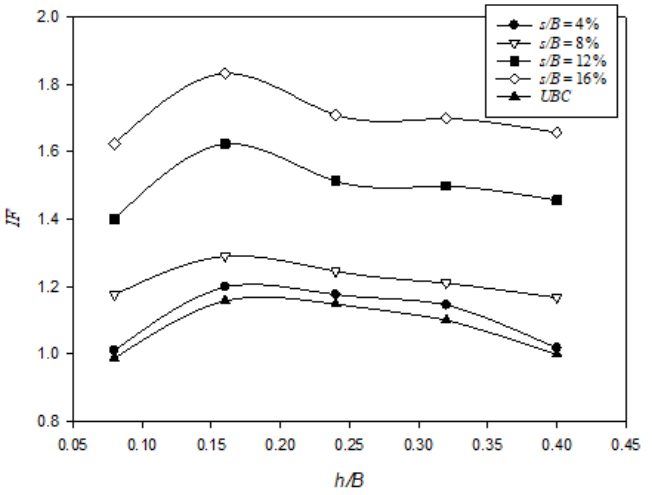

(c)

Fig. 4.9 Improvement factor versus *h/B* for (a) GGR1 (b) GGR2 and (c) GTX

For example, see Fig 4.10 (a-c), for the case of GGR1 at (*s/B* = 4 %) with N=5, the improvement factor increased from 1.51 to 1.57 when *b/B* ratio varied from 4 to 5. Further increment in *b/B* ratio from 5 to 6, the *IF* was increased from IF = 1.57 to 1.58. It is observed that a maximum rise in *IF* values were observed for *b/B* ratio between 4 to 5 than those between 5 to 6. It is clear that satisfactory results may not be obtained with increment in reinforcement width beyond 6B. Same trend has been in case of GTX. Similar to this finding (Latha and Somvanshi, 2009) reported that the optimum width of geogrid to reinforce the square footing resting over the sand observed at *b/B* = 5 - 5.93. The probable reason for this optimum width is that tensile strength is mobilized in only shear zone, which occurs just below the footing, and beyond this shear zone, some additional length of reinforcement is required for the safety of pullout failure. This additional zone is called the anchorage zone. So, the total effective width of the reinforcement is the summation of these two zones, i.e., shear and anchorage zone. Further increment in reinforcement width beyond the optimum value will not be effective and satisfactory results cannot be expected. The similar results can be observed in the case of geotextile.

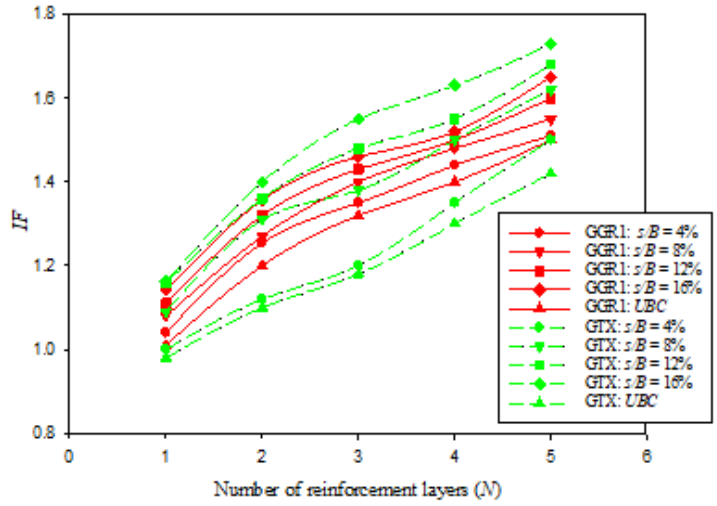

(a)

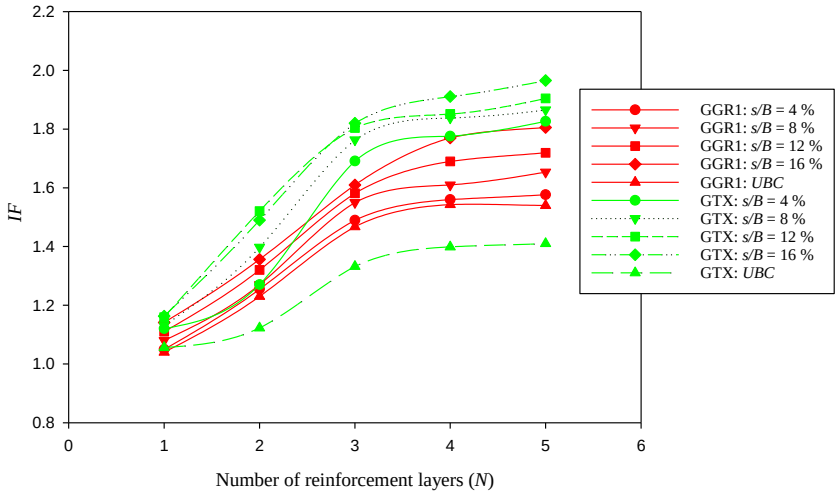

(b)

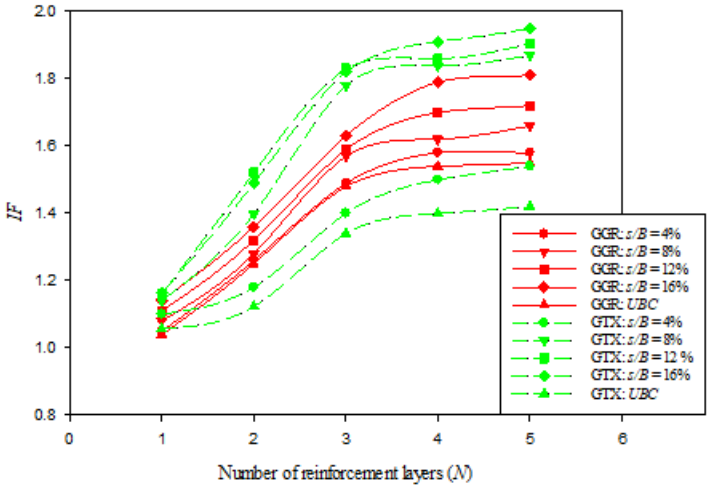

(c)

Fig. 4.10 Improvement factor versus Number of reinforcement layers (N) for GGR1 and GTX (a) b = 4B (b) b = 5B and (c) b = 6B

4.7 Physical strain measurement in the reinforcement

The physical strain in the reinforcement was calculated during the experiment. For this purpose, GGR1 was used as a reinforcement. The strain gauges were installed along with a reinforcement layer located at a depth of 0.34B and 1.36B (N=4) from the center of the footing. In a single layer of reinforcement, in total six strain gauges were attached at different locations. Fig. 4.11 (a-b) and Fig. 4.12 (a-b) shows the typical strain variation of the geogrids at a different *s/B* ratio. It is observed that the strain is tensile in nature and largest just below the center of footing. As the distance from the center of footing increases, the magnitude of the strain decreases and increases with increases in *s/B* ratios. The value of strain becomes almost insignificant at a distance of 2.5B from the center of footing. Thus, it can be concluded that the mobilization of strain in the geogrid is almost negligible at the effective width of reinforcement (5B) beyond which a significant improvement in bearing capacity of reinforced soil cannot be expected. Fig. 4.12 (a-b) shows the variations of strain at the edge of footing in X direction and Y direction for footing size (75 mm× 75 mm). It is observed that the strain mobilized in geogrid at the edge of the footing in X direction (machine direction) is almost equal to the strain in reinforcement in Y direction (cross direction). The reason for the same can be explained that the edge of footing in the X direction is equal to the distance of the edge of the footing in the Y direction**.**

4.8 Summary and conclusions

Geosynthetics inclusion in cohesive soil increases the bearing capacity and reduces the settlement of the footing. The performance of 3D- Geogrid was better than the others at lower settlement. However, geotextile imparts high strength at higher settlement. Based on the above study, the following conclusions were drawn.

1. The optimum depth of top layer reinforcement for GGR1, GGR2 and GTX were obtained at $u/B = 0.34$.

2. The soil reinforced with geotextile behave differently from the geogrids. The improvement in bearing capacity increases with an increase in reinforcement layers. An optimum number of reinforcement layers was obtained at N= 4 for geogrids reinforced soil and N= 3 for geotextile reinforced soil.

3. The optimum depth of reinforcement (d) was obtained at *d/B* ratio of 1.36B and 1.02B for geogrids and geotextile, respectively. After testing for reinforcement at a deeper point, the increase in bearing capacity was not substantial, thus signifying the presence of an optimum depth beyond which inclusion of a geosynthetic is not viable.

4. The width of reinforcement also played a crucial role in amassing maximum benefit from reinforcements. A substantial improvement in the performance of reinforcement was found when the width of reinforcements was equal to 5 times the width of footing for geogrid and geotextile.

5. For the foundation construction point of view, Geogrid was the best performing material. Although geotextile performed better at higher settlement ratios, geogrid provided better reinforcement for lower settlement ratios for which the structures are usually designed for.

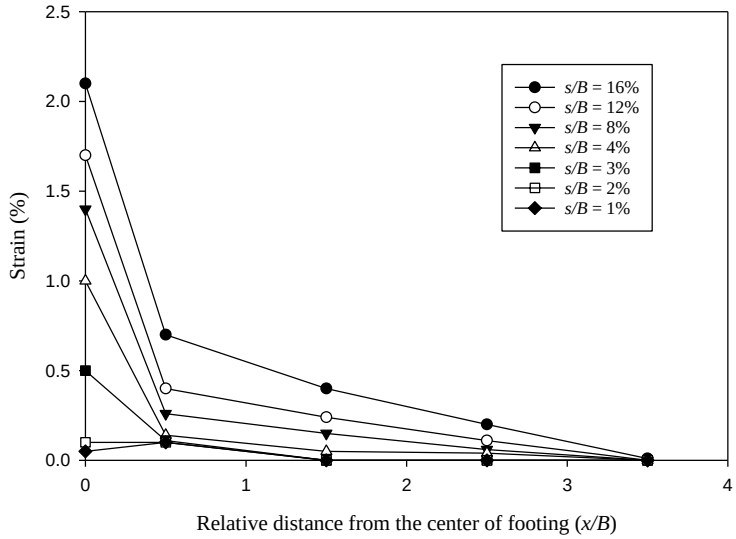

(a)

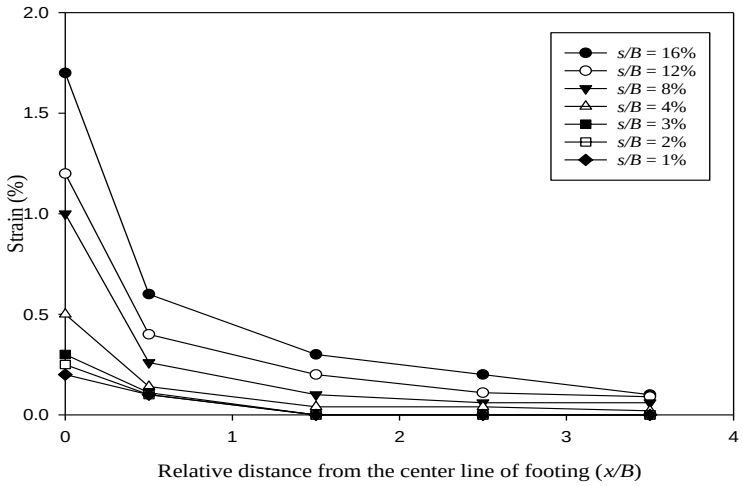

(b)

Fig. 4.11 Strain distribution in geogrid placed at a depth of (a) 30 mm and (b) 120 mm

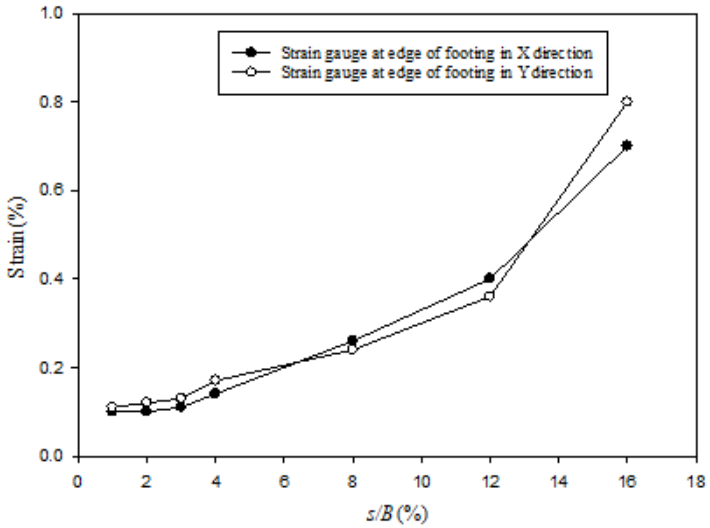

(a)

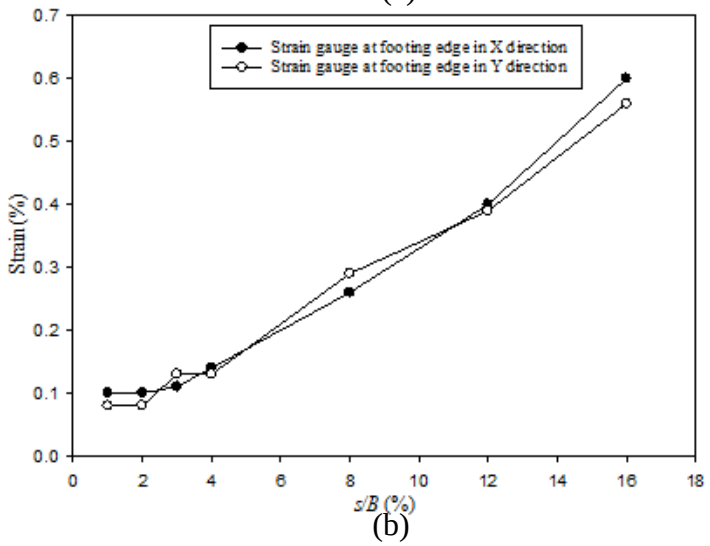

(b)

Fig. 4.12 Distribution of strain in geogrid versus s/B ratios beneath edge (a) X direction and (b) Y direction of footings

Table 4.1 Summary of the tests test results based optimum position of reinforcements

Test No.	**Configuration**	***s/B = 4%***	***s/B = 8%***	***s/B = 12%***	***s/B = 16%***	***UBC***
		IF	***IF***	***IF***	***IF***	***IF***
1.	GGR1 (N=1) (*u/B* = 0.34)	1.067	1.079	1.110	1.141	1.060
2.	GGR1 (N=4) (b/B=5) (*d/B*=1.36)	1.53	1.61	1.69	1.77	1.53
3.	GGR1 (h/B = 0.16)	1.25	1.29	1.35	1.38	1.26
4.	GGR1 (N=1) (*e/B* = 0.04)	1.028	1.065	1.097	1.12	1.011
5.	GGR1 (N=1) (*e/B* = 0.08)	1.022	1.059	1.091	1.107	1.001
6.	GGR1 (N=1) (*e/B* = 0.12)	1.019	1.055	1.076	1.090	1
7.	GGR1 (N=1) (*e/B* = 0.16)	1.017	1.049	1.070	1.081	0.99
8.	GGR1 (N=4) (*e/B* = 0.04)	1.46	1.520	1.590	1.640	1.44
9.	GGR1 (N=4) (*e/B* = 0.08)	1.45	1.50	1.55	1.610	1.42
10.	GGR1 (N=4) (*e/B* = 0.12)	1.43	1.47	1.52	1.57	1.4
11.	GGR1 (N=4) (*e/B* = 0.16)	1.42	1.45	1.49	1.55	1.38
12.	GGR2 (N=1) (*u/B* = 0.34)	1.041	1.051	1.062	1.096	1.038
13.	GGR2 (N=4) (*d/B*= 1.36)	1.46	1.48	1.60	1.61	1.44
14.	GGR2 (*h/B* = 0.16)	1.36	1.44	1.49	1.53	1.26
15.	GTX (N=1) (*u/B* = 0.34)	1.01	1.12	1.13	1.18	0.99
16.	GTX (N=4) (*d/B*= 1.36)	1.31	1.70	1.80	2.10	1.26
17.	GTX (*h/B* = 0.16)	1.19	1.28	1.62	1.83	1.15

REFERENCES

1. Abu-Farsakh, M., Chen, Q., and Sharma, R. (2013). "An experimental evaluation of the behavior of footings on geosynthetic-reinforced sand". *Soils and Foundations*, Vol. 53, pp.335-348.
2. Abu-Farsakh, M., Chen, Q., Sharma, R., and Zhang, X. (2008). "Large-scale model footing tests on geogrid-reinforced foundation and marginal embankment soils". *Geotechnical Testing Journal*, Vol. 31, pp. 413-423
3. Adams, M.T., and Collin, J.G. (1997). "Large model spread footing load tests on geosynthetic reinforced soil foundations". *Journal of Geotechnical and Geoenvironmental Engineering*. Vol. 123, pp. 66-72.
4. Alawaji, H. (2000). "Settlement and bearing capacity of geogrid-reinforced sand over collapsible soil". *Geotextiles and Geomembranes*, Vol. 19. Pp. 75-88.
5. Badakhshan, E., and Noorzad, A. (2015). "Load eccentricity effects on behavior of circular footings reinforced with geogrid sheets". *Journal of Rock Mechanics and Geotechnical Engineering*, Vol. 7, pp. 691-699.
6. Binquet, J., and Lee, K.L., (1975a). "Bearing capacity tests on reinforced earth slabs." *Journal of Geotechnical Engineering Division, ASCE*, Vol. 101, pp. 1241-1255.
7. Binquet, J., and Lee, K.L., (1975b). "Bearing capacity analysis on reinforced earth slabs." *Journal of Geotechnical Engineering Division, ASCE*, Vol. 101, pp. 1257-1276.
8. Chen, Q., Abu-Farsakh, M., Sharma, R., and Zhang, X. (2007). "Laboratory investigation of behavior of foundations on geosynthetic-reinforced clayey soil". *Journal of the Transportation Research Board*, Vol. 2004, pp. 28-38.

9. Guido, V. A., Chang, D. K., and Sweeney, M. A. (1986). "Comparison of geogrid and geotextile reinforced earth slabs". *Canadian Geotechnical Journal*, Vol. 23, pp. 435-440.
10. Lee, K.M., Manjunath, V.R., and Dewaikar., D.M. (1999). "Numerical and model studies of strip footing supported by a reinforced granular fill soft-soil system." *Canadian Geotechnical Journal,* Vol. 36, pp. 793-806.
11. Mandal, J. N., and Sah, H. S. (1992). "Bearing capacity tests on geogrid-reinforced clay". *Geotextiles and Geomembranes,* Vol. 11, pp. 327-333.
12. Omar, M. T., Das, B. M., Yen, S. C., Puri, V. K., and Cook, E. E. (1993). "Ultimate bearing capacity of rectangular foundations on geogrid-reinforced sand". *Geotechnical Testing Journal*, Vol. 16, pp. 246-252.
13. Ramaswamy, S. D., and Purushothaman, P. (1992). "Model footings of geogrid reinforced clay". *In Proceedings of the Indian Geotechnical Conference on Geotechnique Today,* Vol. 1, pp. 183-186.
14. Sakti, J. P., and Das, B. M. (1987). "Model tests for strip foundation on clay reinforced with geotextile layers". *Transportation Research Record,* Vol. 1153. pp. 40-45
15. Sawwaf, M. (2009). "Experimental and numerical study of eccentrically loaded strip footings resting on reinforced sand." *Journal of Geotechnical and Geo-environmental Engineering*, Vol. 135, pp. 1509-1518.
16. Sharma, R., Chen, Q., Abu-Farsakh, M., and Yoon, S. (2009). "Analytical modeling of geogrid reinforced soil foundation". *Geotextiles and Geomembranes,* Vol. 27, pp. 63-72.
17. Shin, E. C., Das, B. M., Puri, V. K., Yen, S. C., and Cook, E. E. (1993). "Bearing capacity of strip foundation on geogrid-reinforced clay". *Geotechnical Testing Journal,* Vol. 16, pp. 534-541.

18. Tafreshi, S. M., and Dawson, A. R. (2010). "Comparison of bearing capacity of a strip footing on sand with geocell and with planar forms of geotextile reinforcement". *Geotextiles and Geomembranes*, Vol.28, pp.72-84.
19. Vesic, A. S. (1975). "Bearing capacity of shallow foundations". *Foundation engineering handbook.*

CHAPTER 5

FOOTING RESTING ON SLOPPING SURFACE

5.1 General

Slope instability is a very frequent problem in soil slopes, road and railway embankment, landfills and deep cuts, etc. Generally, natural slope may lose their stability by sliding, and embankments may fail by a detachment of soil particles or by losing their shear strength. Various civil engineering projects require the construction of foundations on conventional slopes or grounds with high gradients. Such foundations are prone to low bearing capacity and high settlements, depending upon the location where footing is constructed with respect to the soil slope. Higher settlement of foundation can cause damage and cracks of the overlying structures. Many researchers have proffered possible solutions to mitigate this soil instability problem by using various types of reinforcing materials to enhance the bearing capacity of the soil and hence increase the overall strength of the soil to carry excess loads. A profuse amount of research has been carried out by researchers with inclusion of different reinforcing materials and additives to increase the load carrying capacity of the footing over soil slope and reducing their susceptibility towards settlements (Prabakar and Sridhar, 2002**;** Yetimoglu and Salbas, 2003**;** Consoli et al., 2003**;** Prabakar et al., 2004**;** Yetimoglu et al., 2005**;** Jellali et al., 2005**;** Hataf and Rahimi, 2006**;** Tang et al., 2007**;** Akbulut et al., 2007**;** Kumar and Gupta, 2015**;** Butt et al., 2016**).** Since the 1970s, advances in technology in material sciences have led to the production of extensively used geosynthetic materials in various aspects of civil engineering. In this chapter, the results obtained extensive laboratory-scale tests have been presented to analyze the performance of different geosynthetics in the improvement of the bearing capacity of a shallow foundation constructed over soil slopes and reducing the percentage settlement induced due to weak soil strength. Various parameters have been considered in the study, such

as the distance of the slope edge from the point of load application (*D*), slope angle (β), top layer spacing for reinforcements (*u*), vertical spacing between reinforcements (*h*), number of reinforcements (*N*), type of reinforcement, effect of mechanical properties of reinforcement and the optimum depth of reinforcement (*d*). The study has been conducted exclusively for each reinforcement type and the effect of reinforcement properties such as tensile strength, tensile modulus and aperture size has been analyzed and presented in the study. The major emphasis of the study is towards estimating the improved bearing capacity of the foundations being construction over sloping ground, with the application of different geosynthetics, tested under different working conditions. An improvement factor was determined for each settlement ratio (S.R) to give an incisive account of the improvement in the bearing capacity of the soil as a result of the application of reinforcements. The concept of improvement factor (*IF*) in terms of improved bearing capacity is the same as discussed in chapter 4. Four different settlement ratios (*s/B*) of 4%, 8%, 12%, and 16% were used to analyze the improvement factor which covers lower and higher settlement range. Hence, the improvement factor for footing restive over slopping surface can be represented as

$$IF = \frac{Q_r}{Q} \tag{5.1}$$

where Q_r and Q are the bearing capacity of reinforced and unreinforced soil. Along with estimating the increase in load-carrying capacity of the soil in terms of the bearing capacity, reduction in settlement as a result of the application of geosynthetic was also considered using the parameter Percentage Reduction in Settlement or *PRS*, which deduces the percentage reduction in settlement with the addition of geosynthetics as different *s/B* ratios. Hence, *PRS* can be represented as

$$PRS = 1 - \frac{s_r}{s} \times 100 \tag{5.2}$$

Where, S_r and S are the settlement of the reinforced bed and settlement of the unreinforced bed at a given applied pressure. Many researchers have also utilized settlement ratio (S.R) as a parameter to compare the settlement reduction with the application of geosynthetics (Chen et al., 2007). Foundations are designed in accordance to the allowable bearing capacity of the soil. Thus, the computation of ultimate bearing capacity becomes substantial to correctly assess the increase in construction viability of the soil with applications of geosynthetics. For the present study, A double tangent method is adopted for the bearing capacity analysis of reinforced soil.

5.2 Effect of top layer spacing

The first series of tests was carried out to determine the optimum top layer spacing of reinforcement. Experimental computation of the optimum top layer spacing was carried out using a series of laboratory scaled tests using the pre-described testing methodology. Fig 5.1 (a-c) shows the pressure settlement curves for GGR1, GGR2, and GTX respectively. As can be deciphered from the curves, maximum improvement has been obtained at u/B = 0.40 and subsequently, a decrease in improvement can be observed with the increase in the cover provided for reinforcement. For example, the bearing pressure of unreinforced soil was found to be 227.42 kPa corresponding to *UBC*, which increases as 235.57 kPa to 237.36 kPa when GGR1 placed at a depth of 0.2B and 0.4B, respectively (see Fig. 5.1 (a)). Further increasing the first reinforcement depth i.e. u = 0.6B, 0.8B to 1.0B, the value of bearing pressure decreases as 234.40 kPa , 233.78 kPa to 232.54 kPa, respectively. Similarly, for GGR2 (See Fig. 5.1 (b), the bearing pressure at *UBC* increases from 231.12 kPa to 233.34 kPa for u = 0.2B to 0.4B, respectively then it decreases as 227.60 kPa, 227.51 kPato 228.37 kPa for u = 0.6B, 0.8B and B, respectively. However, No pressure bearing pressure increment was observed in the case of geotextile reinforced soil see Fig. 5.1 (c)

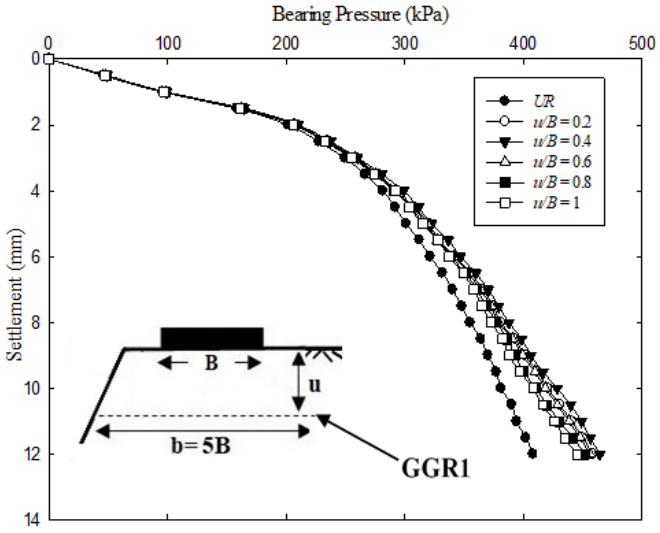

(a)

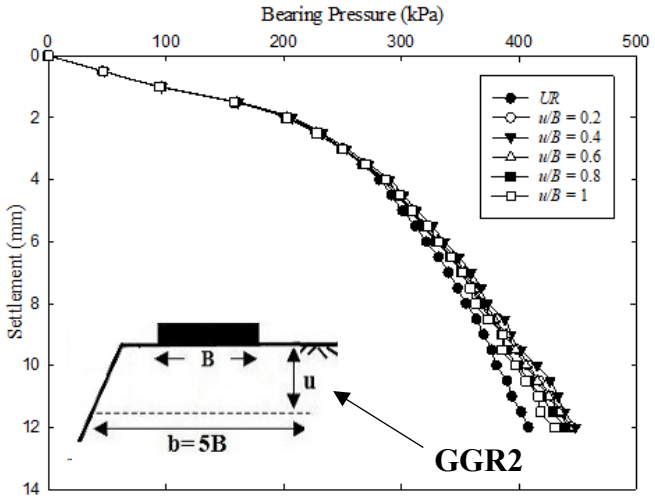

(b)

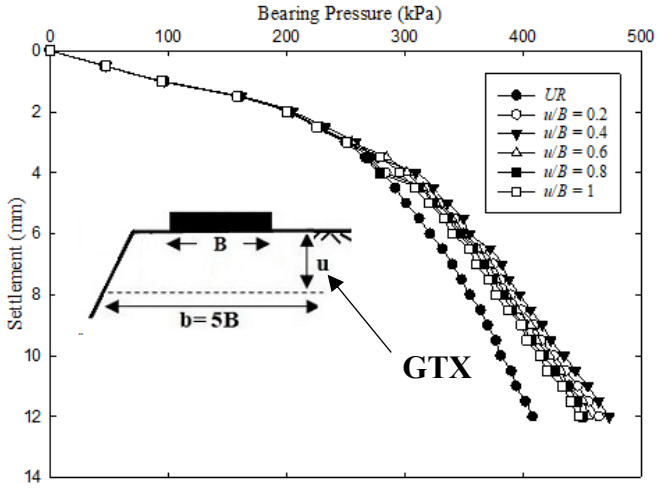

(c)

Fig. 5.1 Pressure Settlement Curve for (a) GGR1 (b) GGR2 (c) GTX at different *u/B* ratios

Fig 5.2 (a-c) depicts the improvement factor versus *u/B* for GGR1, GGR2 and GTX, respectively. As can be observed from the curves, the improvement factor increases with the increase in *u/B* ratio. Also, after the optimum depth of the top layer is reached, that is at *u/B* = 0.4, the decrease in the improvement factor fastens, thus suggesting that any further increase in depth of reinforcement would deteriorate the possible benefits of reinforcement. For example, the improvement factor at *UBC* increases as 1.03 to 1.04 when GGR1 placed at a depth of 0.2B and 0.4B, respectively. Further increasing the first reinforcement depth i.e. *u* = 0.6B, 0.8B to 1.0B, the value of bearing pressure decreases as 1.03, 1.02 to 1.02, respectively. Similarly, for GGR2, see Fig. 5.2 (b) the bearing pressure at *UBC* increases from 1.01 to 1.02 for u = 0.2B to 0.4B, respectively. After increasing further depth, no satisfactory improvement was observed. However, geotextile found to be performed negatively for lower settlement values, as shown in Fig. 5.2 (c)

Similar results have been obtained for all the reinforcement materials, thus signifying that reinforcement type has no bearing on the optimum depth of the top layer. At *u/B* = 0.2, lesser improvement is obtained than *u/B* = 0.4, thus signifying that occurrence of an optimum depth of initial layer reinforcement can be accredited to the lack of sufficient depth at *u/B* < 0.40 to mobilize significant friction between the reinforcements and the soil, which prevents the initiation of lateral resistance of the geosynthetic, thus not yielding then possible beneficial effects of applying a reinforcement. In other words, a lack of cushion of soil above the geosynthetic reinforcement prevents the development of sufficient tensile force in the reinforcement, which prevents the lateral deformation in the footing, from occurring. Also, lack of sufficient confining pressure for the top layer of the soil beyond the footing edges can also be attributed as another reason for obtaining such results.

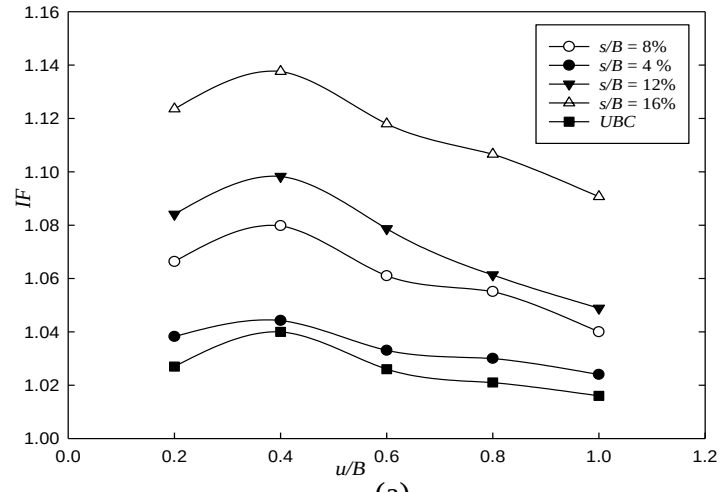

(a)

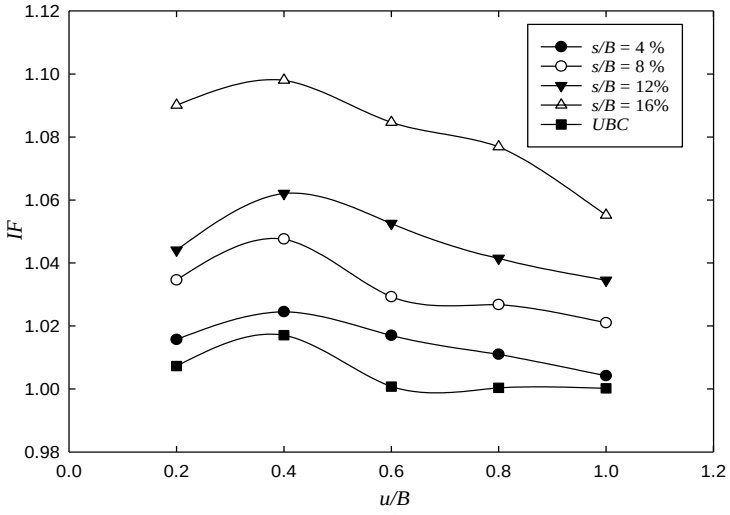

(b)

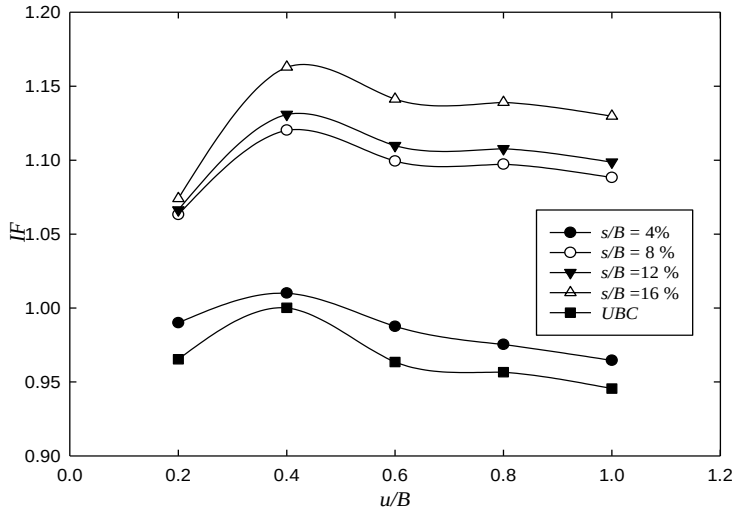

(c)

Fig 5.2 Improvement factor versus *u/B* for (a) GGR1 (b) GGR2 and (c) GTX

Fig 5.3 (a-c) shows the percentage reduction in settlement versus *u/B* curves for different *s/B* ratios. As can be seen from the graphs, GGR1 and GGR2 show a much higher reduction in the settlement at *s/B* ratio 4% in comparison to GTX, whereas, after smaller settlement ratios, geotextile performs better than both the geogrids, see Fig. 5.3 (c). It can thus be proffered that a sufficient embedment depth is required to mobilize significant lateral resistance in the reinforcement to ensure maximum improvement can be achieved with a geosynthetic. Similar results were obtained by (Shin and Das, 1998), who reported *u/B* of 0.4B for strip footing resting over clay slope reinforced with geogrid. (El Sawwaf, 2007) reported *u/B* equal to 0.6 for achieving maximum benefit from geogrid reinforcement on clay slope. The deviation in results could be due to the variation in properties of soil and geosynthetics used for the respective studies.

5.3 Effect of optimum depth and number of reinforcements

For ascertaining the effect of increasing number of reinforcement layers on the bearing capacity of the soil, the top layer was fixed at 0.40B, i.e. the optimum top layer spacing, and the spacing between the reinforcements was varied at 0.40B until addition of additional layers of reinforcements does not have any significant benefit towards improving the bearing capacity or the optimum depth of reinforcement is achieved. Reinforcement depth (*d*) for reinforcements having top layer spacing as *u* and vertical spacing between the *N* numbers of reinforcements being h can be represented as

$$d = u + (N - 1) \times h \tag{5.3}$$

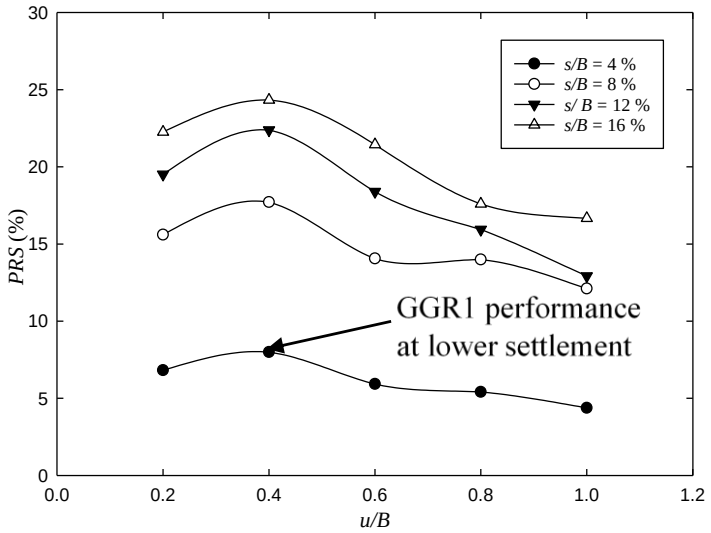

(a)

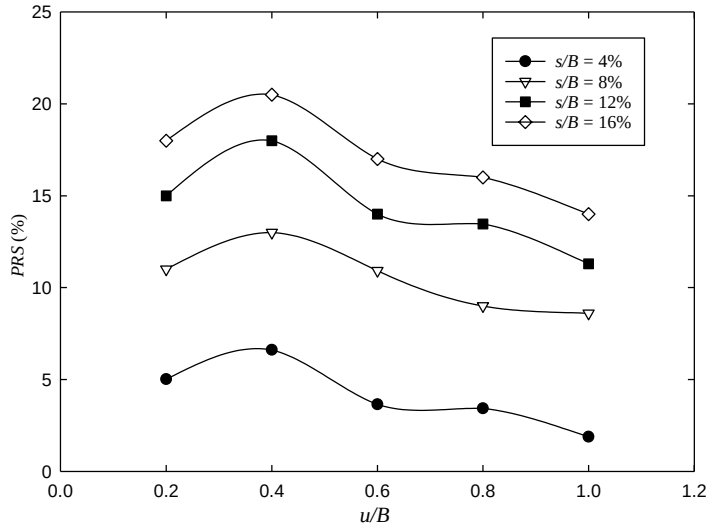

(b)

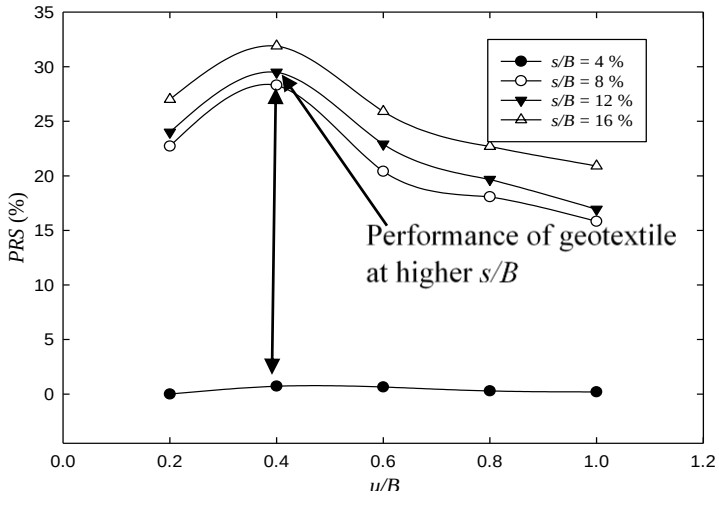

(c)

Fig 5.3 Percentage Settlement Reduction versus u/B for (a) GGR1 (b) GGR2 (c) GTX

Optimum reinforcement is the maximum depth beyond which any addition of geosynthetics thus not have a significant improvement towards the bearing capacity. Initial test was carried out at *D/B* = 1.0 and β = 45^{o}. Fig. 5.4 (a-c) show the pressure settlement curve for the for all the geosynthetics. It can be seen from all three graphs that there is a substantial improvement in bearing capacity of soil with the addition of multiple layers of reinforcements. For example, the foundation soil reinforced with GGR1, (see Fig. 5.4 a) at *s/B* = 4% (lower settlement level) the bearing capacity increases as 260, 328.62, 384.81, 436, and 446 kPa as N values increases from 1 to 5 respectively, similarly at *s/B* = 16% (higher settlement level), the bearing capacity increases as 464.15, 602, 706, 798.47, and 819 kPa as number of reinforcement increases from N = 1 to 5 respectively. Similar observations were observed in case of GGR2 reinforced soil (see Fig. 5.4 b). Whereas, in the case of GTX (see Fig. 5.4 c), at *s/B* = 4%, the bearing capacity increases as 250, 303, 351, 404 and 407 kPa as N values increases from 1 to 5 respectively. Whereas, for higher settlement (*s/B* = 16%), bearing pressure = 491, 652, 816.35, 879 and 892 kPa as N values increases from 1 to 5 respectively. From the above observations, it is observed that a significant amount of bearing capacity increment decreases as the additional number of reinforcement layers increases.

Fig 5.5 (a-c) also depict that effect of reinforcement becomes less substantial with the addition of the fifth layer of reinforcement and the fourth layer of reinforcement in case of geogrids and geotextile respectively, thus signifying that beyond this depth, any addition of extra layers of reinforcement will not be viable towards any further settlement reduction or load capacity enhancement. For example, the foundation soil reinforced with GGR1, (see Fig. 5.5 a) at *s/B* = 4% (lower settlement level) the improvement factor increases as 1.044, 1.31, 1.53, 1.73 and 1.77 as N values increases from 1 to 5 respectively, similarly at *s/B* = 16% (higher settlement level), the bearing capacity increases 1.3, 1.47, 1.73, 1.95 and 2.1 as number of reinforcement increases from N = 1 to 5 respectively.

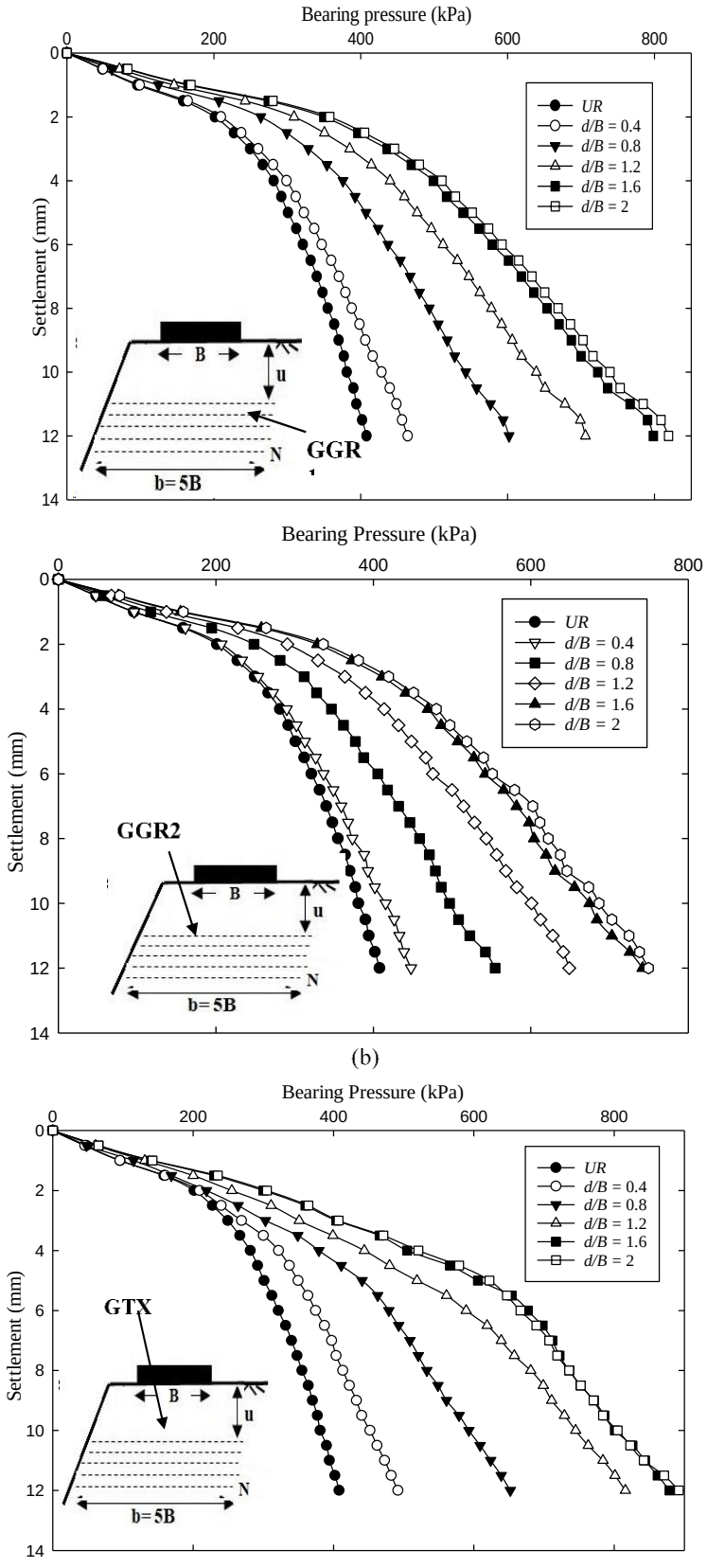

Fig. 5.4 Pressure Settlement Curves for (a) GGR1 (b) GGR2 and (c) GTX at different *d/B* ratios

Similar observations were observed in case of GGR2 reinforced soil (see Fig. 5.5 b). Whereas, in the case of GTX (see Fig. 5.5 c), at *s/B* = 4%, the improvement factor increases 1.07, 1.21, 1.40, and 1.63 % as N values increases from 1 to 5 respectively. Whereas, for higher settlement (*s/B* = 16%), This can be attributed to the stress envelope, which has a specific depth of influence. The increase in the bearing capacity of the soil with the increase in layers of geosynthetics can be attributed to the increase in friction between the reinforcement and the soil, which increases with the increase in geosynthetic layers. Also, better interlocking between the soil and geogrids and passive earth resistance can be attributed as the reason for the improvement of the bearing capacity. Better interlocking between the geogrid and the soil prevented the lateral deformation of the soil. As a result of applied load, tension is mobilized in the geosynthetics, which resist the shear stresses developed in the soil below the loading area and transfer them to the stable soil, thus eventually increasing the depth of the failure zone. Similar observations were observed by (Shin and Das, 1998), who reported that the inclusion of geogrid reinforcements became less substantive after a certain depth of reinforcement. They reported an optimum depth of 1.72B for geogrids and N = 5 as the substantive number of layers of reinforcements for the case of strip footing.

The variation in the depth of reinforcements can be attributed to the deviation in soil, footing shape, and geosynthetic properties being used for the experimental study. (Chen et al., 2007) reported an optimum depth of 1.5B and 1.25B for geogrids and geotextile respectively for square footing resting over clay foundations. (Shin and Das, 1998) however, reported that geotextile reinforcements beyond 1.0B could not improve the footing performance (Badakhshan and Noorzad, 2015) reported that beyond *N*=3, an increase in the number of layers of reinforcements had a reducing effect in case of circular footing under eccentric loading.

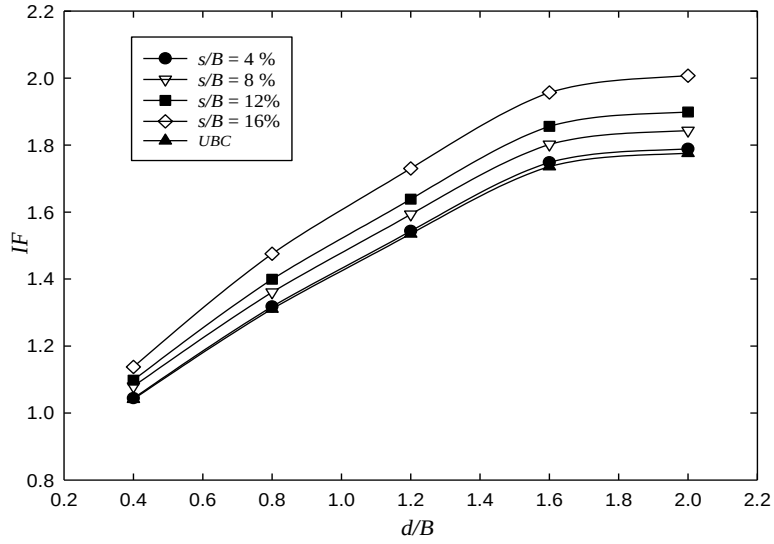

(a)

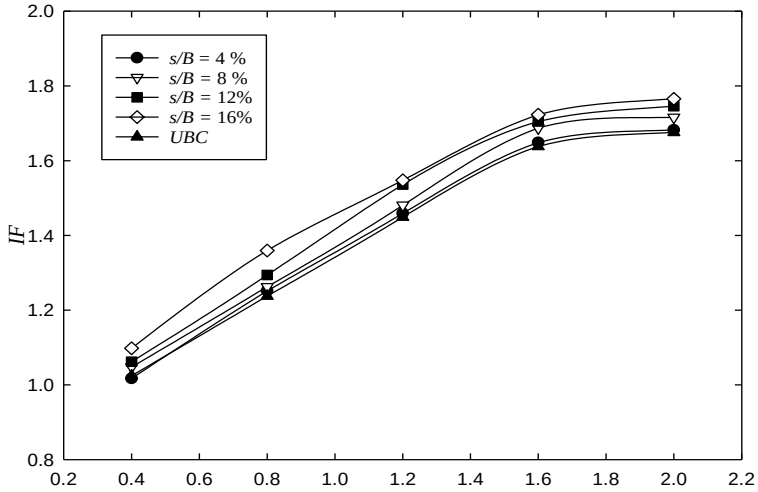

(b)

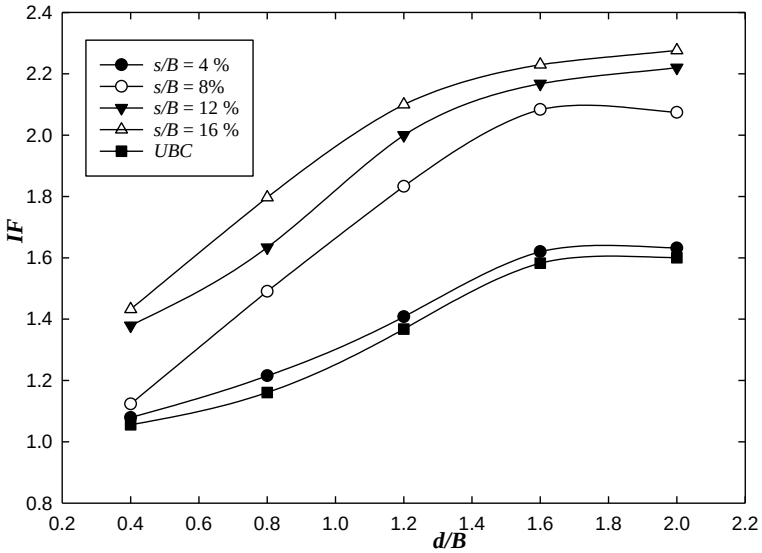

(c)

Fig 5.5 Improvement Factor versus *d/B* Curves for (a) GGR1 (b) GGR2 (c) GTX

5.4 Effect of spacing between reinforcements

A series of laboratory tests to check the effect of vertical spacing of the reinforcement were carried out by fixing the top layer at 0.40B from the base of footing for all the geosynthetics and varying the second layer by 0.2B, 0.4B, 0.6B, 0.8B, and 1B. Fig. 5.6 (a-c) shows the pressure settlement curves for the geosynthetics. From Fig. 5.6 (a) GGR1 case at settlement ratio of s/B = 4% it can be observed that the bearing pressure rises as 29, 31.78 to 41.8% (Bearing pressure = 322.42, 328.62 and 353.59) then decreases to 26.72 and 25.6% (Bearing pressure 316, 313.4 kPa) for *h/B* ratios 0.2, 0.4, 0.6, 0.8 and 1 respectively. Similarly, in case of GGR2 see Fig 5.6 (b) bearing pressure rises as 21, 25 to 27.9% (Bearing pressure = 302.68, 312 and 318.53) then decreases to 25.64 and 25.9% (Bearing pressure = 312.86 313.6 kPa) for *h/B* ratios 0.2, 0.4, 0.6, 0.8 and 1 respectively. But in case of GTX for s/B = 4%, a different trend has been observed which shows that the bearing pressure increases as 11, 24.3% (Bearing Pressure = 278, 310, kPa) then it falls like 23.2, 22.3, 20.3% (307, 305.4, 301.2 kPa). The same trend has been observed for higher settlements. From the above observations it is cleared that 0.4B is the optimum vertical spacing for GTX and 0.6B for GGR1 and GGR2, respectively. The tests were carried out at *D/B* = 1 and β=45˚. Fig. 5.7 (a-c) show the graphs of improvement factor graphs for all the geosynthetics.

It is cleared from the graphs that an optimum value of *h/B* exists for which there is a maximum improvement in the bearing capacity, and beyond this depth, there is a decrease in the improvement factor for the reinforced foundation soil. Fig. 5.7 (a-c) also show that the influence of reinforcement on vertical spacing is very effective for higher settlement ratios, whereas for lower settlement, the value of *IF* is not varied much with rising the spacing of reinforcement. (Shin and Das, 1998) reported a vertical spacing of 0.8B in case of geogrids, whereas, (Guido et al., 1986) and (Chen et al., 2007) reported a vertical spacing of 0.167B for square footing resting over clay foundation.

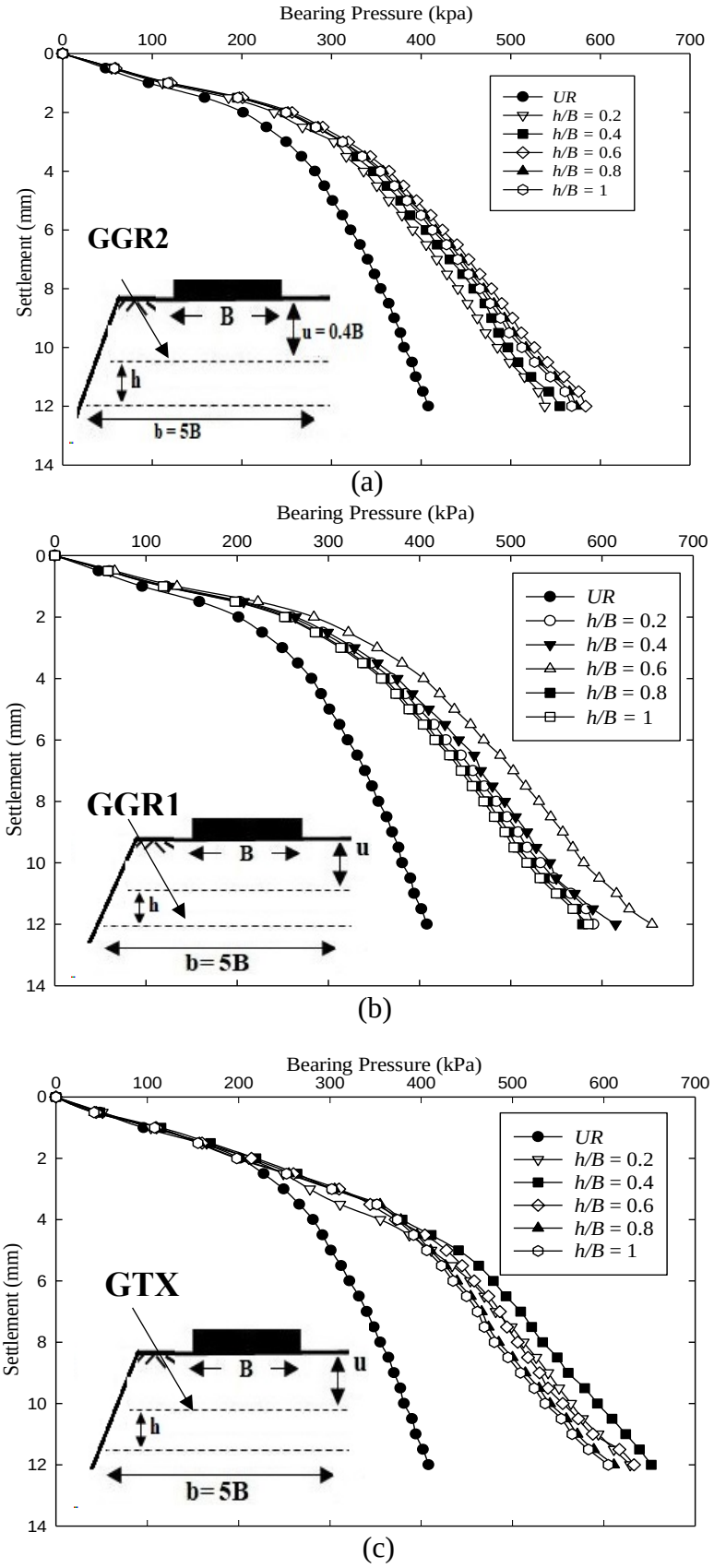

Fig. 5.6 Pressure Settlement Curves for (a) GGR1 (b) GGR2 and (c) GTX at different *h/B* ratios

(Yoo, 2001) obtained an optimum vertical spacing of 0.7B for slope formed completely of sand. The reason for this can be attributed to the necessity of a suitable cover between reinforcements to mobilize substantial lateral resistance in them.

5.5 Effect of type of reinforcement

Three different types of geosynthetics were used in the study to compare the influence of different geosynthetic properties on the bearing capacity of foundation over soil slope. GGR1 has higher stiffness and larger aperture size with respect to GGR2. Fig. 5.8 (a-c) show the percentage reduction in settlement curves at different depth of reinforcements for the three chosen geosynthetics. As can be seen from the curves, GGR1 performs better than GGR2 and shows a much higher reduction in the settlement. This signifies that geogrid properties, such as tensile strength, tensile modulus/ stiffness and aperture size, have a significant role in the performance of the geogrid towards providing efficient reinforcement. (Lee and Manjunath, 2000) also reported that geogrids with higher tensile modulus provided the best results in the case of geosynthetic reinforced sand slopes. It can be observed that GGR1 and GGR2 performed better than geotextile for lower settlement ratios, but for higher settlement GTX performed much better and provided a much higher improvement than others. See Fig. 5.8 (c) when three geotextiles were provided, PRS value at s/B = 4% was found as 42% whereas at s/B = 16% a significant rise i.e. 108 % have been observed in PRS value. The reason for the same can be explained by the fact that geotextile has much higher tensile strength than the geogrids and thus requires greater deformation to completely mobilize its capacity. Geogrids, however, can efficiently mobilize its lateral stress resistance capacity at lower settlement ratios, due to the confinement effect, which is the major reinforcement mechanism in geogrids, and thus performs better than geotextile for smaller s/B ratios.

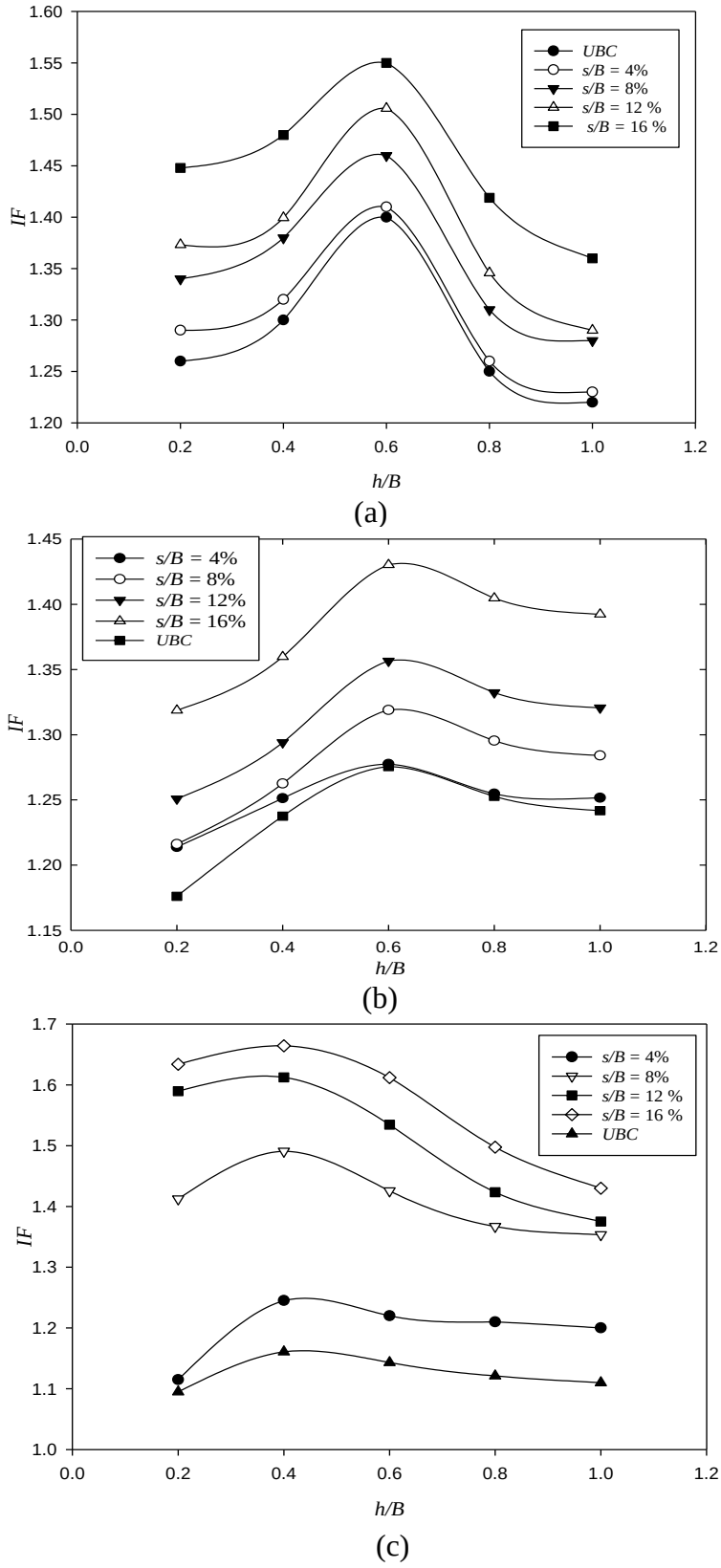

Fig. 5.7 Improvement factor versus *h/b* for (a) GGR1 (b) GGR2 and (c) GTX at different *h/B* ratios

Generally, construction requirements require a foundation to be constructed for the ultimate bearing capacity of the soil. It can be clearly observed that geogrids perform better than the geotextile for improvement in the ultimate bearing capacity of the soil. GGR1 is the best performing material out of the three chosen materials for limited settlement requirements. However, geotextiles primary function is to act as a filter or in drainage purposes, such as in landfills, and thus can be considered as reinforcement material where small tensile strength is required. (Lee and Manjunath, 2000) reported similar findings when they compared the two types of geosynthetics, i.e. geogrids and geotextiles.

To analyze the characterization of the geosynthetics before and after the failure, SEM analysis was conducted for GGR1, GGR2, and GTX before and after performing $u/B = 0.4$ tests. For this purpose, a representative sample of the same was procured from where maximum yielding has been observed. SEM photographs of Non-deformed and deformed geotextile are shown in Fig.5.9 (a-c). From Fig. 5.9 (a) it is confirmed that the geotextile is woven type as it indicates that both warp and weft are interlocked with each other, and they are made of multifilament. The fiber arrangement is orthogonal, and very fewer openings are visible in the whole structure. A comparison of non-deformed and deformed geotextiles indicates that there could be two modes of the failure of geotextile. First, a tearing of yarn from the fabric and another is the higher elongation of multifilament in the loading direction. Tearing of yarn from the fabric could be due to the friction between the soil particles and reinforcement and also due to the tensile failure of yarn. From Fig. 5.9 (b-c), it is clearly seen that the orientation of the multifilament has changed after the failure, which creates a number of openings at the junction of warp and weft. The formation of openings imparts a poor retention capacity of soil and results in a reduction of bearing capacity of the soil. The opening of yarns in the geotextile after the application of a certain strain facilitates the confinement of the soil particles within the geotextile mass, thus promoting confinement

effect, which is a major reinforcement mechanism in geogrids, along with the membrane effect, which is the common reinforcement mechanism of the geotextiles. The higher tensile strength of the geotextiles in comparison to the geogrids thus promotes better confinement effect in comparison to the geogrids, which could be the reason for better performance of the geotextiles in comparison to the geogrids. Fig. 5.10(a and b) shows the SEM pictures of the 3D geogrid. Form Fig. 5.10 (a and b) it is cleared that the surface texture is uniform when sample was not loaded, but after loading wave formation and cracks can be seen in the geogrid see Fig.5.10 (c and d). Fig.5.11 (a-b) shows the SEM photographs of Non-deformed and deformed glass grids respectively. While Fig. 5.12 (a-b) show the loss of glass coating before and after the failure. It can be easily seen that the glass grid crystals have uniform coating along with its structure. However, after the failure in the glass grid isolates the crystals attached to the surface. Presence of these damages indicates a possible reduction in the strength of the glass grid.

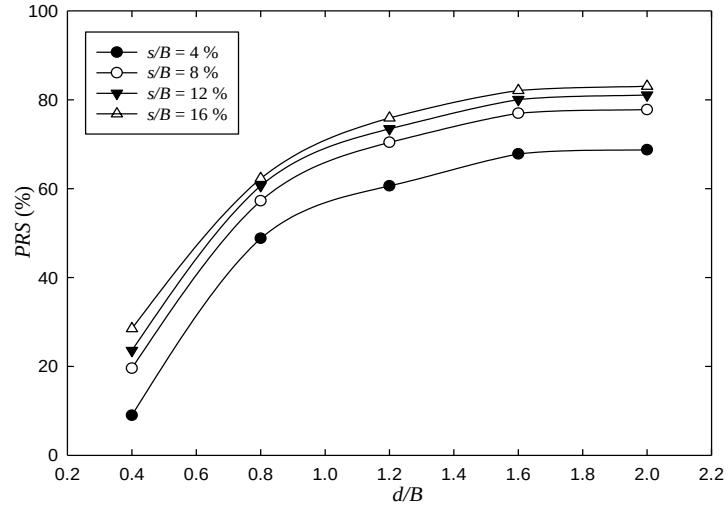

(a)

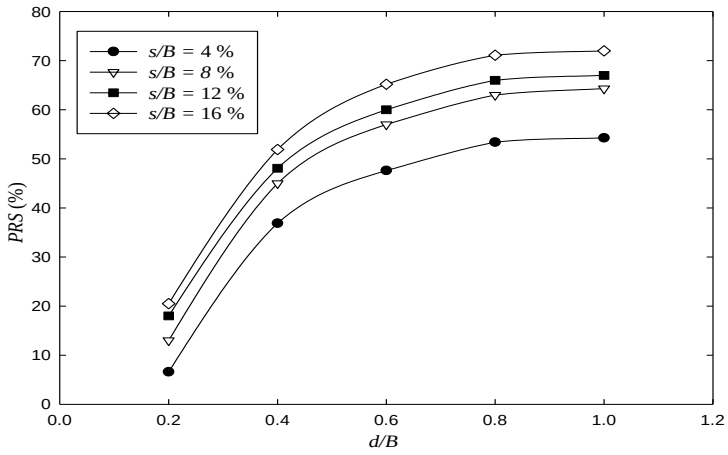

(b)

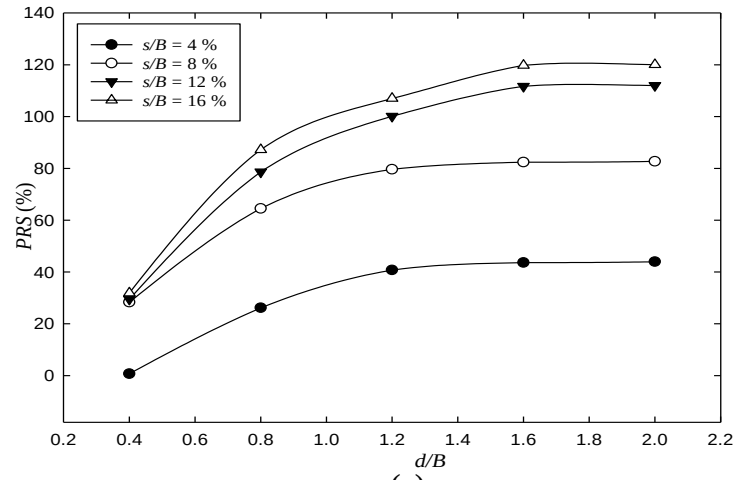

(c)

Fig 5.8 Percentage Settlement Reduction versus d/B for (a) GGR1 (b) GGR2 (c) GTX

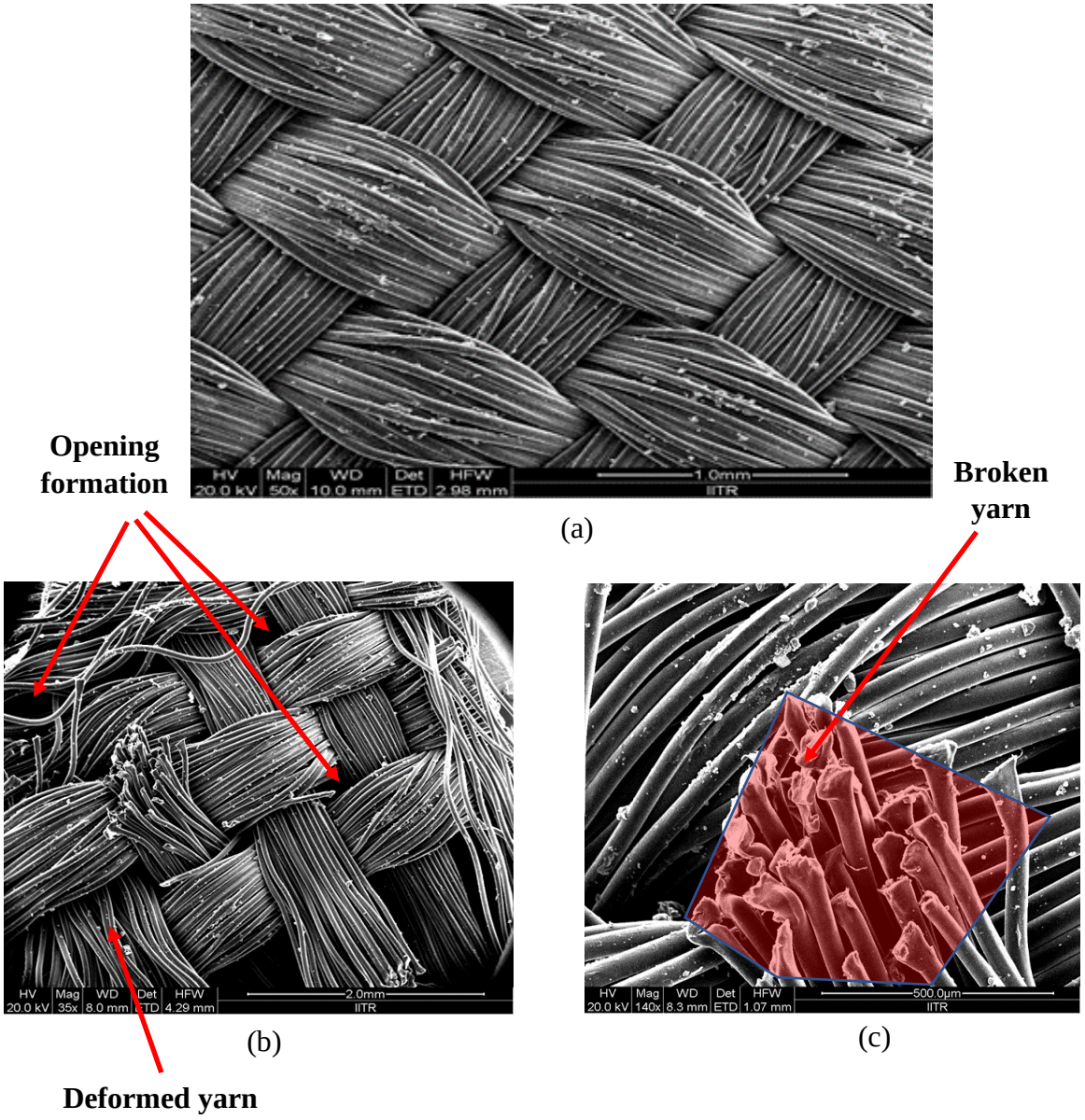

Fig. 5.9 SEM images of (a) geotextile before testing (b) and (c) geotextile after testing

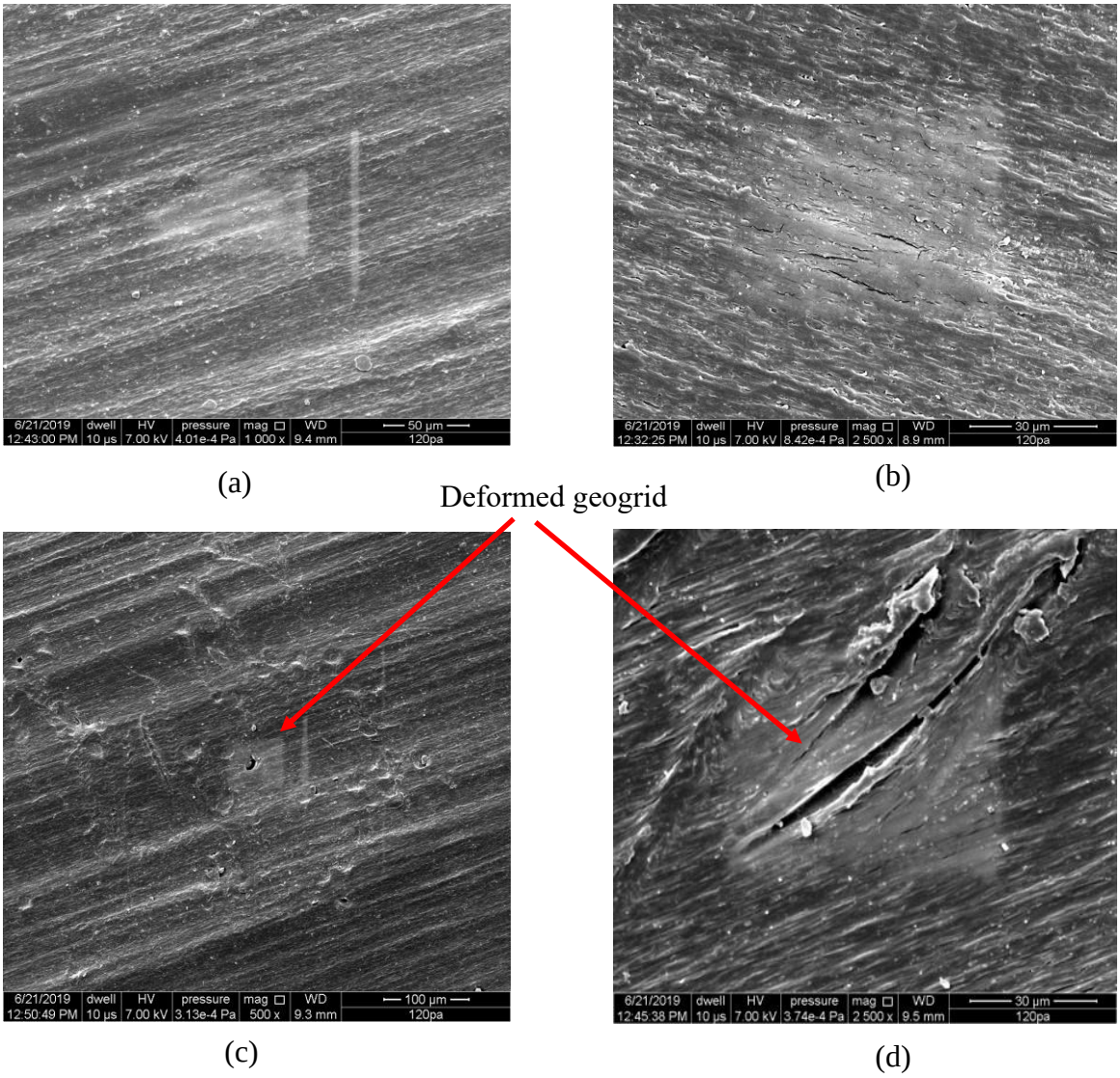

Fig. 5.10 SEM images of 3D geogrid (a & b) before testing (c & d) after testing

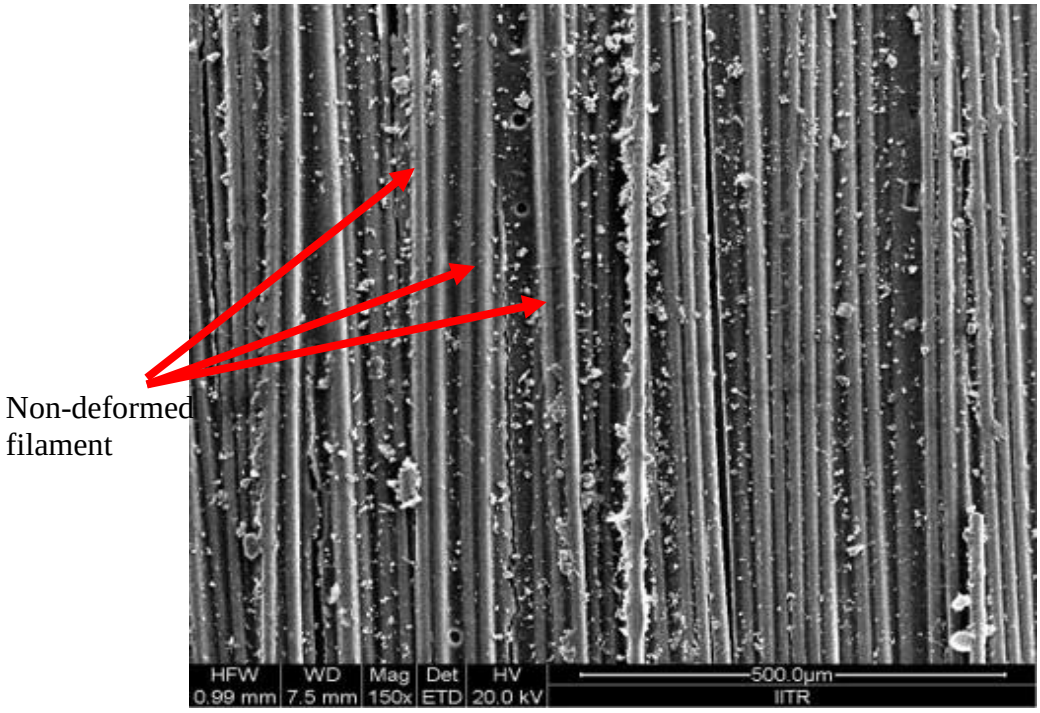

(a)

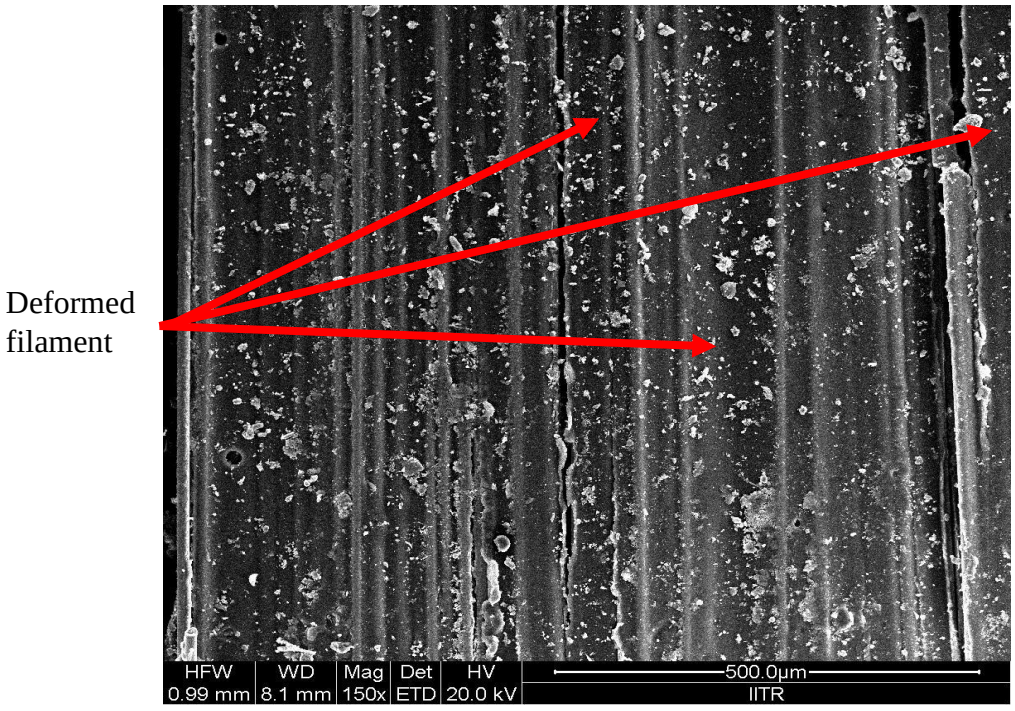

(b)

Fig. 5.11 SEM images of gasgrid (a)Non deformed geogrid (b) Deformed geogrid

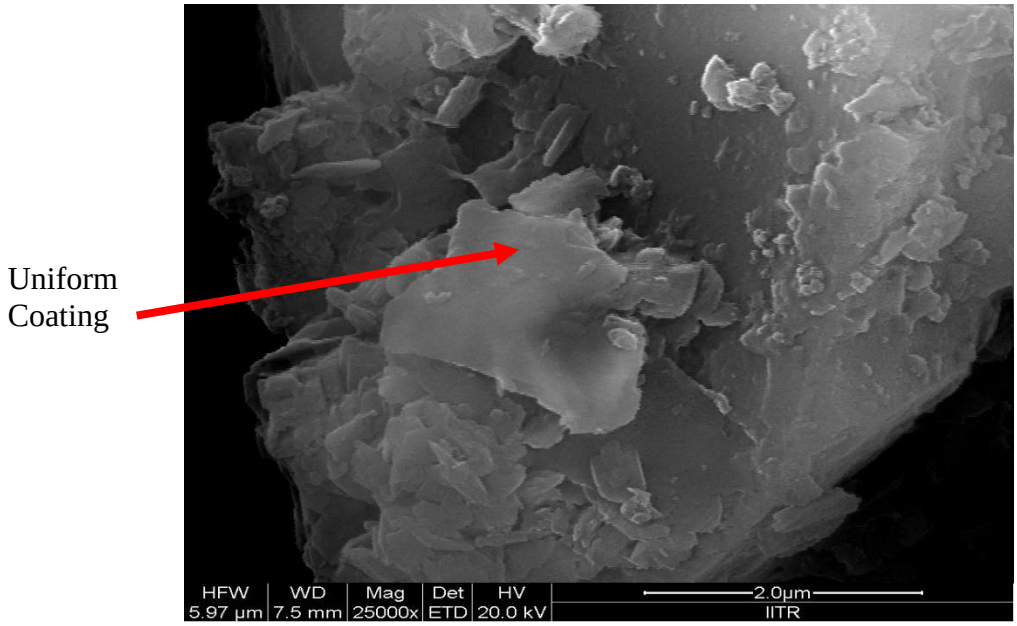

(a)

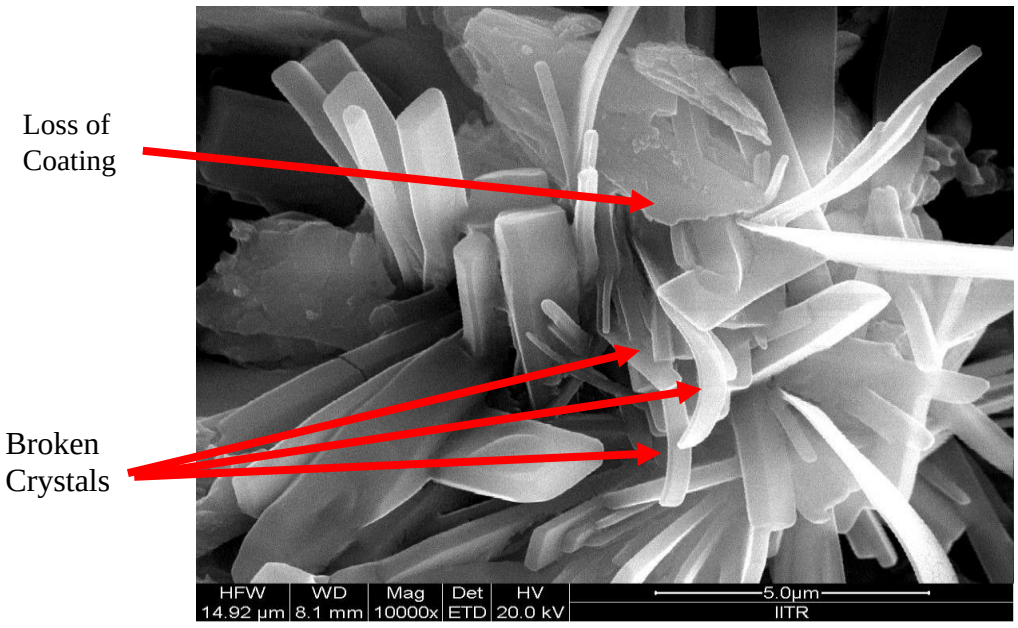

(b)

Fig. 5.12 SEM images of (a) Uniform coating of glass crystals on glasgrid (b) Deformed glass crystals

5.6 Effect of slope geometry

A number of tests were performed in the laboratory to find the effect of edge distances and slope angles on the bearing capacity of the slope. Fig. 5.13 (a-c) show the improvement factor versus *d/B* curves for different slope angles at *D/B* =1. It can be clearly observed that the

bearing capacity decreases with the increase in the slope angle. Also, the change in the slope angles does not change or alter the position of the optimum depth of reinforcement, with the number of optimum layers of reinforcement remaining 4 for each of the cases, although the magnitude of improvement factor is the highest at β=35º. Three series of tests were conducted to analyze the influence of *D/B* ratios on the bearing capacity as represented in Fig 5.14 The bearing capacity increased with the increase in the edge of the slope and the loading area. The change in load-carrying capacity with edge distance can be explained by the increasing passive earth pressure with increasing distance from the slope. More passive pressures cause wider and deeper failure zones, thus causing an increase in load-carrying capacity. The effect of the slope is minimized when the load is placed at an edge distance of two times of loading area. (Shin and Das, 1998) reported that at $D/B > 3$, slope angle β thus not have any effect on the bearing capacity. Although the bearing capacity of the soil decreases as the distance from the slope edge increases, Fig.5.14 also shows that maximum improvement in bearing capacity is obtained when the reinforcement is kept at the slope crest without providing any slope edge distance in the case of a single layer reinforcement kept at $u/B = 0.40$. Although the improvement in bearing capacity is greater than that obtained for $D/B = 1$ and 2, the magnitude of bearing capacity is much greater in the case of the later. This observation can be attributed to the greater tensile force mobilized in the reinforcements at $D/B = 0$ due to greater settlement of foundation soil overlying the reinforcement layer, which prevents lateral deformation and facilitates better improvement in bearing capacity. However, the overall magnitude of the bearing capacity increases with increasing *D/B* ratio. This result is in line with the result obtained by (Sawwaf et.al., 2007) who reported a similar trend for geogrid reinforced slope.

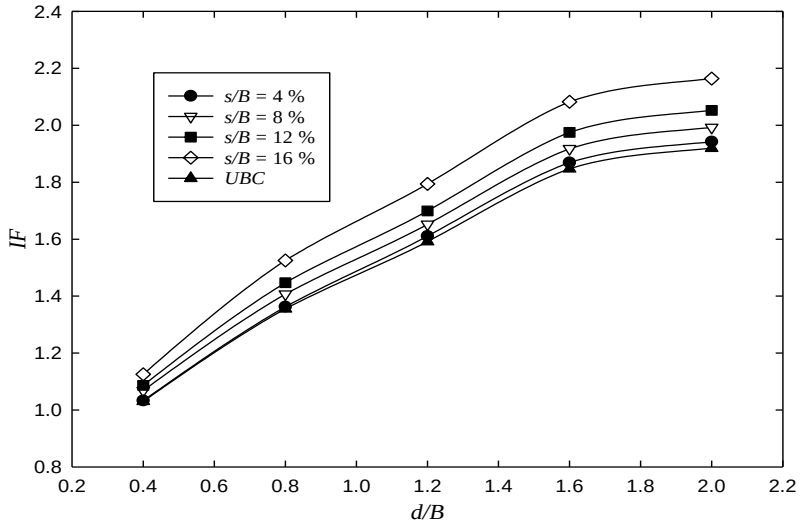

(a)

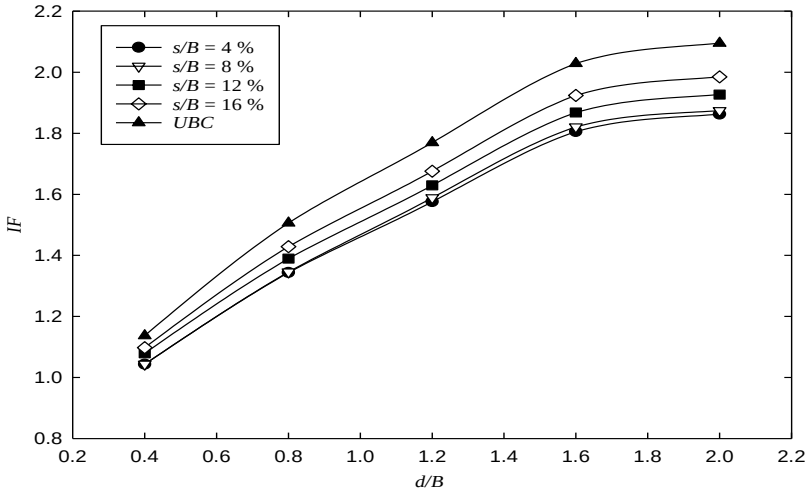

(b)

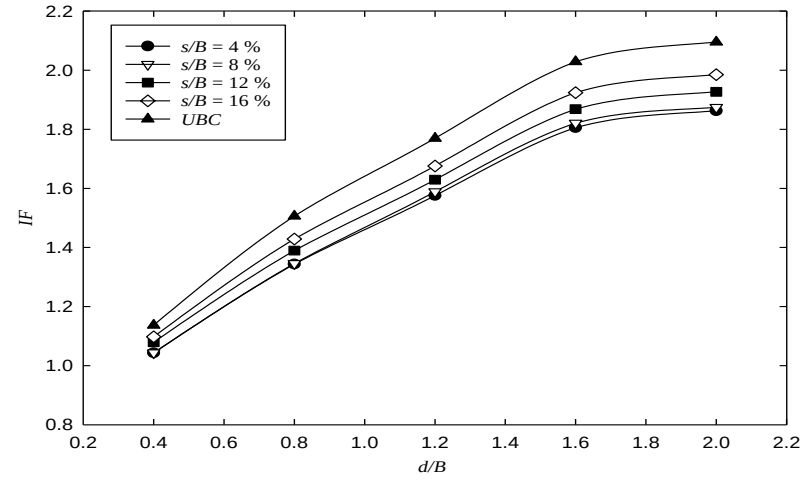

(c)

Fig. 5.13 Improvement factor curves for (a) β=35º (b) 40º (c) 45º

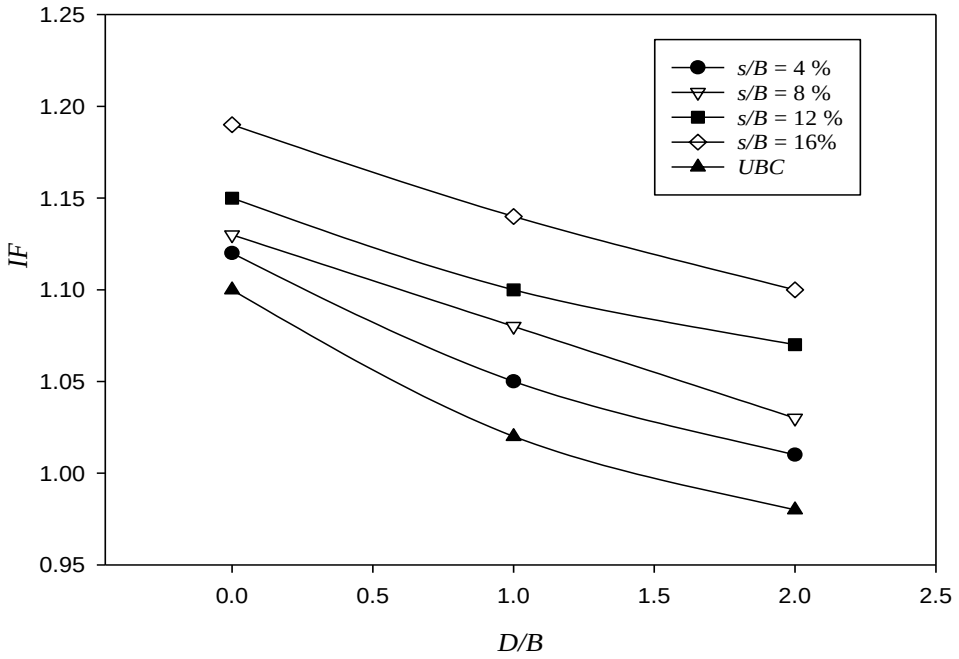

Fig. 5.14 Improvement factor versus D/B curve

5.7 Summary and conclusions

In this study, a series of laboratory tests were conducted to analyze the performance of various geosynthetics towards increasing the bearing capacity of shallow foundations built over soil slope. Geosynthetic reinforcement significantly increased the bearing capacity of the soil and facilitated in settlement reduction, subject to the location of placement of the geosynthetic within the slope. The key findings from the study, which can be significant in computation of allowable bearing capacity of geosynthetic reinforced foundations in the field are as follows:

1. The optimum depth of top layer reinforcement for GGR1, GGR2 and GTX were obtained at u/B = 0.4. This signifies the need for a cover for the reinforcement to completely mobilize the tensile strength within them. Also, optimum depth for a single layer reinforcement was obtained as 0.40B for all the three reinforcement materials, signifying that the reinforcement type did not have a bearing on the top layer spacing.
2. The optimum depth of reinforcement (*d*) was obtained at *d/B* ratio of 1.6B and 1.2B respectively for geogrids and geotextile. After testing for reinforcement at a deeper point, the increase in bearing capacity was not substantial, thus signifying the presence of an

optimum depth beyond which inclusion of a geosynthetic is not viable and the maximum number of reinforcements for geogrid and geotextile was obtained as 4 and 3 respectively.

3. Vertical spacing between reinforcements also played a crucial role in amassing maximum benefit from reinforcements. Optimum vertical spacing was obtained at 0.6B and 0.4B for geogrids and geotextiles respectively.
4. The maximum benefit from reinforcement was obtained at *D/B* ratio equal to 0, although the highest magnitude of bearing capacity was obtained as the distance between the loading area and the slope edge increased.
5. The maximum bearing capacity was achieved at $\beta=35^{o}$, with respect to $\beta=40^{o}$ and 45^{o}.

Table 5.1 Summary of the tests test results based on optimum positions of reinforcements

Test No.	**Configuration**	***s/B = 4%***	***s/B = 8%***	***s/B = 12%***	***s/B = 16%***	***UBC***
		IF	***IF***	***IF***	***IF***	***IF***
1.	GG1 (N=1) (u/B=0.4)	1.04	1.07	1.09	1.14	1.04
2.	GG1 (N=2) (d/B=0.8)	1.31	1.36	1.39	1.47	1.31
3.	GG1 (N=3) (d/B=1.2)	1.54	1.59	1.63	1.73	1.53
4.	GG1 (N=4) (d/B=1.6)	1.74	1.8	1.85	1.95	1.73
5.	GG1(N=2) h/B = 0.6	1.41	1.46	1.5	1.6	1.41
6.	GG2 (N=1) u/B=0.4	1.02	1.04	1.06	1.09	1.01
7.	GG2 (N=2) d/B=0.8	1.25	1.26	1.29	1.35	1.23
8.	GG2 (N=3) d/B=1.2	1.45	1.48	1.53	1.54	1.44
9.	GG2 (N=4) d/B=1.6	1.64	1.68	1.7	1.72	1.63
10.	GG2 (N=2) h/B=0.6	1.27	1.31	1.35	1.43	1.27
11.	GTX (N=1) u/B=0.4	1	1.12	1.13	1.162	1
12.	GTX (N=2) d/B=0.8	1.21	1.49	1.63	1.79	1.16
13.	GTX (N=3) d/B=1.2	1.4	1.83	2	2.1	1.36
14.	GTX (N=4) d/B=1.6	1.62	2.08	2.16	2.23	1.58
15.	GTX (N=2) h/B=0.6	1.01	1.12	1.13	1.16	1

REFERENCES

1. Akbulut, S., Arasan, S., and Kalkan, E. (2007). “Modification of clayey soils using scrap tire rubber and synthetic fibers”. *Applied Clay Science,* Vol. 38, pp. 23-32.
2. Badakhshan, E., and Noorzad, A. (2015). “Load eccentricity effects on behavior of circular footings reinforced with geogrid sheets”. *Journal of Rock Mechanics and Geotechnical Engineering*, Vol. 7, pp. 691-699.
3. Butt, W. A., Mir, B. A., and Jha, J. N. (2016). “Strength behavior of clayey soil reinforced with human hair as a natural fibre”. *Geotechnical and Geological Engineering*, Vol 34, pp. 411-417.
4. Chen, Q., Abu-Farsakh, M., Sharma, R., and Zhang, X. (2007). “Laboratory investigation of behavior of foundations on geosynthetic-reinforced clayey soil”. *Journal of the Transportation Research Board,* Vol. 2004, pp. 28-38.
5. Consoli, N. C., Vendruscolo, M. A., and Prietto, P. D. M. (2003). “Behavior of plate load tests on soil layers improved with cement and fiber”. Journal of *Geotechnical and Geoenvironmental engineering,* Vol. 129, pp. 96-101.
6. Sawwaf, E., M. (2007). “Behavior of strip footing on geogrid-reinforced sand over a soft clay slope. *Geotextiles and Geomembranes,* Vol. 25, pp. 50–60. doi.org/10.1016/j .geotexmem.2006.06.001
7. Guido, V. A., Chang, D. K., and Sweeney, M. A. (1986). Comparison of geogrid and geotextile reinforced earth slabs. *Canadian Geotechnical Journal,* Vol. 23, pp. 435-440.
8. Hataf, N., and Rahimi, M. M. (2006). “Experimental investigation of bearing capacity of sand reinforced with randomly distributed tire shreds”. *Construction and Building Materials,* Vol. 20, pp. 910-916.
9. Jellali, B., Bouassida, M., and De Buhan, P. (2005). “A homogenization method for estimating the bearing capacity of soils reinforced by columns”. *International Journal for Numerical and Analytical Methods in Geomechanics,* Vol. 29, pp. 989-1004.
10. Kumar, A., and Gupta, D. (2016). “Behavior of cement-stabilized fiber-reinforced pond ash, rice husk ash–soil mixtures”. *Geotextiles and Geomembranes,* Vol. 44, pp. 466-474.
11. Lee, K.M. and Manjunath, V.R., (2000). "Experimental and numerical studies of geosynthetic-reinforced sand slopes loaded with a footing". *Canadian Geotechnical Journal*, Vol. 37, pp. 828-842.

12. Osman, A.S., and Bolton, M.D., (2005). "Simple plasticity-based prediction of the undrained settlement of shallow circular foundations on clay." *Geotechnique*, Vol. 55, , pp. 435-447.
13. Prabakar, J., and Sridhar, R. S. (2002). "Effect of random inclusion of sisal fibre on strength behaviour of soil". *Construction and Building Materials*, Vol.16, pp. 123-131.
14. Prabakar, J., Dendorkar, N., and Morchhale, R. K. (2004). "Influence of fly ash on strength behavior of typical soils". *Construction and Building Materials,* Vol. 18, pp. 263-267.
15. Shin, E.C., and Das, B.M. (1998). "Ultimate Bearing Capacity of Strip Foundation on Geogrid-Reinforced Clay Slope". *KSCE Journal of Civil Engnieering*, Vol. 2, pp. 481-488.
16. Tang, C., Shi, B., Gao, W., Chen, F., and Cai, Y. (2007). "Strength and mechanical behavior of short polypropylene fiber reinforced and cement stabilized clayey soil". *Geotextiles and Geomembranes*, Vol 25, pp. 194-202.
17. Yetimoglu, T., and Salbas, O. (2003). "A study on shear strength of sands reinforced with randomly distributed discrete fibers". *Geotextiles and Geomembranes,* Vol. 21, pp. 103-110.
18. Yetimoglu, T., Inanir, M., and Inanir, O. E. (2005). "A study on bearing capacity of randomly distributed fiber-reinforced sand fills overlying soft clay". *Geotextiles and Geomembranes*, Vol. 23, pp.174-183.
19. Yoo, C., 2001. Laboratory investigation of bearing capacity behavior of strip footing on geogrid-reinforced sand slope. *Geotextile and Geomembranes*, Vol. 19, pp. 279-298.

CHAPTER-6

VALIDATION OF NUMERICAL RESULTS WITH EXPERIMENTAL RESULTS AND SCALE EFFECT STUDY

6.1 General

The finite element method is increasingly being used in bearing capacity computations of foundation soil bearing capacity analysis in recent years. The finite element method is well identified as being a very precise tool, and numerous examples of its application to modeling of reinforced soil foundations can be found in the literature (Abu-farsakh et al., 2012; Adem and Vanapalli, 2014; Arab et al., 2017; Azzam and Farouk, 2010; Griffiths and Lane, 1999; Karim et al., 2011; Lal and Mandal, 2012; Liu and Zhao, 2013).

Finite element analysis was carried out on the different size of footings using Plaxis 2D. In the present study, a square footing was used over reinforced soil. So, to observe the actual behavior of footing, a 3D modeling of footing is required. However, 3D modeling is time-consuming and very hard to run in manifold cases. Many researchers have successfully converted square footing into a circular footing with an equivalent area in bearing capacity analysis (Bolton and Osman, 2005; Chen, 2007; Jie Gu 2011). (Skempton, 1951) also considered a square footing as a circular footing with the equivalent area. The finite element analysis with approximation has been chosen in the study. Initially, the square footing has been converted in circular footing with following relations (Chen, 2007)):

$$D = \frac{2\,B}{\sqrt{\pi}} \tag{6.1}$$

where *B* is the width of the square footing; *D* is the diameter of the equivalent circular footing.

6.2 Dimensioning of the model

Dimensions of the finite element model employed were chosen so that it was sufficiently large and, thus, the constraints imposed at the boundaries will have very little influence on the stress distribution in the system. Axisymmetry conditions were chosen to simulate the reinforced soil conditions. Since the foundation bed symmetrical so one part of the footing has been analyzed. During mesh development, clusters were divided into triangular elements. The meshes are composed of 15 noded triangular elements that can more conveniently measure continuously varying stress-strain fields in comparison to the 6 noded elements. Standard fixities were applied to set up the boundary conditions for the model. The behavior of the soil was modeled using the Mohr-Coulomb soil model. The Mohr-Coulomb model assumes that the failure occurs when shear stress at any point in the material reaches a value which depends linearly on the normal stress in the same plane. The soil was modeled under undrained conditions. The footing was modeled as a rigid steel plate. The initial model was set up by defining the geometry and boundary conditions of the model. The prepared model of reinforced soil foundation resting over flat ground is presented in Fig. 6.1.

6.3 Properties of the materials used in modeling

Three types of materials soil, geogrid, and plate were used in the modeling. GGR1 is used as reinforced material in the soil foundation. The properties of the material required for modeling are shown in Table 6.1.

Table 6.1 Properties of the material used in FEM

Parameters	**Soil**	**Geogrid**	**Footing**
Elastic Modulus (kPa)	15×10^3	-	2×10^8
Poisson's ratio (υ)	0.3	-	-
Friction angle	22^o	-	-
Cohesion (kPa)	16	-	-
Stiffness (kN/m)	-	550	-

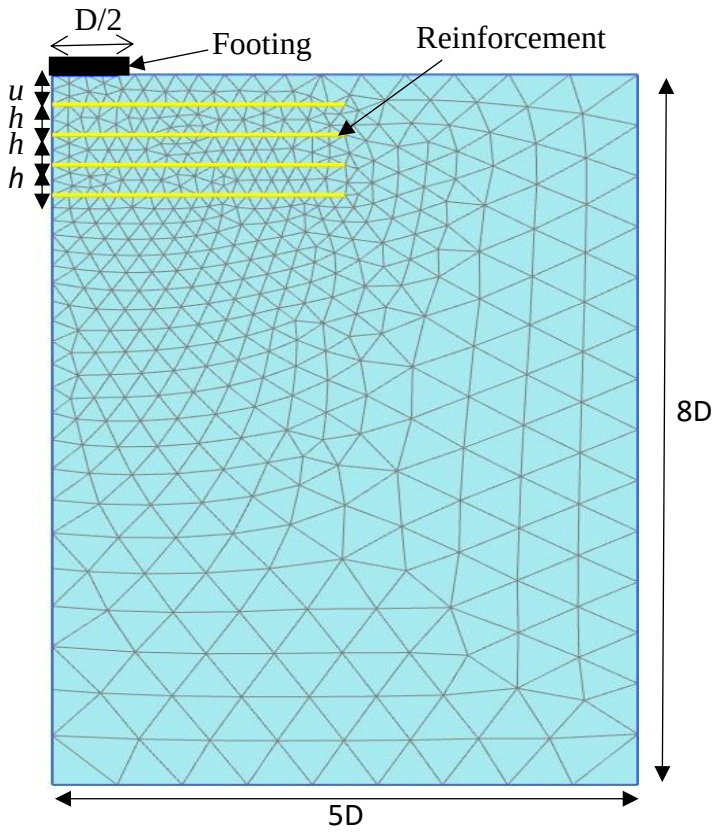

Fig. 6.1 Finite element model footing over flat ground

6.4 Verification of the model for foundation soil

In order to verify the FEM analysis, initially, both reinforced and reinforced soil was modeled. Fig. 6.2 shows the comparative graph between the experimental results and the FEM curve for footing resting over flat ground. It can be clearly seen from the graph that, for lower settlement, the shape of the curve is almost similarly until about s/*B* = 4 - 6%. Thus, it is clear that the obtained values of pressure settlement form experimental work with the FEM analysis agree well. Although, for higher settlement values, a difference begins to be seen, thus signifying that the lower settlement can be easily validated by FEM. However, for larger settlement and higher loading soil starts to compact due to the footing loading, and the particles of the soil come closers to each other thus, changing the mechanical behavior of soil. In this respect, this leads to limitations of the FEM analysis.

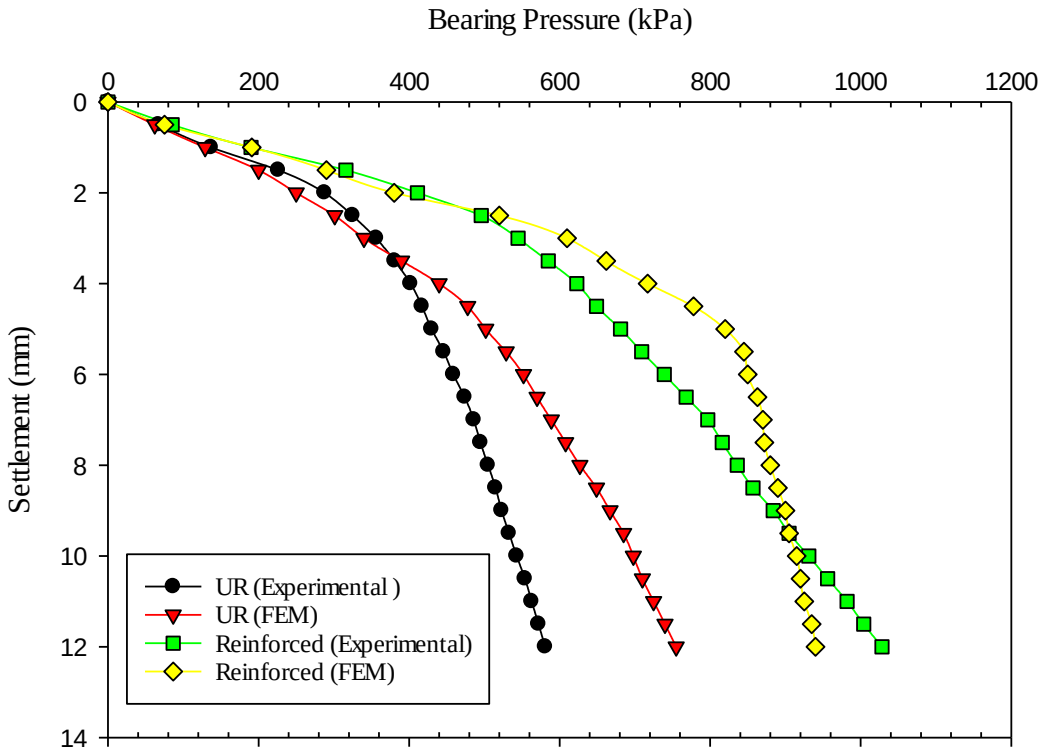

Fig. 6.2 Verification of model of soil

6.5 Numerical analysis for scale effect

FEM analysis has been conducted to check the scale effect of model footing tests resting over flat ground. Initially, the FEM analysis has been conducted on square footing of 75 mm × 75 mm size then size of footing was increased as 300 mm × 300 mm (4 times), 600 mm × 600 mm (8 times), 900 mm × 900 mm (12 times), 1200 mm × 1200 mm (16 times). The size of reinforcement, soil block was also increased in the same way as increased in the footing size. However, input parameters like soil properties, reinforcement properties, plate properties were kept the same for all footing size.

The FEM analysis has been divided into three series to investigate the scale effect on the footing.

(1) Considering number of reinforcement (N), spacing between the reinforcement (h/B), and total depth ratio (d/B) constant. GGR1 was used as a reinforcing material for different size of footing resting over flat ground.

(2) Considering spacing between the reinforcement (*h*), and total depth ratio (*d/B*) constant while increasing the number of reinforcement layers and GGR1 was used as a reinforcing material for different size of footing resting over flat ground.

(3) Considering number of reinforcement (*N*), spacing between the reinforcement (*h/B*), and total depth ratio (*d/B*) constant but increasing the tensile strength of reinforcement in the same way as increased the footing size and GGR1 was used as a reinforcing material for different size of footing resting over flat ground.

Pressure settlement curves obtained by FEM analysis of model footing resting over flat ground of different sizes are presented in Fig. 6.4 (a-c), for series one, series two and series three respectively.

6.6 Analysis of FEM results

Fig. 6.4 (a) shows pressure settlement curves of unreinforced soil for all size of footings. It is observed from the curves that all the tests conducted on different size of footings having similar shapes. It is confirmed that the model footing resting over unreinforced soil has no scale effect. The scale effect using reinforced foundation soil system has been investigated using the reinforcement ratio. The reinforcement ratio ($R_{r)}$ has been used by (Jie Gu 2011) in his study to investigate the scale effect reinforced foundation soil. The formulation of the reinforcement ratio is discussed below. The reinforcement ratio R_r is defined as

$$R_r = \frac{E_r A_r}{E_S A_S} \qquad (6.2)$$

where E_r is the modulus of elasticity of reinforcement which is equal to J/t_r, E_s is modulus of elasticity of soil, $A_{r\,=}$ area of reinforcement pre-unit width which is equal to N tr × 1, E_s = modulus of elasticity of soil, A_s = Area of soil block per unit width which is equal to d × 1. Where d = total reinforcement depth $d = u + (N - 1)\,h$, in most of the cases first reinforcement depth *i.e.* u is taken equal to vertical spacing between the reinforcements i.e. h. If $u = h$ is put in equation (6.2) then reinforcement ratio can be modified as

$$R_r = \frac{\frac{J}{tr} N\, t_r}{E_s d}, \; = \frac{J}{E_s h} \tag{6.3}$$

From the above equation it is cleared that R_r is directly proportional to the tensile modulus of reinforcement and inversely proportional to vertical spacing between two reinforcements (*h*). Series one was considered by assuming the total depth ratio (*d/B*), number of reinforcement (*N*), and spacing between the reinforcement (*h/B*) for flat ground. GGR1 was used as a reinforcing material for all size of footings. From graph 6.4 (a) it is cleared that the bearing pressure of reinforced soil decreases with increasing the footing size. The improvement factor (*IF*), size of footing and reinforcement ratio relation at different *s/B* ratios (4%, 8%, 12% and 16%) are shown in Fig. 6.3, It is cleared from the graphs that *IF* value decreases with increasing the footing size and decreasing the reinforcement ratio. From the curves, it can be observed that the reinforcement ratio decreases as increasing the vertical spacing between the reinforcements which revels that the reinforcement ratio decreases with increasing in footing size.

In the case of series two, 6.4 (b) the total depth ratio (*d/B*), the vertical spacing between reinforcements (*h*), were kept constant for all footings with different sizes. GGR1 was used as a reinforcing material for all footings with different size. It is clear from the graph that bearing pressure increment is the same for all different size footings. Maximum difference in bearing pressure of reinforced soil at the same settlement was found 6%. The observation for series two can suggest that there is no influence of scale effect when settlement is indicated as a non-dimensional relative settlement (s/*B*).

In case of series three, the total depth ratio (*d/B*), vertical spacing between reinforcements (*h*), were kept constant for all footings with different size but the tensile modulus of geogrid was increased in the same manner as increased in footing size from 900 mm to 1200 mm. Fig.6.4 (c) shows the bearing pressure settlement curves for all size of footing when number of

reinforcement and reinforcement ratio kept constant. It can be suggested that the scale effect on the response of pressure settlement curves of reinforced soil foundation is not significant for series three. From the above three results, it is concluded that scale effect is mainly related to reinforcement ratios of the reinforced foundation soil if the depth ratio is kept constant. (Chen, 2007) noticed the same observation when they studied the scale effect on reinforced soil foundation.

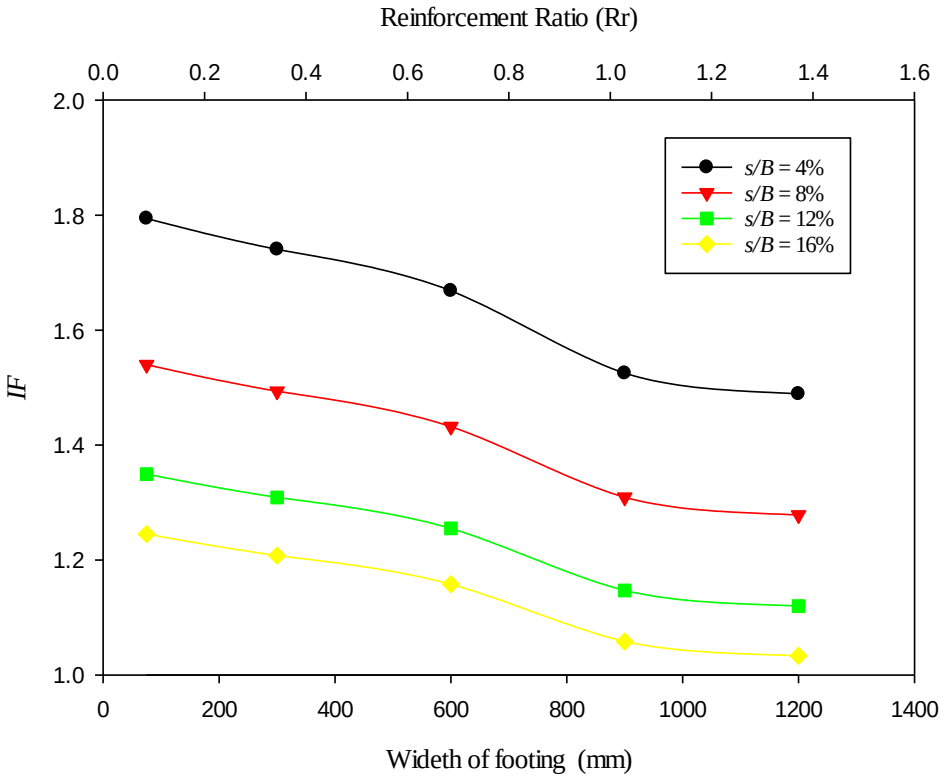

Fig. 6.3 *IF* vs footing size (B) and Reinforcement ratio (Rr) for footing over flat ground

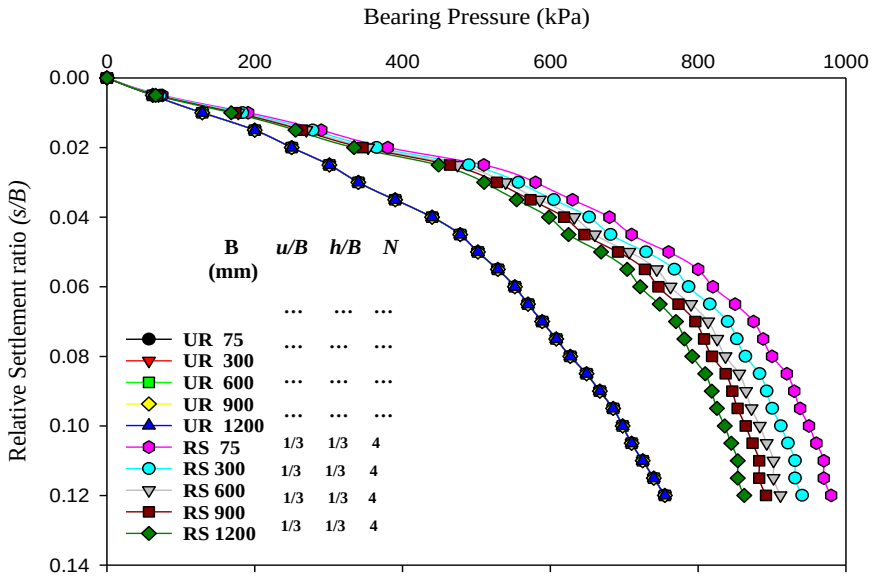
Bearing Pressure (kPa)
0
200
400
600
800
1000
0.00
0.02
0.04
0.06
0.08
0.10
0.12
0.14
Relative Settlement ratio (s/B)
B (mm)
u/B
h/B
N
UR 75 ... ...
UR 300 ... ...
UR 600 ... ...
UR 900 ... ...
UR 1200 ... ...
RS 75 1/3 1/3 4
RS 300 1/3 1/3 4
RS 600 1/3 1/3 4
RS 900 1/3 1/3 4
RS 1200 1/3 1/3 4

(a)

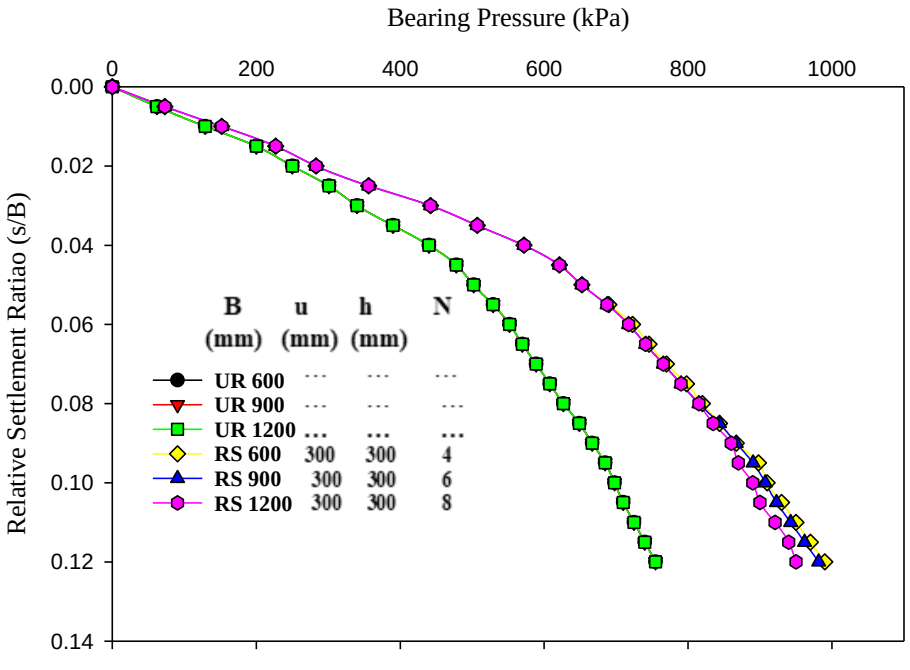
Bearing Pressure (kPa)
0
200
400
600
800
1000
0.00
0.02
0.04
0.06
0.08
0.10
0.12
0.14
Relative Settlement Ratiao (s/B)
B (mm)
u (mm)
h (mm)
N
UR 600 ... ...
UR 900 ... ...
UR 1200 ... ...
RS 600 300 300 4
RS 900 300 300 6
RS 1200 300 300 8

(b)

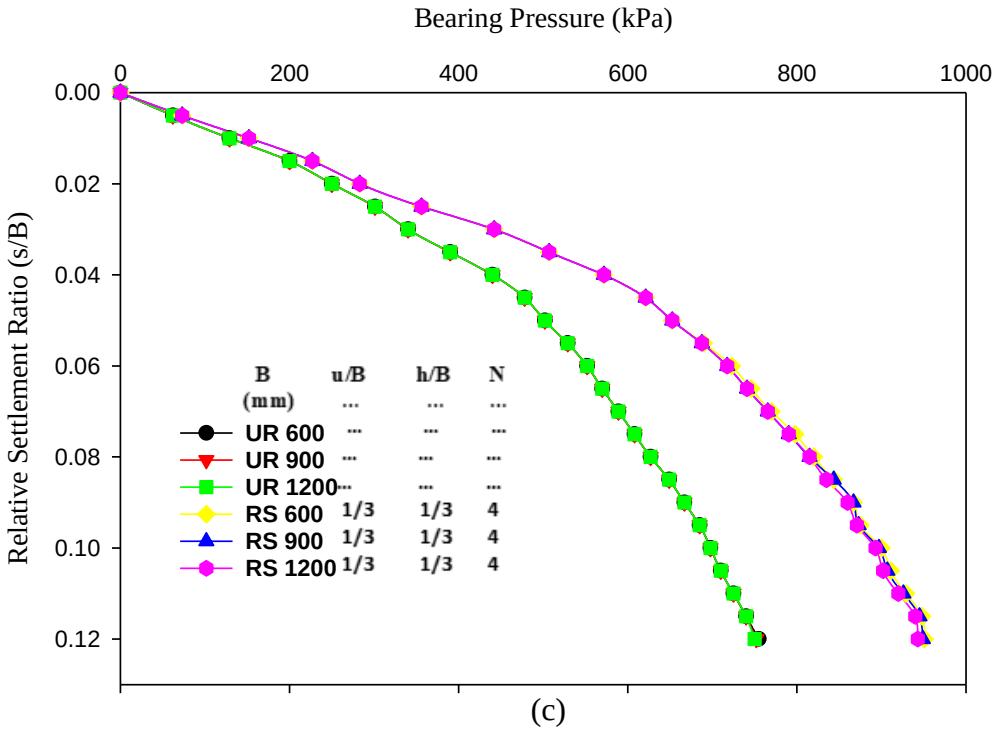

(c)

Fig. 6.4 Pressure Relative settlement ratio relation of square footing over flat ground for (a) series one (b) series two (c) series three

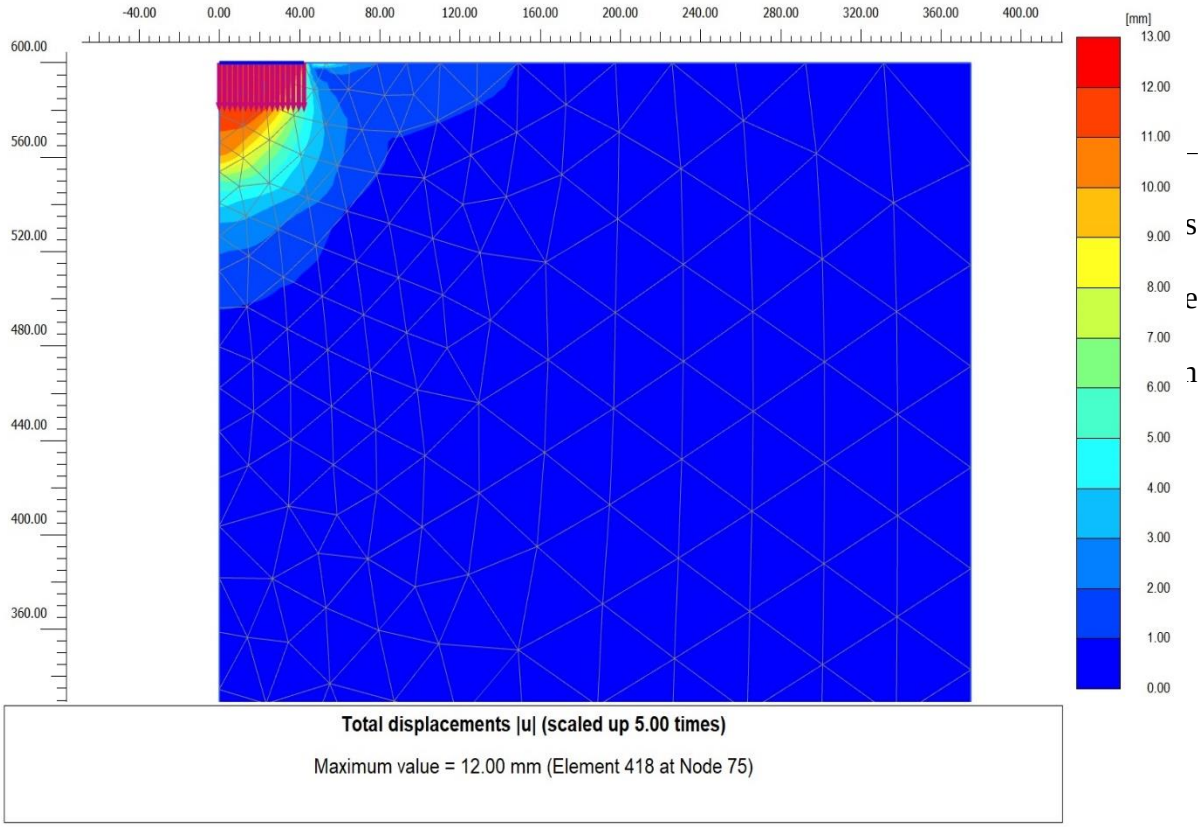

(a)

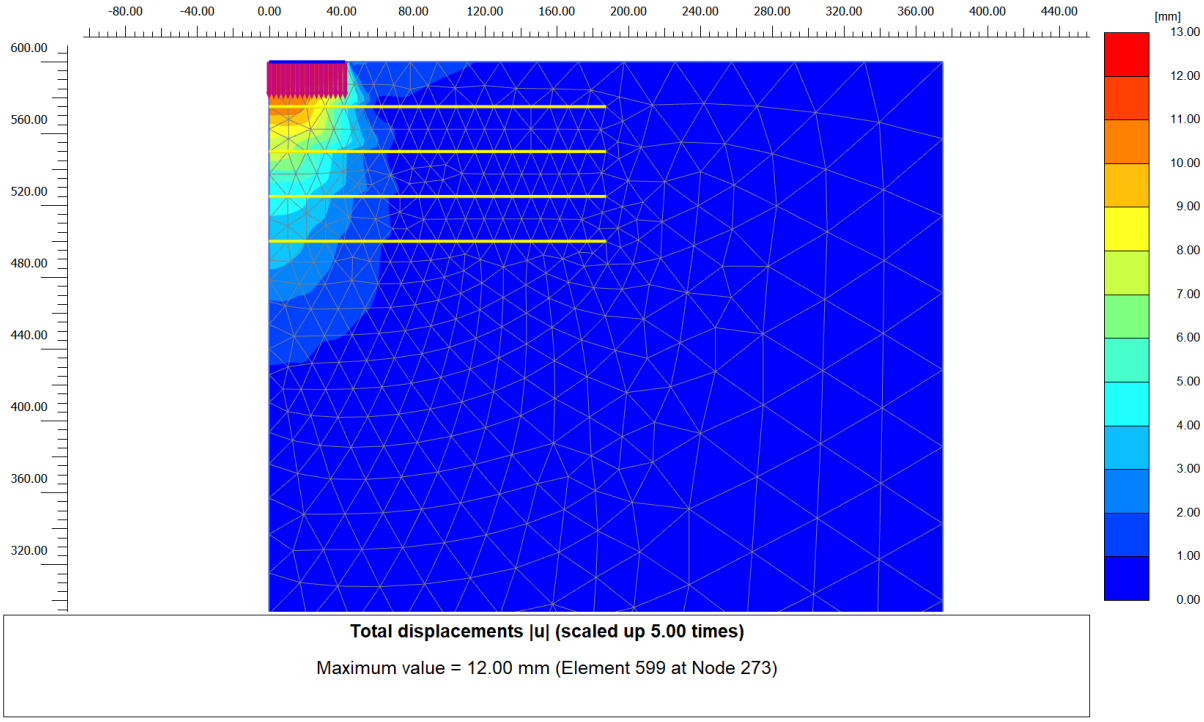

(b)

Fig. 6.5 Displacement distribution diagram of Footing (a) with out reinforcements (b) with reinforcements

6.7 Summary and conclusions based on FEM analysis

Finite element analysis of square footing with different sizes shows that the pressure – settlement graphs for unreinforced soil are always similar if the settlement is expressed in terms of relative settlement. In case of reinforced soil the bearing capacity decreases as size of the footing increases if the spacing ratio between two reinforcement layers (h/B), effective depth ratio of reinforcement (d/B) and number of reinforcement layers are kept constant.

REFERENCES

1. Abu-farsakh, M., Voyiadjis, G., and Chen, Q., (2012) . "Finite Element Parametric Study on the Performance of Strip Footings on Reinforced Crushed Limestone over Embankment Soil". *Electronic Journal of Geotechnical. Engineering.* Vol. 17, pp. 723-742.
2. Adem, H.H., and Vanapalli, S.K. (2014). "Prediction of the modulus of elasticity of compacted unsaturated expansive soils". *International Journal of Geotechnical Engineering,* Vol. 9, pp. 163-175.
3. Arab, M.G., Omar, M., and Tahmaz, A., (2017). "Numerical analysis of shallow foundations on geogrid reinforced soil", *MATEC Web of Conferences*. Vol. 120.
4. Azzam, W., and Farouk, A. (2010). "Experimental and Numerical Studies of Sand Slopes Loaded with Skirted Strip Footing". *Electronic Journal of Geotechnical Engineering*, Vol. 15, pp. 795-812.
5. Chen, Q., (2007). "An experimental study on characteristics and behavior of reinforced soil foundation". *PhD Thesis, Louisiana State University.*
6. Chen, Q., Abu-Farsakh, M., Sharma, R., and Zhang, X. (2007). "Laboratory investigation of behavior of foundations on geosynthetic-reinforced clayey soil". *Journal of the Transportation Research Board,* Vol. 2004, pp. 28-38.
7. Griffiths, D.V., and Lane, P.A., (1999). "*Slope stability analysis by finite elements". Geotechnique,* Vol. 49, pp. 387-403.
8. Ju, Jie. (2011). "Computational modeling of geogrid reinforced soil foundation and geogrid reinforced base in flexible pavement". *P.hD thesis,* Louisiana State University, and Agricultural and Mechanical College, LA, USA
9. Karim, M.R., Manivannan, G., Gnanendran, and C.T., Lo, S.-C.R. (2011). "Predicting the long-term performance of a geogrid-reinforced embankment on soft soil using two-dimensional finite element analysis". *Canadian Geotechnical Journal,* Vol. 48, pp. 741-753. doi.org/10.1139/T10-104
10. Lal, B.R.R., and Mandal, J.N. 2012. Feasibility study on fly ash as backfill material in cellular reinforced walls. *Electronic Journal of Geotecnical Ennieering,* Vol. 17, pp. 1437-1458.
11. Liu, F., and Zhao, J. (2013). "Limit analysis of slope stability by rigid finite element method and linear programming considering rotational failure". *Inernational Journal of Geomechnics,* Vol. 13, pp. 827–839. doi.org/10.1061/(ASCE)GM.1943-5622.0000283.

CHAPTER 7

MODEL DEVELOPMENT AND ANALYTICAL SOLUTIONS FOR BEARING CAPACITY COMPUTATION OF REINFORCED SOIL FOUNDATION

7.1 Model development for case footing resting over sloping ground

Regression analysis was carried out on the results obtained from the experimental analysis after validation through FEM. The analysis was carried out on a R Integrated Development Environment (IDE) RStudio, which provides open source environment for data visualization and analysis. The analysis was carried out by considering six dimensionless parameters, i.e. *u/B, h/B, D/B, N,* Normalized stiffness (N_s) and Normalized tensile strength (N_t) and estimating the degree of significance of each parameter with the improvement factor, computed at ultimate bearing capacity of soil. Regression analysis was performed using pairwise testing as well as using individual parameters. The analysis was carried out for a linear model of the form

$$Y = \alpha_0 + \alpha_1 X_1 + \alpha_2 X_2 + \alpha_3 X_3 + \alpha_4 X_4 + \alpha_5 X_5 + \alpha_6 X_6 \quad (7.1)$$

For the purpose of analysis, data set was created using the results obtained from the experimental analysis, and imported into the RStudio framework. Improvement factor was kept as the Y intercept for the purpose of analysis and functioned as the dependent variable, and all the other parameters were analyzed for their influence on the improvement factor at the ultimate bearing capacity for all the reinforcements and their corresponding configurations. The relative importance of each independent parameter for computation of ultimate bearing capacity of a reinforced foundation was assessed by computing the individual t values for each of the

variable. The higher the value of |t|, the greater is the variable significance. Table 7.1 shows the fittings obtained with different parameters taken one at a time.

Table 7.1 Various possible linear models and their fittings

Multiple R^2	**R^2 adjusted**	**Parameters**
0.9565	0.9494	*D/B, u/B, h/B, N,* Norm. Stiffness and Norm. Tensile Strength
0.9562	0.9504	*D/B, u/B, h/B, N* and Norm. Tensile Strength
0.9561	0.9515	*D/B, u/B, N* and Norm. Tensile Strength
0.9556	0.9498	*D/B, u/B, h/B, N* and Norm. Stiffness
0.9555	0.9509	*D/B, u/B, N* and Norm. Stiffness
0.9539	0.9478	*u/B, N, h/B,* Norm. Stiffness and Norm. Tensile Strength
0.9534	0.9499	*u/B, N* and Norm. Tensile Strength
0.9529	0.9493	*u/B, N* and Norm. Stiffness
0.9515	0.9451	*D/B, h/B, N,* Norm. Stiffness and Norm. Tensile Strength
0.9466	0.9440	*u/B* and *N*
0.9427	0.9414	N
0.4424	0.3691	*D/B, u/B, h/B,* Norm. Stiffness and Norm. Tensile Strength
0.2996	0.2277	*D/B, h/B,* Norm. Stiffness and Norm. Tensile Strength
0.2768	0.2226	*D/B, u/B* and *h/B*
0.2323	0.2141	*h/B*
0.1884	0.1448	Norm. Stiffness and Norm. Tensile Strength
0.1871	0.1678	Norm. Tensile Strength
0.1796	0.1601	Norm. Stiffness
0.1339	0.1133	*u/B*
0.002626	0.00212	*D/B*

From Table 7.1 it can be observed that linear model including all dimensionless parameters is the best fitted for computation. Conducting linear regression including all parameters yields the following results as reported in Table7.2.

Table 7.2 Linear regression computations with all dependent variables

Parameters	**Coefficients**	**t Value**
D/B	-0.0586	-1.495
u/B	-0.1212	-2.064
N	0.1895	20.911
h/B	0.01623	0.454
Normalized Stiffness	0.008645	0.502
Normalized Tensile Strength	-0.66975	-0.852

From the results obtained from the regression study, it can be observed that *N* is the most significant factor when computing the ultimate bearing capacity of reinforced foundation, with an overall t value of 20.911. Also, edge distance is the least significant of the design parameters selected with a |t| value of 1.495 out of the four selected parameters. From the experimental study, it can be seen that geosynthetic stiffness is a very significant parameter in computing the improvement factor for any reinforced foundation. It is thus viable to include normalized tensile stiffness in the equation to compute the improvement factor of any reinforced foundation. Hence, from the results obtained in the regression analysis, it can be proffered that it is more feasible to vary the vertical spacing between the reinforcements than to vary the tensile strength or the tensile modulus of the reinforcements for improving the bearing capacity of foundation constructed over soil slope. In order to assure high accuracy and also to provide a concise equation valuable for computation of ultimate bearing capacity of geosynthetic reinforced soil foundation, the proposed equation including the aforementioned parameters is

$$I.F. = 0.19\,N - 0.06\frac{D}{B} - 0.14\,\frac{u}{B} - 0.3\,N_t + 1.028 \qquad 7.3$$

7.2 Model development for case footing resting over flat ground

The analysis was conducted by considering five dimensionless parameters, i.e. *u/B, h/B, N,* Normalized stiffness (N_s) and Normalized tensile strength (N_t) and estimating the degree of significance of each parameter with the improvement factor, computed at ultimate bearing capacity of soil. The analysis was carried out for a linear model of the form

$$Y = \alpha_0 + \alpha_1 X_1 + \alpha_2 X_2 + \alpha_3 X_3 + \alpha_4 X_4 + \alpha_5 X_5 \quad 7.4$$

Table 7.3 shows the fittings obtained with different parameters. From Table 7.3 it can be observed that linear model including all dimensionless parameters is the best fitted for computation. Conducting linear regression including all parameters yields the following results as reported in Table 7.4

From the analysis, it can be observed that N is the most significant factor when computing the ultimate bearing capacity of reinforced foundation, with an overall t value of 20.911. Also, from the analysis of the obtained results, it can be concluded that spacing between reinforcements is more significant that the tensile modulus of the reinforcement for a range of

$$0.08 \leq h/B \leq 0.4 \quad (7.5)$$

which is a critical observation, as the project cost is usually associated with the spacing between reinforcements. From Table 7.3 it can be observed that the highest adjusted R^2 value is obtained when *u/B, N* and Norm. Tensile Strength are taken as the parameters for computation of the ultimate bearing capacity, even though the multiple R^2 value reduces (confidence level still greater than 95%). In order to assure high accuracy and also to provide a concise equation valuable for computation of ultimate bearing capacity of geosynthetic reinforced soil foundation, the proposed equation including the aforementioned parameters is

$$I.F. = 0.23\ N - 0.26\ \frac{u}{B} - 0.194\ N_t + 0.99 \quad (7.6)$$

Table 7.3 Various possible linear models and their fittings

Multiple R^2	**R^2 adjusted**	**Parameters**
0.9685	0.9524	*u/B, h/B, N,* N_s and Nt
0.9657	0.9516	*u/B, h/B, N* and Nt
0.9644	0.9537	*u/B, N* and Nt
0.9599	0.9508	*u/B, h/B, N* and N_s
0.9547	0.9499	*u/B, N* and N_s
0.9539	0.9478	*u/B, N, h/B,* N_s and Nt
0.9521	0.9466	*u/B, N* and Nt
0.9513	0.9447	*u/B, N* and N_s
0.9511	0.9433	*h/B, N,* N_s and Nt
0.5197	0.4416	*u/B, h/B,* N_s, Nt
0.4785	0.4315	N
0.2996	0.2277	*h/B,* N_s and Nt
0.2768	0.2226	*u/B* and *h/B*
0.2323	0.2141	*h/B*
0.1884	0.1448	N_s and Nt
0.1871	0.1678	Nt
0.1796	0.1601	*u/B*
0.1117	0.1107	N_s

Table 7.4 Linear regression computations with all dependent variables

Parameters	**Coefficients**	**t Value**
u/B	-0.1187	-3.009
N	0.1948	23.911
h/B	0.0159	2.175
N_s	0.01956	0.678
Nt	-0.4798	-1.51

7.3 Analytical solutions for bearing capacity of reinforced soil

Different researchers have proposed the analytical solutions for estimation of the bearing capacity foundation resting over reinforced soil bed (Binquet and Lee., 1975a); Huang and Tatsuoka., 1990; Wayne et al., 1998; Kumar and Saran., 2003; Sharma et al., 2009; Chen and Abu-Farsakh., 2015). Wayne et al., (1998) presented an analytical model for the determination of bearing capacity of rectangular footing on reinforced soil without inculcating the confinement effect of the reinforcement in improving the ultimate bearing capacity of the soil. The solutions assumed a two layered soil structure approach for the estimation of the ultimate bearing capacity of the foundation, thus it is considered that the punching shear failure takes place in the reinforced zone general shear failure in the unreinforced zone. (Sharma et al., 2009) presented the analytical solutions for predicting the ultimate bearing capacity by including the effects of reinforcement on the soil. The proposed failure mechanisms can be cited as failure above the reinforcement, failure between the reinforcements failure as if two-layered soil system exists and bearing failure. Based on the above mechanisms for a reinforced soil foundation following three bearing capacity equations are presented

For (Wayne et al., 1998): (Rectangular footing)

$$q_{u(R)} = q_{(u)b} + \frac{2c_a d}{B}\left(1+\frac{B}{L}\right) + \gamma_t d^2\left[1+\frac{2D_f}{d}\right] \times \frac{K_S tan\emptyset_t}{B}\left(1+\frac{B}{L}\right) + \frac{2}{B}\left(1+\frac{B}{L}\right)\sum_{i=1}^{N} T_{ui} - \gamma_t d \quad (7.2)$$

For (Sharma et al., 2009): (Square footing)

$$q_{u(R)} = q_{(u)b} + \frac{4c_a d}{B} + 2\gamma_t d^2\left[1+\frac{2D_f}{d}\right] \times \frac{K_S tan\emptyset_t}{B} + \frac{4}{B}\sum_{i=1}^{N} T_i tan\delta - \gamma_t d \quad (7.3)$$

For (Chen and Abu-Farsakh, 2015): (Strip footing)

$$q_{u(R)} = q_{(u)b} + \frac{2c_a d}{B} + \gamma_t d^2\left[1+\frac{2D_f}{d}\right] \times \frac{K_S tan\emptyset_t}{B} + \frac{2}{B}\sum_{i=1}^{N} T_i cos\alpha_i tan\delta + \frac{2}{B}\sum_{i=1}^{N} T_i sin\alpha_i - \gamma_t d \quad (7.4)$$

where, $q_{u(R)}$ and $q_{(u)b}$ are the ultimate bearing capacity of the foundation under reinforced and unreinforced zone respectively; D_f is the embedment depth of the footing; ;γ_t is the unit weight of the soil in the reinforced region; K_S is a coefficient of punching shear; L and B are the length and the width of the footing respectively; $\emptyset_t$ is the frictional angle of the soil; N is

the number of reinforcement layers; T_i is the tensile force mobilized in the ith reinforcement layer; T_u is the ultimate tensile strength of the reinforcement; δ is the mobilized frictional angle at the punching shear upper surface and α_i is the horizontal angle of the reinforcement. Wayne et.al., (1998) considered the failure between two reinforcement whereas (Sharma et al., 2009; Chen and Abu-Farsakh, 2015) assumed general failure mechanism of reinforced soil foundation, is identified as a punching shear failure followed by general shear failure. Fig.7.1 (a) shows the failure mechanism of reinforced soil under strip loading. It can be seen that the location of first layer of reinforcement lies within the punching shear zone. While other reinforcements are situated in zone of general shear failure. The forces act on the punching surface aa' and bb', Fig. 7.1 (a) include adhesive force $C_a D_P$, acting upwards, the total passive earth pressure P1, inclined at angle δ. Here c_a is unit adhesion of the soil along the line D_P. When the reinforcement comes under the action, an upward force acts due to the tension effect of reinforcement along the failure surface. When the soil reaches a ultimate failure state, the reinforcement deforms, and the tensile force T makes an angle α in the horizontal direction. The tensile force T has two components, i.e., the horizontal and vertical components. The horizontal component gives a confinement effect, whereas the vertical component provides the membrane effect. In this study, the mechanisms presented by (Chen and Abu-Farsakh, 2015) have been used for the bearing capacity computations.

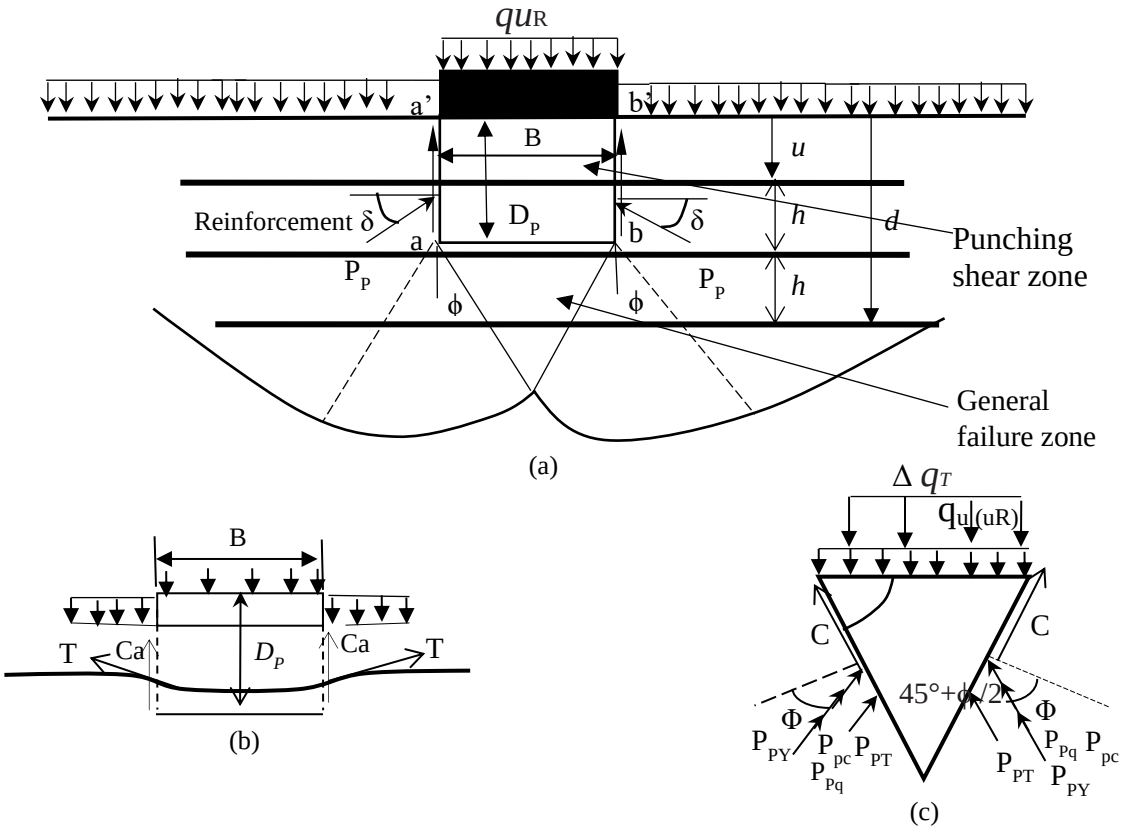

Fig. 7.1 (a) Strip foundation on geosynthetic reinforced soil based on the study (Chen and Farsakh, 2014) shear punching failure followed by general shear failure (b) Punching shear zone (c) General shear zone

Equation (7.4) can only be used for strip footing calculations and thus has to be modified so as it can be used for footings of other shapes. The equation can thus be modified as follows,

$$q_{u(R)} = q_{(u)b} + \frac{2c_a d}{B}\left(1+\frac{B}{L}\right) + \gamma_t d^2\left[1+\frac{2D_f}{d}\right] \times \frac{K_S tan\emptyset_t}{B}\left(1+\frac{B}{L}\right) + \frac{2}{B}\sum_{i=1}^{N} T_i cos\alpha_i tan\delta\left(1+\frac{B}{L}\right) + \frac{2}{B}\sum_{i=1}^{N} T_i sin\alpha_i\left(1+\frac{B}{L}\right) - \gamma_t d \quad (7.5)$$

The failure mechanism of reinforced soil foundation under eccentric loading assumed by (Sahu et al., 2016) is shown in Fig. 7.2 For the present study, a punching shear failure followed by general shear failure under eccentric loading is assumed and shown in Fig. 7.3

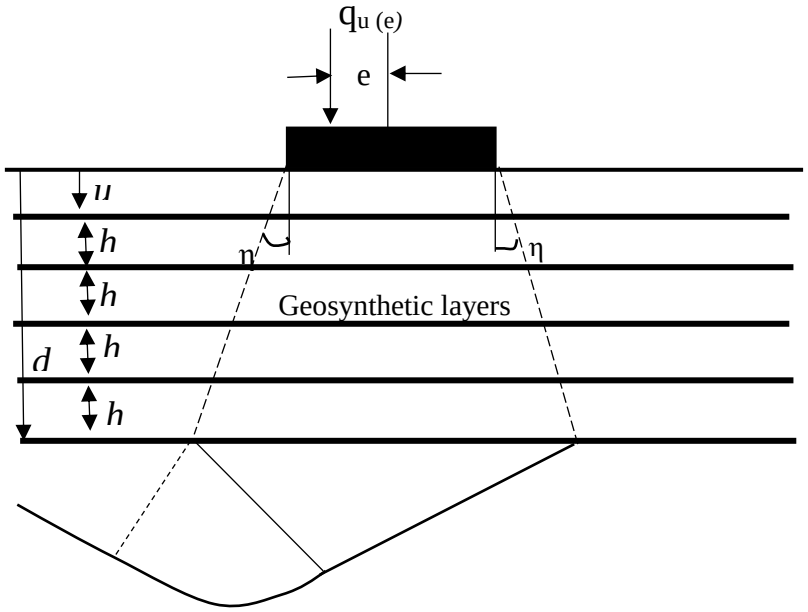

Fig.7.2 Failure mode of eccentrically loaded strip footing on reinforced sand Sahu et al. (2016)

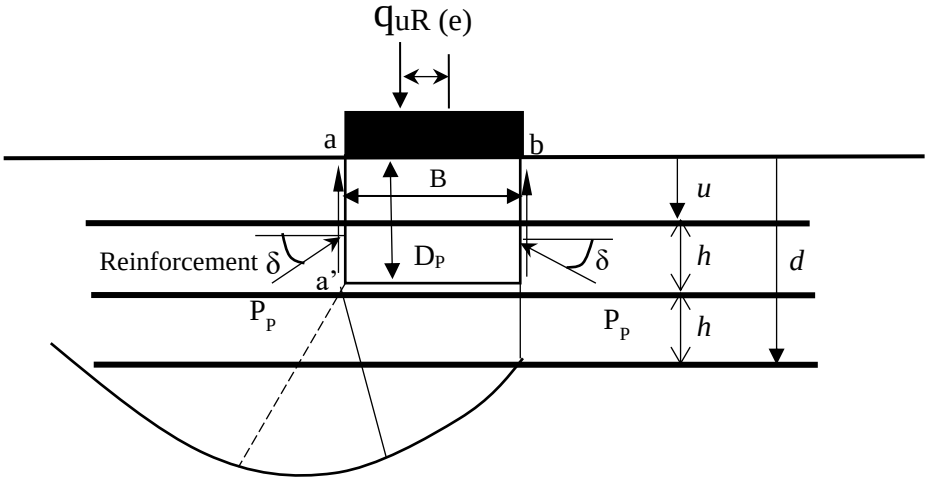

Fig. 7.3 Assumed failure mode of reinforced soil foundation under eccentric loading- shear punching failure followed by general shear failure

Modified equation (7.5) can now be used for deducing ultimate bearing capacity of any given footing shape, such as rectangular footing, square footing, circular footing, or strip footing. Also, it must be noted that the new proposed equation (7.6) has to be further modified to inculcate the effect of eccentricity. (Meyerhof, 1953) developed analytical solutions for computation of eccentrically loaded footing by analyzing the footing as a footing with reduced width. (Purkayastha and Char, 1977) carried out stability analysis of eccentrically loaded foundation, based on which reduction factor, was proposed. Using these two theories, two new models have been proposed to suggest solutions for foundations of any shape under eccentric loading. For the convenience of understanding, the two models have been called ANM1 and ANM2, respectively. ANM1 has first been suggested. Assuming a footing of reduced width, i.e. a footing with an assumed width of ω, where $\omega = B - 2e_x$,a new equation has been proposed, which is as follows

$$q_{u(R)} = q_{(u)b} + \frac{2c_a d}{\omega}\left(1 + \frac{\omega}{L}\right) + \gamma_t d^2\left[1 + \frac{2D_f}{d}\right] \times \frac{K_S tan\emptyset_t}{\omega}\left(1 + \frac{\omega}{L}\right) + \frac{2}{\omega}\sum_{i=1}^{N} T_i cos\alpha_i tan\delta\left(1 + \frac{\omega}{L}\right) + \frac{2}{\omega}\sum_{i=1}^{N} T_i sin\alpha_i\left(1 + \frac{\omega}{L}\right) - \gamma_t d \quad (7.6)$$

For the present study, square footing has been considered and hence *B/L*=1. Also, as the test procedure uses a surface footing, embedment depth is equal to zero.

The second analytical model being presented from the study is based on the reduction factor theory presented by (Purkayastha and Char, 1977).

As defined before, a reduction factor can be written in the form,

$$R_k = 1 - \frac{q_{u(eccentric)}}{q_{u(centric)}} \quad (7.7)$$

Based on the results presented in the study, it can be clearly observed that the values of reduction factor, which are typically expected to be dependent on the embedment depth, are also dependent on the number of reinforcement layers applied in the foundation. This provokes the design of a new analytical model, which inculcates the effects of number of reinforcement

layers on the reduction factor values, and can be utilized in the calculation of ultimate bearing capacity in case of geosynthetic reinforcement. The new model (ANM2) being proposed for square footing for a given value of N is represented below.

$$RF = 1 - \frac{q_{u(eccentric,N)}}{q_{u(centric,N)}} \tag{7.8}$$

where, $q_{u(eccentric,N)}$ is the ultimate bearing capacity of an eccentrically loaded square footing with N layers of reinforcements and $q_{u(centric,N)}$ is the ultimate bearing capacity of a centrally loaded square footing with N layers of reinforcements. A nonlinear regression model was developed in MATLAB software to analyze the rise and fall in the values of the reduction factor. The nonlinear model thus created was based on the following equation,

$$\text{RF}= \mu \left\{\frac{e}{B}\right\}^{\gamma} \tag{7.9}$$

where , μ and γ are the unknown parameters in the model. As the equation is linear in the parameters, linear least square analysis can also be conducted to obtain the values of μ and γ in the equation. But to reduce the possibility of squared errors, nonlinear functions originally available in MATLAB for computations were used. From the two-equations presented above, it can be clearly said that the model ANM2 can be written in the form,

$$q_{u(eccentric,N)}=q_{u(centric,N)} \left\{1 - \mu(\frac{e}{B})^{\gamma}\right\} \tag{7.10}$$

The value of $q_{u(centric,N)}$ can be obtained from the new modified equation (7.6) presented by the authors, and thus equation (7.10) can be written as,

$$q_{u(eccentric,N)} = \left(q_{(u)b} + \frac{2c_a d}{B}\left(1 + \frac{B}{L}\right) + \gamma_t d^2 \left[1 + \frac{2D_f}{d}\right] \times \frac{K_S tan\emptyset_t}{B}\left(1 + \frac{B}{L}\right) + \frac{2}{B}\sum_{i=1}^{N} T_i cos\alpha_i tan\delta \left(1 + \frac{B}{L}\right) + \frac{2}{B}\sum_{i=1}^{N} T_i sin\alpha_i \left(1 + \frac{B}{L}\right) - \gamma_t d\right) \times \left\{1 - \mu(\frac{e}{B})^{\gamma}\right\} \tag{7.11}$$

The values of the unknown parameters obtained from nonlinear regression of the presented model have been shown in Table 7.3

Table 7.5 Values of dimensionless parameters using MATLAB

Loading Condition	$\boldsymbol{\mu}$	$\boldsymbol{\gamma}$
N=1	1.198	1.591
N=2	1.291	1.517
N=3	1.319	1.499
N=4	1.392	1.481

Based on the values obtained in Table 7.3, it can be observed that there are minimal deviations in the values obtained for the two unknown parameters for the new proposed equation. The average of the values for the parameters μ and γ are1.3 and 1.522, or approximately 1.52 respectively. Hence, the final equation of the new proposed model ANM2 is

$$q_{u(eccentric,N)} = \left(q_{(u)b} + \frac{2c_a d}{B}\left(1+\frac{B}{L}\right) + \gamma_t d^2\left[1+\frac{2D_f}{d}\right] \times \frac{K_S tan\emptyset_t}{B}\left(1+\frac{B}{L}\right) + \frac{2}{B}\sum_{i=1}^{N} T_i cos\alpha_i tan\delta\left(1+\frac{B}{L}\right) + \frac{2}{B}\sum_{i=1}^{N} T_i sin\alpha_i\left(1+\frac{B}{L}\right) - \gamma_t d\right) \times \left\{1-\mu\left\{\frac{e}{B}\right\}^{\gamma}\right\} \quad (7.12)$$

It has to be however noted that the values of reduction factor have been predicted at a single embedment depth ratio, i.e. D_f/B=0. Fig 7.4 (a-b) shows the prediction of results Versus Experimental Results for ANM1 and ANM2 respectively. As can be observed, ANM2 shows R^2 value of 0.96 for computation of ultimate bearing capacity and also applicable for the calculation of bearing capacity of reinforced foundations. However, ANM1 shows conservative results. Probable reason behind this can be explain by the fact that in ANM1 it is considered that when footing is subjected to eccentric load, it tilts towards the side of the eccentricity and the contact pressure below the base is generally taken to decrease linearly towards the heel from a maximum at the toe. Thus, reduction is more in ultimate bearing capacity of soil.

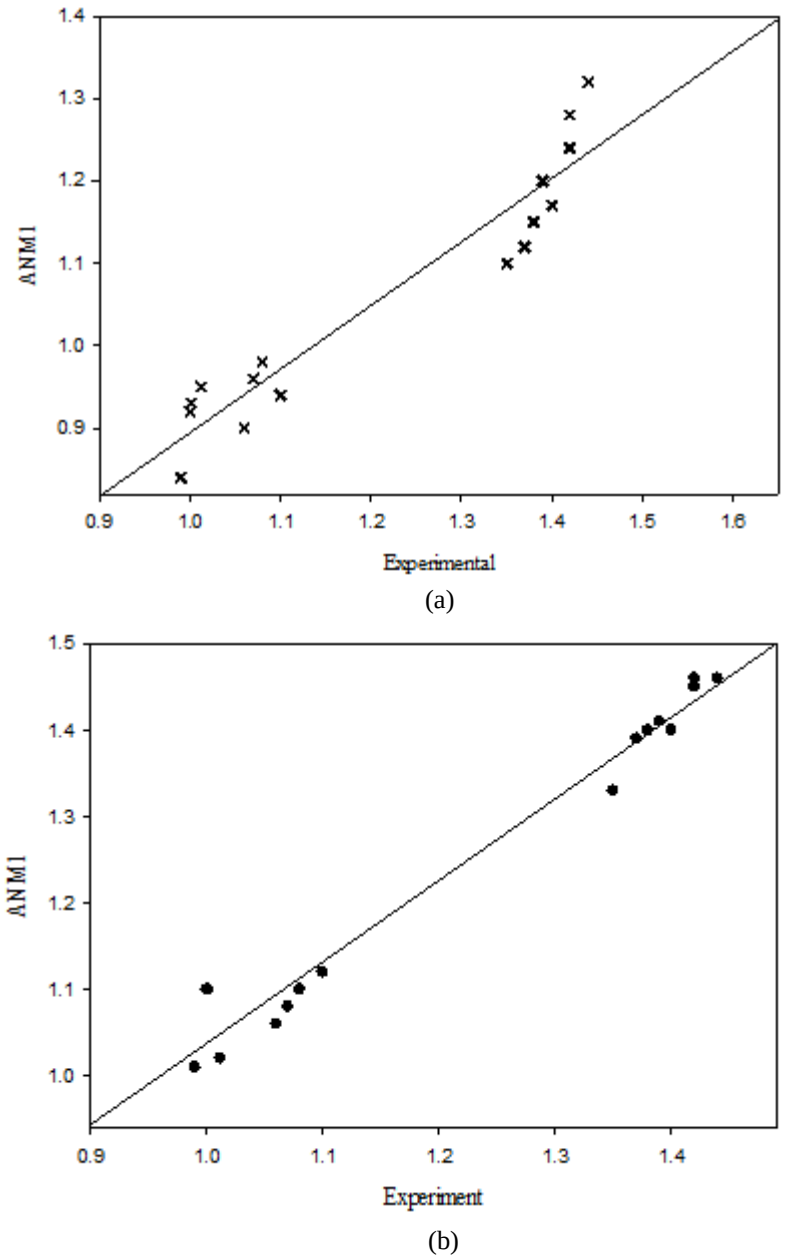

Fig 7.4 Prediction of results Versus Experimental Results for (a) ANM1 and (b) ANM2

7.4 Summary and conclusions

From the regression analysis of the experimental results, number of reinforcements was obtained as the most significant parameter for improving the bearing capacity at ultimate bearing capacity and tensile modulus of the reinforcement was obtained as the least significant parameter. The proposed ANM2 model, based on the reduction factor, provided high accuracy, and can thus be used for computation of ultimate bearing capacity of reinforced clay foundations under eccentric loading whereas ANM1 model, based on the Meyerhof's effective width method provided conservative results with lower accuracy in comparison to ANM2 .

REFERNCES

1. Binquet, J., and Lee, K.L., (1975a). "Bearing capacity tests on reinforced earth slabs." *Journal of Geotechnical Engineering Division, ASCE,* Vol. 101, pp. 1241-1255.
2. Chen, Q., and Abu-Farsakh, M. (2015). "Ultimate bearing capacity analysis of strip footings on reinforced soil foundation". *Soils and Foundations,* Vol. 55, pp. 74-85.
3. Huang, C. C., and Tatsuoka, F. (1990). "Bearing capacity of reinforced horizontal sandy ground". *Geotextiles and Geomembranes,* Vol. 9, pp. 51-82.
4. Kumar, A., and Saran, S. (2003). "Bearing capacity of rectangular footing on reinforced soil". *Geotechnical and Geological Engineering,* Vol. 21, pp. 201-224.
5. Meyerhof, G. T. (1953). "The bearing capacity of foundations under eccentric and inclined loads". *In Proceeding of the third International Conference on SMFE,* Vol. 1, pp. 440-445.
6. Sharma, R., Chen, Q., Abu-Farsakh, M., and Yoon, S. (2009). "Analytical modeling of geogrid reinforced soil foundation". *Geotextiles and Geomembranes,* Vol. 27, pp. 63-72.
7. Sharma, R., Chen, Q., Abu-Farsakh, M., and Yoon, S. (2009). "Analytical modeling of geogrid reinforced soil foundation". *Geotextiles and Geomembranes,* Vol. 27, pp. 63-72.
8. Wayne, M. H., Han, J., and Akins, K. (1998). "The design of geosynthetic reinforced foundations". *Geosynthetics in Foundation Reinforcement and Erosion Control Systems,* Vol. 10, pp. 1-18.
9. Wayne, M. H., Han, J., and Akins, K. (1998). "The design of geosynthetic reinforced foundations". *Geosynthetics in Foundation Reinforcement and Erosion Control* Systems, Vol. 10, pp. 1-18.

CHAPTER 8

CONCLUSIONS AND RECOMMENDATION FOR FUTURE STUDY

8.1 Conclusions

A comprehensive study was conducted to analyse the effects of inclusion of geosynthetics in cohesive soil foundation on its bearing capacity using a laboratory scaled model. The essential results reported in the study conducted on reinforced soil foundation are enlisted below:

(1) The optimum depth of top layer reinforcement for GGR1, GGR2 and GTX were obtained at u/B = 0.34. While in case footing resting over sloping ground, the optimum depth of top layer reinforcement for GGR1, GGR2 and GTX were obtained at u/B = 0.4. This signifies the need for a cover for the reinforcement to completely mobilize the tensile strength within them.

(2) The number of layers upto which the effect of reinforcement was felt was obtained at N=4 and N=3 for geogrids and geotextile respectively. After increasing the number of reinforcement layers further, the increase in bearing capacity was not substantial, thus signifying the presence of an optimum depth beyond which inclusion of a geosynthetic is not viable. While in case of footing resting over slope, the optimum depth of reinforcement (d) was obtained at d/B ratio of 1.6B and 1.2B respectively for geogrid and geotextile respectively. After testing for reinforcement at a deeper point, the increase in bearing capacity was not substantial, thus signifying the presence of an optimum depth beyond which inclusion of a geosynthetic is not viable. And the maximum number of reinforcements for geogrid and geotextile was obtained as 4 and 3 respectively.

(3) Vertical spacing between reinforcements also played a crucial role in amassing maximum benefit from reinforcements. Optimum vertical spacing was obtained at 0.16B for all the geo reinforcements. While in case of footing over slope, Vertical spacing between reinforcements

also played a crucial role in amassing maximum benefit from reinforcements. Optimum vertical spacing was obtained at 0.6B for both GGR1 and GGR2 and 0.4B for GTXs respectively.

(4) GGR1 was the best performing material from construction standpoint. Although, GTX performed better at higher settlement ratios, GGR1 provided better reinforcement for lower settlement ratios for which the structures are usually designed for.

(5) GGR1 performed better than GGR2 at every settlement ratio, i.e. s/B =4%, 8%, 12%, 16%, thus signifying that mechanical properties of the geosynthetics such aperture size, tensile strength and tensile modulus have a significant role in reinforcement in reinforcement efficiency of the geosynthetic.

(6) Maximum benefit from reinforcement was obtained at D/B ratio equal to 0, although the highest magnitude of bearing capacity was obtained as the distance between the loading area and the slope edge increased and maximum bearing capacity was achieved at $\beta=35^{\circ}$, with respect to $\beta=40^{\circ}$ and 45°.

(7) FEM study shows a good agreement with experimental results at lower settlement hence it could be used to model unreinforced soil and reinforced soil model very well at lower settlement ratios. Since, the foundations are designed for allowable bearing pressure which requires limited settlement, it can be concluded that FEM model can be successfully used in the design of reinforced soil foundation.

(8) FEM study also shows that scale effect depends on reinforcement ratio of the reinforced zone.

(9) The proposed ANM2 model, based on the reduction factor, provided high accuracy, and can thus be used for computation of ultimate bearing capacity of reinforced cohesive soil foundations under eccentric loading.

(10) ANM1 model, based on the Meyerhof's Effective Width method provided conservative results with lower accuracy.

(11) From the regression analysis of the experimental results, number of reinforcements was obtained as the most significant parameter for improving the bearing capacity at ultimate bearing capacity and tensile modulus of the reinforcement was obtained as the least significant parameter.

(12) Use of geotextiles for reinforcement of soil is uneconomical as the strength improvement is achieved only slightly, and use of woven geotextiles should be considered only where low tensile strength is required.

8.2 Recommendation for future research

Present research work reveals the impact of reinforcement in the development of the bearing capacity of cohesive soil. Various factors have been considered in this study to check the behaviour of reinforced soil foundations. However, some more factors can be considered in the study which influenced the performance of the reinforced soil foundation.

(1) All the experimental and numerical tests have been conducted on maximum dry unit weight. But moisture content of the soil can vary with seasonal variations. Due to variations of moisture content performance of reinforced soil foundation can be influenced. So, the study recommends the effect of moisture content in the performance of reinforced soil foundation.

(2) The present work is based on small scaled footing tests. These tests can have some variations in results with actual field conditions. Large-scale footing tests are recommended on reinforced soil foundation.

(3) A study on effect of various dynamic forces due to earthquake, landslide and volcanic eruptions on actual footing can also be conducted and how reinforcements play a role in the performance of bearing capacity of actual footing under dynamic loading conditions can also be studied.